NATIONAL ADVISORY COMMITTEE FOR AERONAUTICS

WARTIME REPORT

ORIGINALLY ISSUED

October 1942 as
Memorandum Report

INVESTIGATION OF DIVING MOMENTS OF A PURSUIT AIRPLANE IN THE AMES 16-FOOT HIGH-SPEED WIND TUNNEL

By Albert L. Erickson

Ames Aeronautical Laboratory
Moffett Field, California

NACA

WASHINGTON

NATIONAL ADVISORY COMMITTEE FOR AERONAUTICS

MEMORANDUM REPORT

for the

Materiel Command, Army Air Forces

INVESTIGATION OF DIVING MOMENTS OF A PURSUIT AIRPLANE IN THE AMES 16-FOOT HIGH-SPEED WIND TUNNEL

By Albert L. Erickson

SUMMARY

A pursuit-type airplane encountered severe diving moments in high-speed dives which make recovery difficult. For the purpose of investigating these diving moments and finding means for their reduction, a 1/6-scale model of the airplane was tested in the 16-foot high-speed wind tunnel at Ames Aeronautical Laboratory. The test results indicate that up to a Mach number of at least 0.75, the limit of the tests, the dive-recovery difficulties can be alleviated and the longitudinal maneuverability improved by the substitution of a long symmetrical fuselage for the standard fuselage.

INTRODUCTION

A pursuit airplane developed powerful diving moments in high-speed dives, and these moments have made recovery from high-speed dives very difficult. The difficulties have been discussed in reference 1, and they have been investigated in the full-scale wind tunnel and in the 8-foot high-speed wind tunnel at Langley Memorial Aeronautical Laboratory (references 2, 3, and 4).

At the request of the Army Air Forces, a model of the airplane was tested in the 16-foot high-speed wind tunnel at AAL. The purpose of these tests was to extend the range of the previous high-speed tests with a view toward developing means for eliminating the diving difficulties and improving the maneuverability of the airplane at high speeds. A number of fuselage shapes, several changes in the span load distribution, bulges and spoilers on the wing and fuselage, and a modification of the wing center-section profile were tested.

APPARATUS AND METHOD

The 1/6-scale tip-mounted model used in the 8-foot high-speed wind tunnel at LMAL (reference 2) was modified by the addition of wing tips and fitted with trunnion-support fittings in the booms for mounting the model on struts. Reference 5 shows details of the model. Stings were attached 18 inches back of the strut trunnions, as shown in figure 1, for controlling the angle of attack. A pitot survey head was used to explore the air flow in the region of the tail. This head measured the total and static pressures and the pitch and yaw angles of the air stream. In those of the present tests wherein the effects of drooped ailerons and partially extended Fowler flaps were studied, the ailerons and flaps were simulated by split flaps having chords approximately 30 percent of the wing chord at each spanwise station. In addition to the tests with the standard airplane wing, the model was tested using a wing with revised twist. Except for the twist, this revised wing was identical to the standard wing. The twist was changed only from the boom center lines outboard so that the angle of attack relative to the standard wing was increased from 0° at the boom center lines to 3° at the station where the rounding of the wing tips started.

RESULTS

The data in this report have been corrected for tunnel-wall effects, and approximately for tare drags and tare moments. The moment center was 3.23 inches vertically above the trunnion point with the airplane in the zero angle-of-attack attitude. Upflow or downflow with the strut supports in place has not been evaluated. A slight upflow or downflow would affect only the absolute values of drag and, for comparative purposes, would have no effect.

The results are discussed in the following order:

1. Standard configuration
2. Effect of fuselage shape
3. Effect of bulges, fillets, and spoilers
4. Effect of changes to wing center section
5. Effect of ailerons and flaps
6. Effect of the change in wing twist

7. Elevator effectiveness

8. Improvements resulting from use of the long symmetrical fuselage

9. Buffeting

Standard Configuration

Tests of the standard configuration, complete and in parts, revealed the nature and cause of the dive-recovery difficulties. With the complete standard model, the longitudinal stability increased enormously as the Mach number was increased above 0.65. This increase in stability is illustrated by the decrease in the slopes of the curves showing the variation of moment coefficient with lift coefficient in figures 2(a) and 2(b). Figure 2(c) consists of cross plots from these curves and shows the variation with Mach number of the moment coefficient at constant values of the lift coefficient. The lift coefficient at which the moment curves for various Mach numbers intersect is of special significance and will henceforth be referred to as the constant-moment lift coefficient. For all lift coefficients greater than the constant-moment value (approximately -0.15 for the standard configuration), the pitching moment decreases; that is, it becomes a diving moment as the speed is increased. For smaller values of lift coefficient, the moment becomes a climbing moment as the speed increases. Thus, it is seen that at high speeds the airplane becomes extremely stable. This stability is so great that deflection of the elevator, as will be shown later, produces little change in lift, hence, the difficulty in recovering from dives.

Removing all the accessories (Prestone, oil, and spark-plug cooling scoops, carburetor scoops, and turbosupercharger installations) from the standard configuration made no important change in the moment characteristics. Removing the fuselage, however, increased the critical speed at which the stability started its rapid increase, and also changed the value of the constant-moment lift coefficient from a small negative value (about -0.15) to a positive value of about 0.2 (fig. 3(c)). With the balance occurring at a positive value of the constant-moment lift coefficient, the airplane would tend to automatically recover from high-speed dives because a pull-out moment would become effective as the speed increased. Modification of the airplane so that the constant moment occurs at a suitable positive value of the lift coefficient, as with the fuselage removed, should provide a means of alleviating the dive-recovery difficulties.

With the horizontal tail surfaces removed from the model, relatively small changes in pitching-moment coefficient occurred as the speed was increased above the critical (fig. 4(e)), and the changes that did occur were in the opposite direction to those with the tail in place. This result indicated that the moments produced by the tail were undergoing large changes as the speed increased thereby causing the difficulties. Figure 5 shows downwash angles that were measured at the tail position while the tail was absent. As the Mach number increased above the critical, the downwash angle decreased as much as 2° or 3°, and the variation of downwash with angle of attack became only a small fraction of its low-speed value. The decrease in downwash was a direct result of the loss in lift as the Mach number was increased above the critical value (fig. 4(c)). The magnitude of the reduction in downwash corresponded approximately to the change in tail angle of attack that would be required to produce the changes in pitching moment shown in figure 3(e).

It was concluded that the dive-recovery difficulties of the airplane are due to the center section of the wing losing lift as the speed increases above the critical. The reduction in lift is accompanied by a reduction in downwash at the tail and a reduction in the rate of change of downwash angle with airplane angle of attack. The latter change produces a great increase in longitudinal stability at speeds above the critical speed of the center section. With the standard fuselage in place, the constant-moment lift coefficient centers about a negative value of the lift coefficient, and the stability becomes so great that the elevator can produce only small changes in airplane lift coefficient; consequently, recovery from high-speed dives is difficult. With the fuselage removed, a positive value of the constant-moment lift coefficient occurred, so in this configuration the airplane would tend to automatically recover from high-speed dives.

Effect of Fuselage Shape

As it was shown that the standard fuselage caused the moments to break at a lower Mach number and the constant-moment lift coefficient to be negative, several fuselage modifications were tested. These were the standard fuselage with modified canopy, an underslung fuselage, a long symmetrical fuselage, a long symmetrical fuselage with flat-front cab, and a long symmetrical fuselage with the cab from the standard fuselage. The results are compared in figure 6.

These curves are plotted for three representative lift coefficients: 0.1, 0.2, and 0.4. The results show that the fuselage designated "the long symmetrical fuselage" (fig. 7) carried the moment curve to the highest Mach number before breaking, and caused the constant-moment lift coefficient to center about a small positive value of the lift coefficient (approximately 0.07). This fuselage also had a lower drag at Mach numbers above 0.68. The underslung fuselage gave similar moment characteristics, but it was not considered as practical a shape (fig. 8).

Adding a flat front to the cab of the long symmetrical fuselage (fig. 9) in order to permit the use of flat bullet-proof glass windshield made the moment characteristics slightly worse (fig. 6). Two cab changes were tried in an effort to find an arrangement that gave satisfactory moment characteristics, but that would not make it necessary to move the pilot and the controls from their positions in the standard airplane. The flat-front cab was moved aft 2 inches (corresponding to 12 in. full-scale), and the cab from the standard fuselage was tried on the long symmetrical fuselage. Both of these cab arrangements gave poor moment characteristics (fig. 6) as compared with the forward cab. The inferior characteristics with these two cabs were probably due to the peak velocities induced by the cabs being near to, and adding to, the peak velocities induced by the wing.

Figures 10 and 11 give the complete basic results for the long symmetrical fuselage. Figure 10 gives results for the regular Prestone scoops; figure 11, for modified Prestone scoops. Little difference in the results is noted, although there is a slight reduction in drag indicated with the modified scoops.

Effect of Bulges, Fillets, and Spoilers

Abrupt bulges were placed on the under side of the fuselage, as shown in figures 12, 13, and 14, to find their effect in causing a shock on the under surface of the fuselage. The first bulge was placed on the under side of the standard fuselage with a revised canopy. This bulge caused the moment curves to rise slightly from Mach numbers of 0.3 upward, but there was no noticeable change in the general effect (fig. 15). This indicates that the upper wing surface had the most powerful influence on the pitching moment. Other bulges tried on the long symmetrical fuselage with the cab off had little effect on the pitching moments. Figure 16 gives comparative results with and without the bulges.

Several types of fillets were tried on the symmetrical fuselage (figs. 17, 18, and 19), but none of these gave any special benefit (fig. 20) over the constant-radius fillet used on all other tests. The fillet used for most of the tests had a constant radius of one-half inch (3 in. on the airplane) and would be the easiest to build.

Some spoilers and bulges were tried on the under side of the wing. The first spoiler tried was set 90° to the wing surface, protruded 1/4 inch from the surface at 33-1/3 percent of the wing chord from the leading edge, and was extended between the booms. A second test was made with this same spoiler extended to the wing tips. For a third test, the spoilers were removed and a smooth bulge one-fourth inch high was located between the booms at the same chord position. These tests were predicated on pressure-distribution data which showed that, at constant angle of attack, as the speed was increased the negative lift on the lower wing surface increased more rapidly than the positive lift on the upper surface at high speeds. The tests were made to determine whether the negative lift increases could be reduced or eliminated. The effects of these various changes are shown on figures 21(a), 21(b), and 21(c). The flow over the lower surface was spoiled to such an extent that from a very low speed, a steady rise in the moment curve took place until the upper surface reached its critical speed, and then at lift coefficients of 0.2 and above, the moment broke in a negative direction.

Effect of Changes to Wing Center Section

As the presence of critical pressures had been shown to cause the trouble, it appeared that a wing with lower pressure peaks would delay the compressibility break. Accordingly, a glove was built around the original wing between the booms. This glove was set at a lower angle of attack and had a larger chord (fig. 22) than the original wing. This glove had much lower pressure peaks and, with the symmetrical fuselage, raised the critical speed and the balancing lift coefficient to a value slightly higher than that for the same configuration but without the glove (figs. 23(a), 23(b), and 23(c)). With the standard fuselage and the glove, on the other hand, the curves broke in the same way and at the same Mach number as for the standard fuselage without the glove.

Effect of Ailerons and Flaps

As the loss in lift on the center section caused the large adverse tail moments for a given total lift a change in span load distribution that would shift a greater part of the lift outboard of the booms would relieve the center section of some lift and delay the pressure rise on this section. Accordingly, tests were made with simulated flaps and ailerons deflected 15° down and extending from the wing tips into the booms. Without the fuselage (fig. 24), an improvement in the characteristics is indicated. The moments increased at speeds above the critical for lift coefficients of 0.3 or less (fig. 24(e)); whereas without the simulated flaps and ailerons (fig. 3(e)), the moments increased for lift coefficients only up to 0.1. In addition, the flaps increased the Mach numbers at which the sudden change in moment occurred. Several additional runs were made (figs. 23(a), 23(b), and 23(c)) with simulated flaps and ailerons 15° down. It can be seen from these comparative curves that the flaps improved the moment characteristics in all cases except when the standard fuselage was used. At a lift coefficient of 0.1, although all other configurations broke in a positive direction, the configuration with the standard fuselage broke negatively and at a much earlier Mach number than the others.

Effect of the Change in Wing Twist

It appeared that an effect similar to that obtained with the split flaps could be obtained in a practically applicable manner by modifying the wing twist. Accordingly, a wing having the twist modified by increasing the angle of attack at the tips by 3° was tested. This change in wing twist improved the characteristics very little, whether used with the long symmetrical fuselage or with the standard fuselage (fig. 25). Complete results of the tests of the revised wing with the long symmetrical fuselage are given in figure 26. The ineffectiveness of the change in wing twist as compared to the split flaps apparently was largely due to the fact that the twist increased the lift coefficient at each angle of attack only a small amount compared to the increase in lift coefficient produced by the flaps.

Elevator Effectiveness

Figure 27 indicates, for one configuration, the lift coefficient at which the airplane would balance at various Mach numbers with several elevator angles. This figure shows that at high speeds a given elevator deflection produced relatively small changes in the lift coefficient at which the airplane would balance. Analysis indicates that the loss of elevator effectiveness at high speeds is largely a result of the great increase in stability of the airplane and not to any important extent due to reduction in the change in tail lift brought about by a given elevator deflection. The results for other configurations were similar, the only important difference being in the value of the constant-moment lift coefficient.

Improvements Resulting From Use of the Long Symmetrical Fuselage

The model with the symmetrical fuselage showed better diving characteristics than the standard configuration. By taking the points on the curves of figure 25 where the moment broke, figure 28 was plotted, which shows the maximum lift coefficient attainable without the moment curves breaking in a diving direction. The Mach numbers at which the moment coefficient curves broke agree closely with the Mach numbers at which the lift coefficient curves broke for corresponding conditions. These results (fig. 28) show that at zero lift and at Mach numbers up to at least 0.75, the limit of the tests, with the symmetrical fuselage the airplane will not have difficulty in recovering from dives, because the moment is a climbing moment when it does break. If the airplane exceeds the critical speed, it will tend to come out of the dive, not stay in it. As a matter of interest, there are also plotted on this figure curves of the lift coefficient required to maintain level flight at various altitudes.

The long symmetrical fuselage improved the longitudinal maneuverability in the critical speed region. The improvement is shown in figure 28. For example, at a Mach number of 0.65, with the standard fuselage, the maximum lift coefficient available without encountering the severe diving moments is 0.2. Replacing the standard fuselage with the long symmetrical fuselage increases the lift coefficient available for the same condition to 0.5. At an altitude of 25,000 feet, a lift coefficient of 0.2 produces only enough lift for level flight at a Mach number of 0.65. Therefore, accelerations that would require higher lift would put the airplane into the critical diving-moment region. By changing to the long symmetrical fuselage, acceleration of 2.5g could be executed under the conditions of the example without entering the critical region.

Buffeting

Neither the results of force tests nor observations of the model behavior during tests gave any indication as to whether or not tail buffeting occurred. Figures 29 and 30, which give results of measurements of the wake at the position of the tail, show that with the standard tail position, the tail will come within the wake of the wing and fuselage at high Mach numbers. These results indicate that raising the horizontal tail surfaces 32 inches above the standard position should keep them out of the wake, except for Mach numbers above 0.75 at angles of attack above 2°, and should thereby largely eliminate buffeting. Reference 2 makes a similar conclusion. Tests were made with the tail altered as shown in figure 31. The model dimensions indicated correspond to raising the tail 32 inches and moving it back 24 inches on the airplane. Figure 32 shows the aerodynamic characteristics resulting from this change. The only effect as compared to the standard tail position was an increase in stability.

CONCLUSIONS

1. The difficulty encountered by this pursuit airplane in recovering from high-speed dives is caused by a compressibility shock on the wing center section. This shock causes a loss in lift and a reduction in the downwash, which results in a large change in the tail moments.

2. With the standard fuselage, none of the modifications tested eliminated the difficulties.

3. A long symmetrical fuselage increased the Mach number at which the adverse diving moments occurred by at least 0.05. At Mach numbers up to at least 0.75, the limit of the tests, the long symmetrical fuselage caused the airplane to balance at a sufficiently positive lift coefficient so that recovery from dives could be effected.

4. The longitudinal maneuverability of the airplane at high speeds can be improved by the use of the long symmetrical fuselage. For example, at 25,000 feet and at a Mach number of 0.65, the airplane can obtain 2.5g accelerations, as compared with only one g for the standard configuration.

Ames Aeronautical Laboratory,
National Advisory Committee for Aeronautics,
Moffett Field, Calif.

REFERENCES

1. Johnson, C. L.: A Study of the Diving Characteristics of the Lockheed P-38 Airplane. Lockheed Aircraft Corporation Rep. No. 2646, May 8, 1942.

2. Draley, Eugene C.: Tests of 1/6-Scale P-38 Model in the 8-Foot High-Speed Tunnel. NACA RMR, May 1942.

3. Preston, G. Merritt, and Guryansky, Eugene R.: Drag Analysis of the Lockheed YP-38 Airplane. NACA MR, March 1942.

4. Guryansky, Eugene R., and Preston, G. Merritt: Full-Scale Wind Tunnel Investigation of Buffeting and Diving Tendencies of the YP-38 Airplane. NACA MR, March 1941.

5. Model Design Group: P-38 1/6-Scale High-Speed Wind Tunnel Model. Lockheed Aircraft Corporation Rep. No. L.A.L., 17 Parts, I, II, III, IV, and Appendix, Dec. 16, 1941, and Apr. 10, 1942.

Figure 1. - Model used in tests with standard equipment.

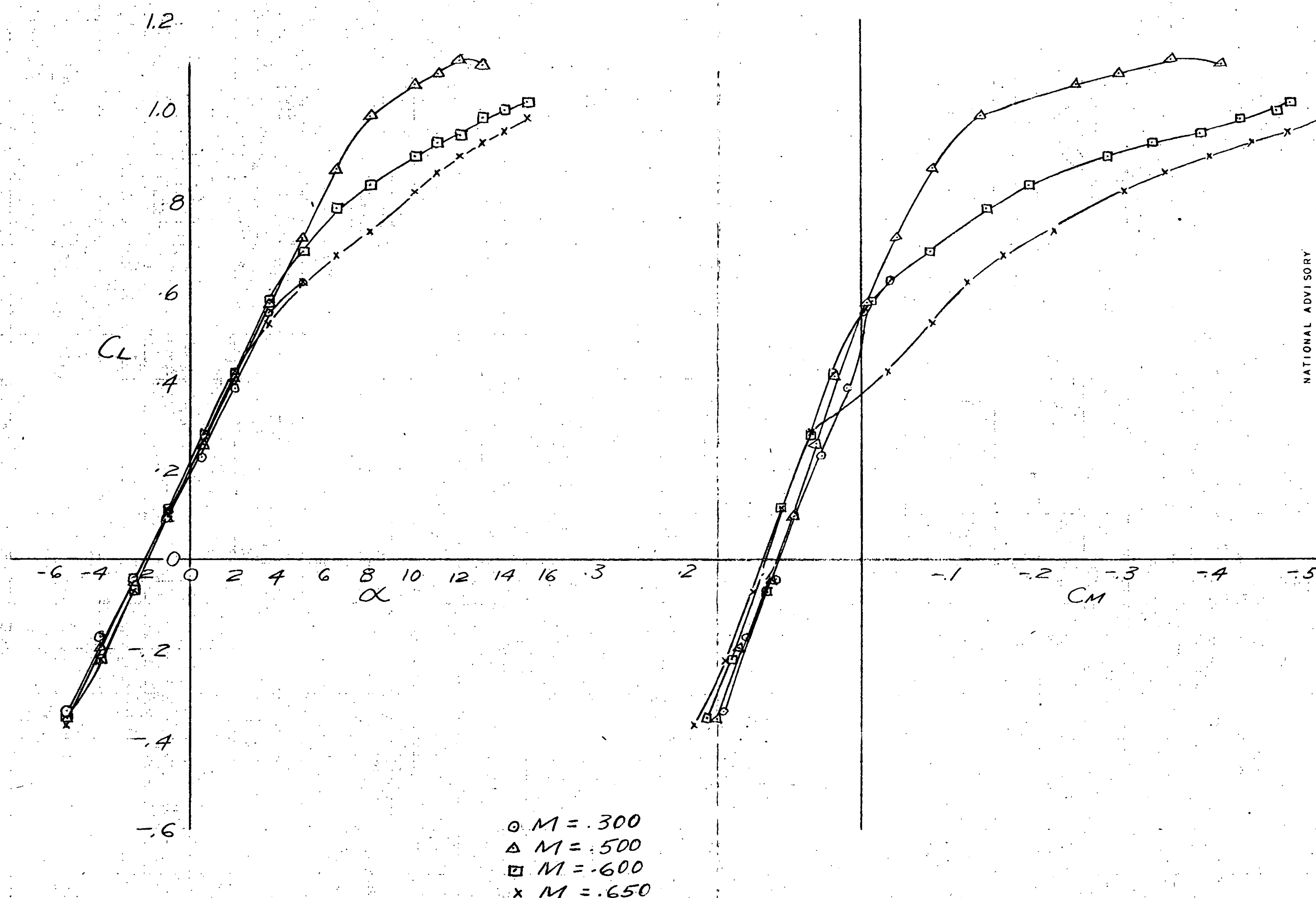

NATIONAL ADVISORY
COMMITTEE FOR AERONAUTICS

(a) Concluded. Basic data from Mach number 0.300 to 0.650.

Figure 2. - Continued. Wing, booms, standard fuseläge, tail, and all accessories.

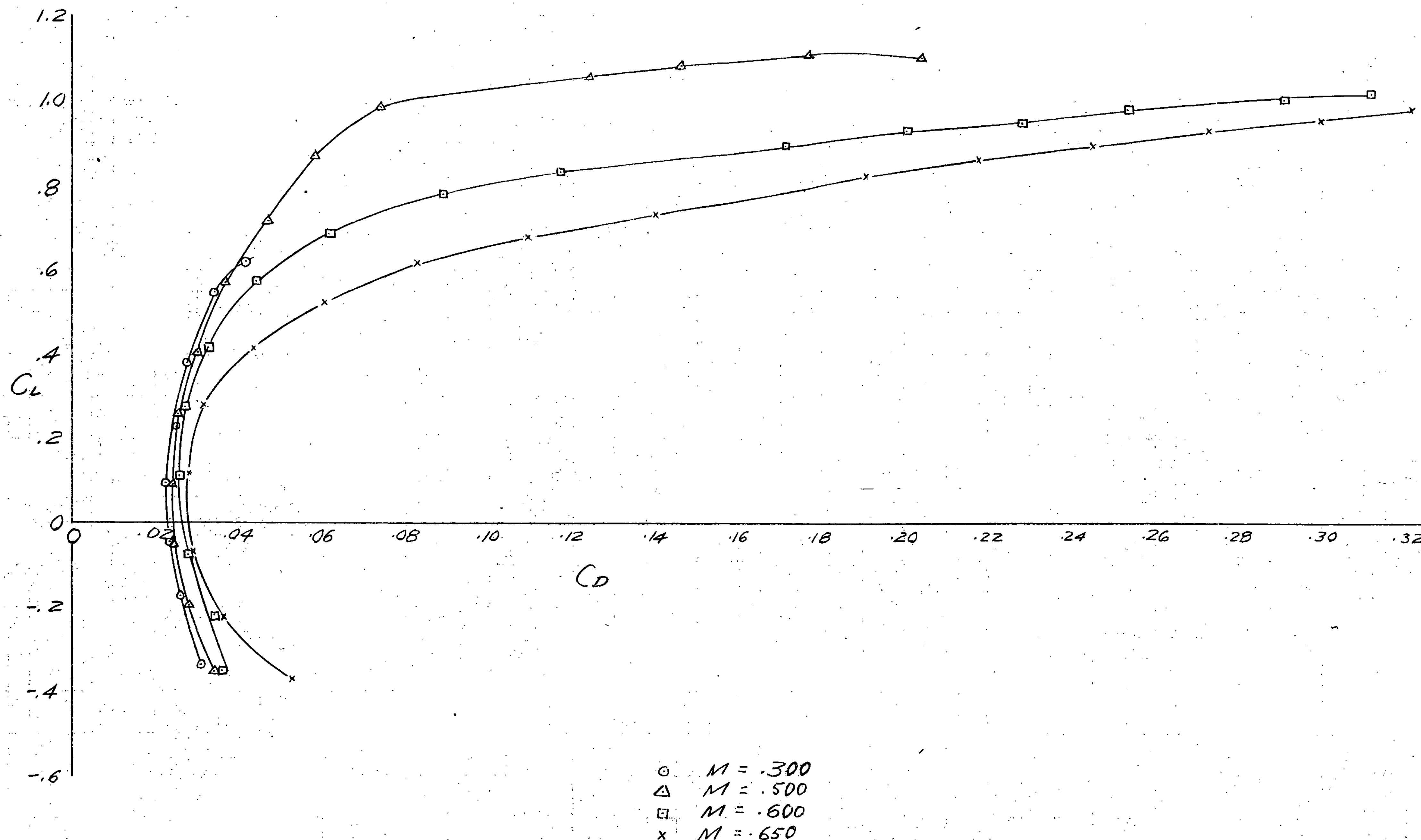

NATIONAL ADVISORY
COMMITTEE FOR AERONAUTICS

(a) Basic data from Mach number 0.300 to 0.650.

Figure 2. - Wing, booms, standard fuselage, tail, and all accessories.

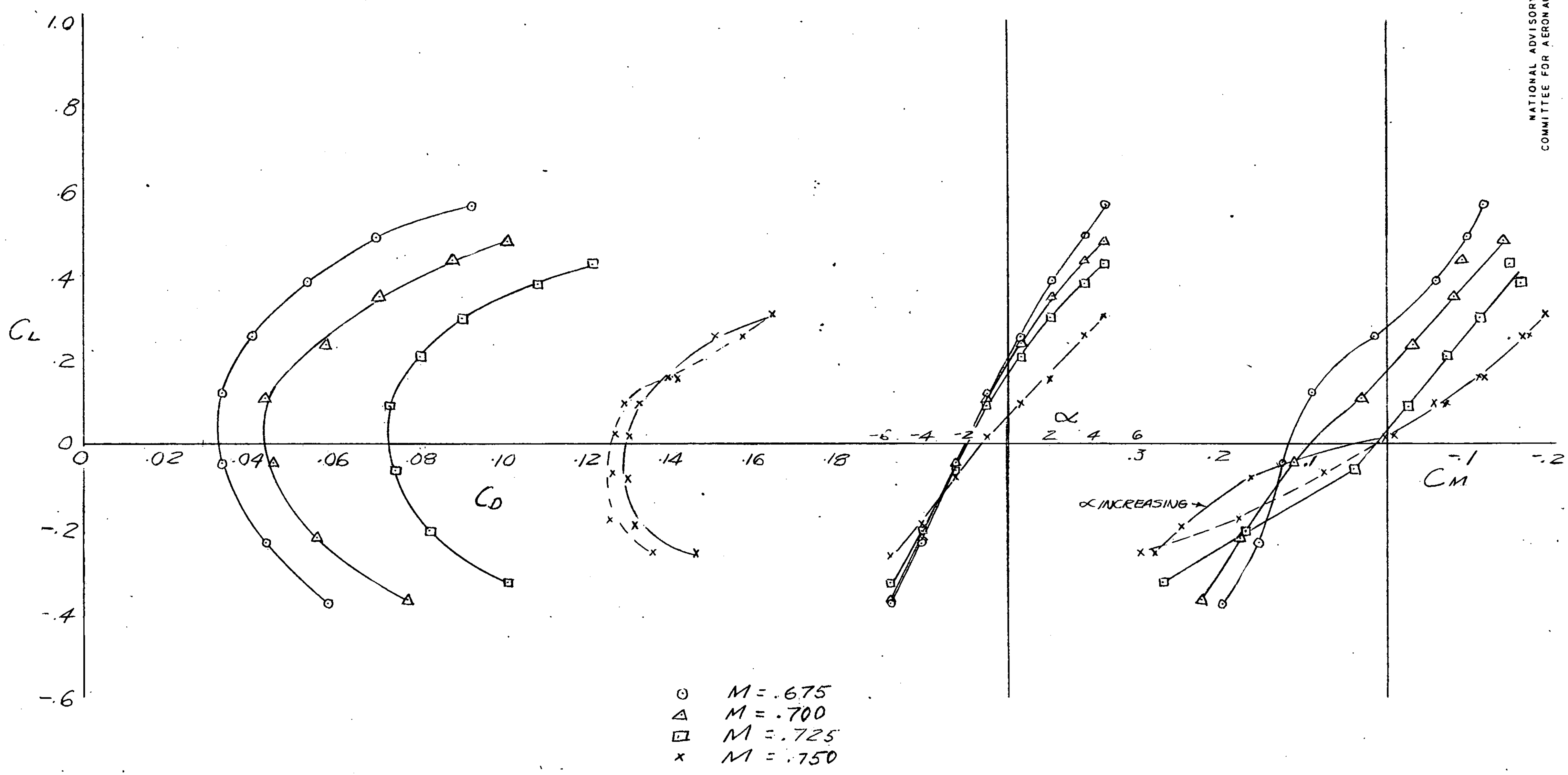

(b) Basic data from Mach number 0.675 to 0.750.

Figure 2. - Continued. Wing, booms, standard fuselage, tail, and all accessories.

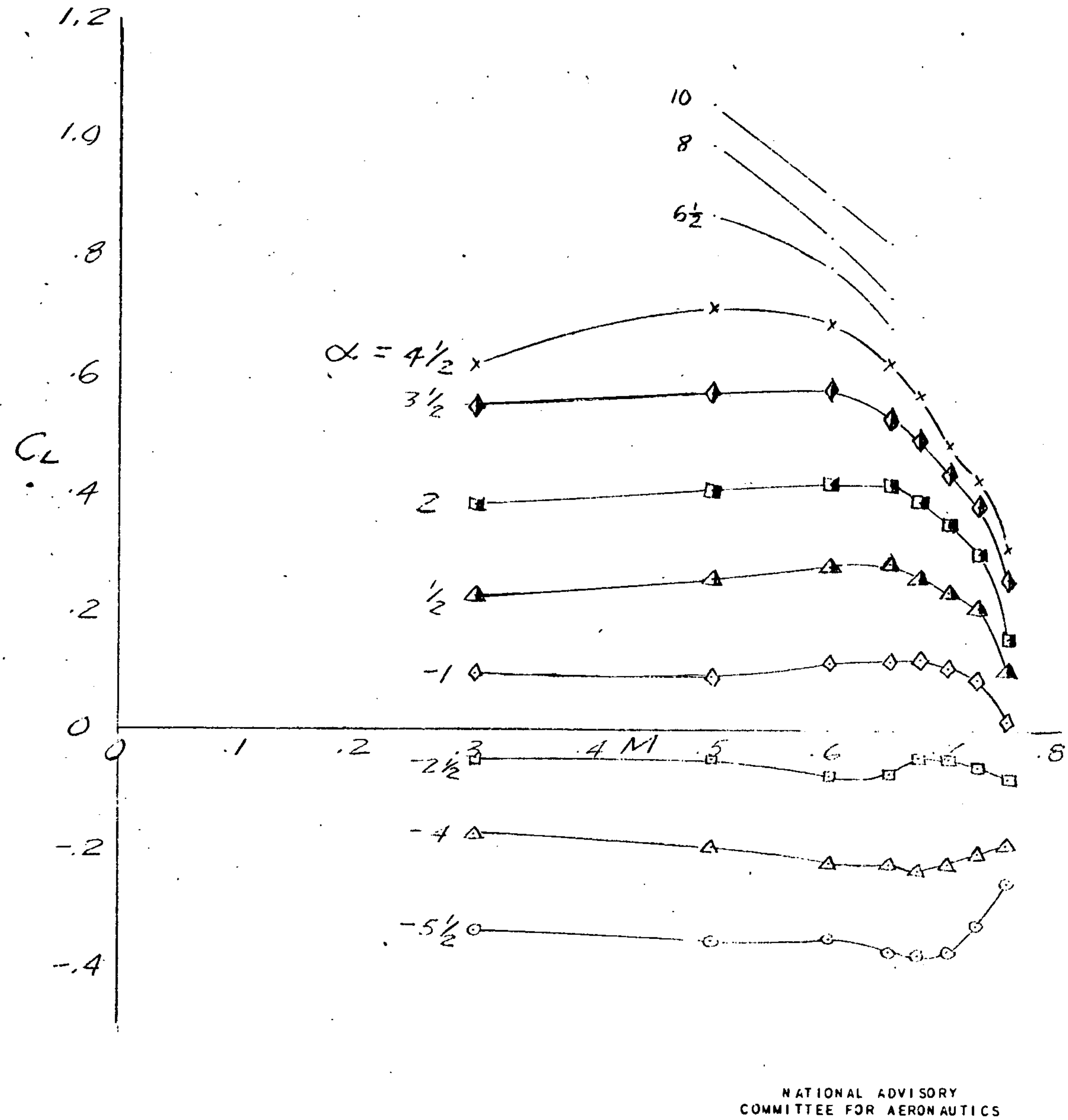

(c) Variation of C_L with Mach number at constant angles of attack.

Figure 2. - Continued. Wing, booms, standard fuselage, tail, and all accessories.

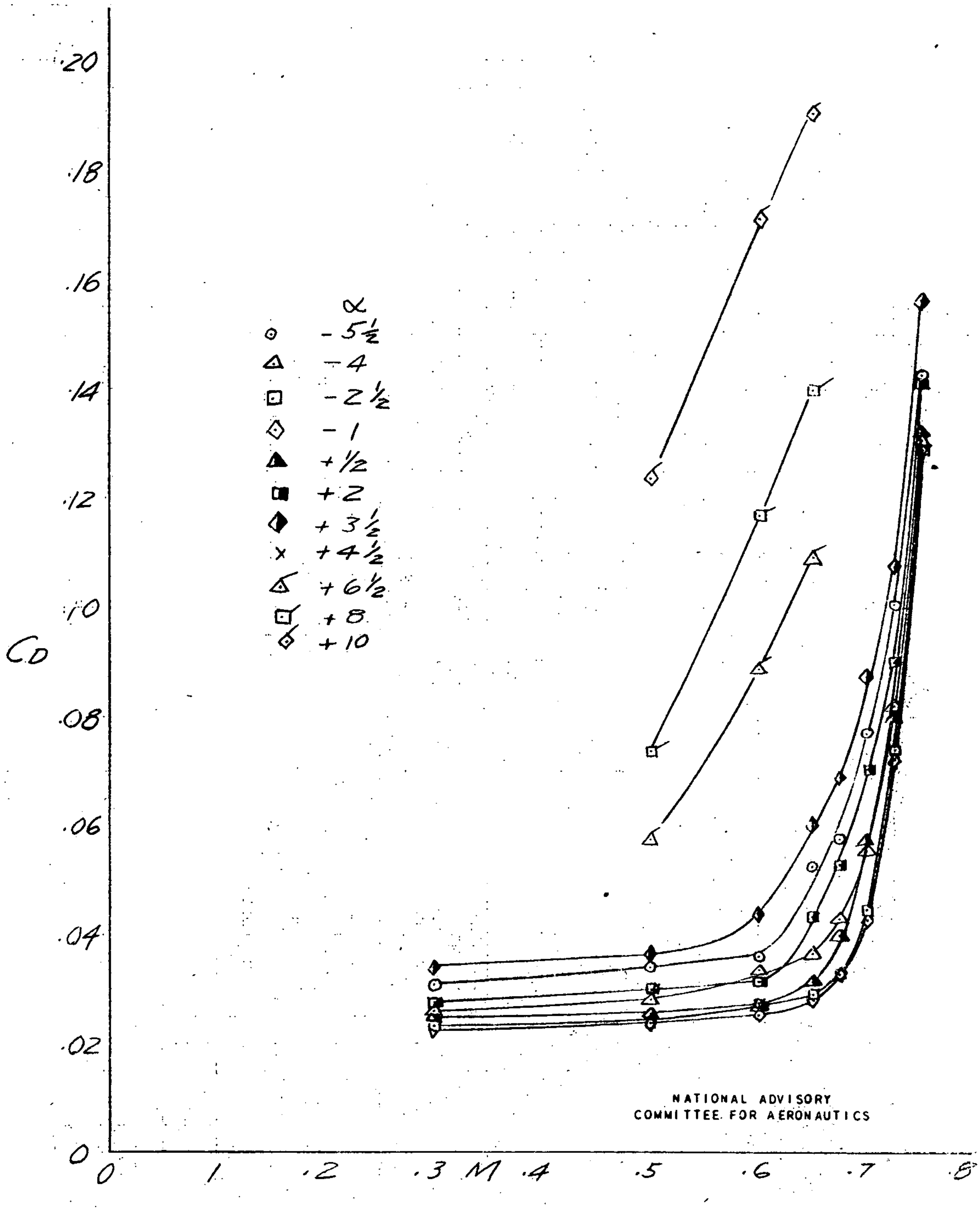

(d) Variation of C_D with Mach number at constant angles of attack.

Figure 2. - Continued. Wing, booms, standard fuselage, tail, and all accessories.

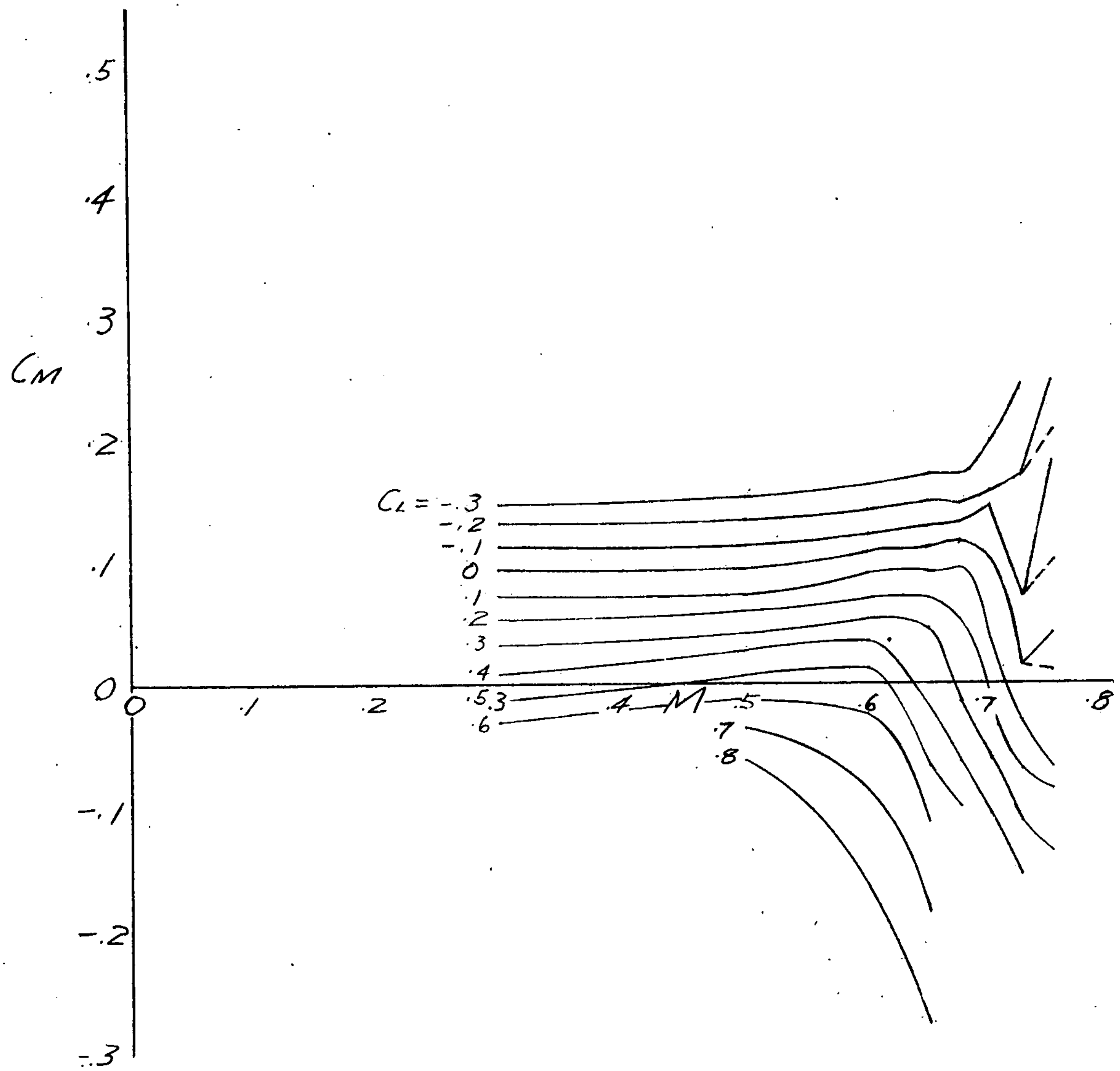

NATIONAL ADVISORY
COMMITTEE FOR AERONAUTICS

(e) Variation of C_M with Mach number at constant lift coefficients.

Figure 2. - Concluded. Wing, booms, standard fuselage, tail, and all accessories.

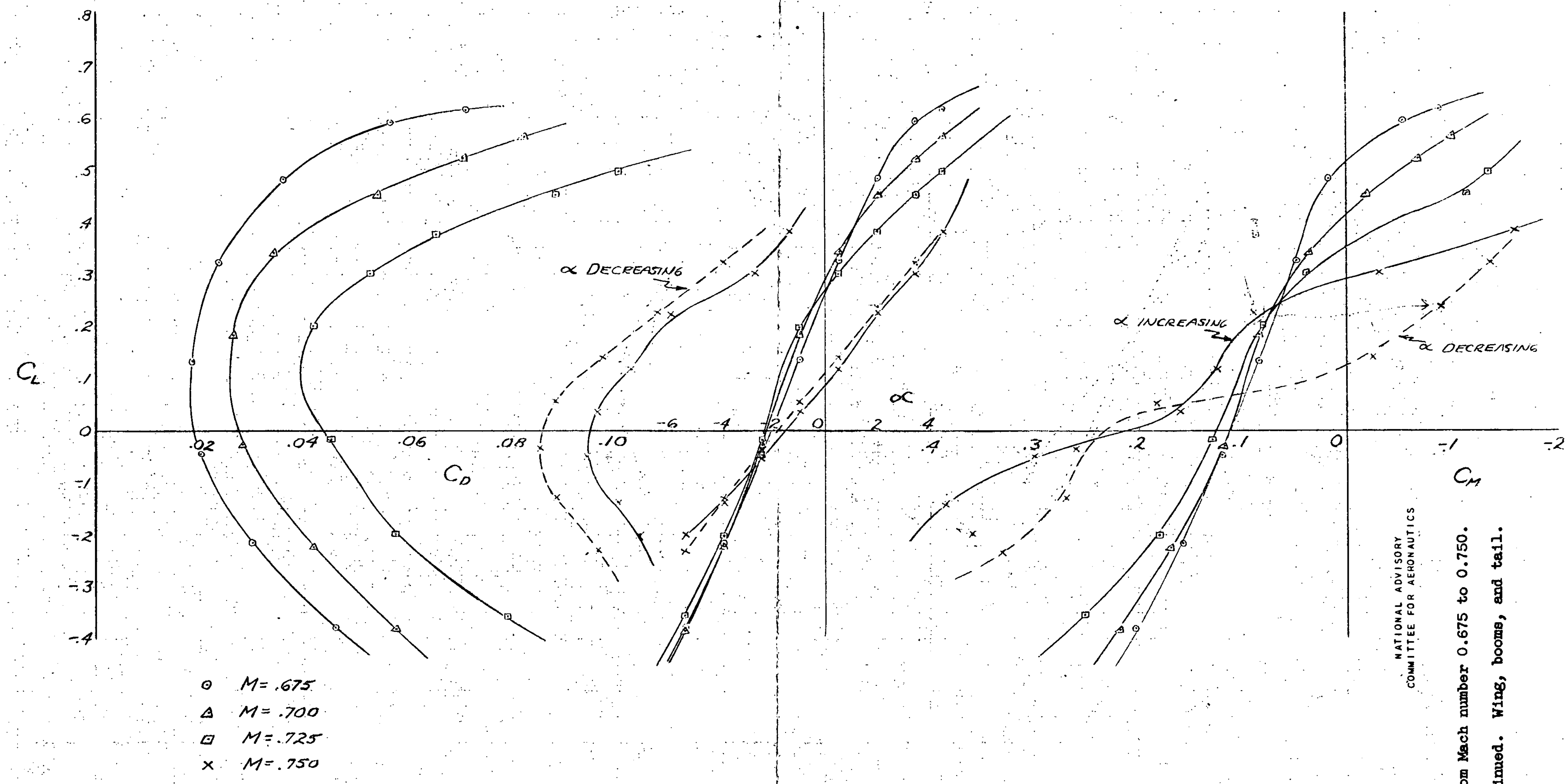

NATIONAL ADVISORY COMMITTEE FOR AERONAUTICS

(b) Basic data from Mach number 0.675 to 0.750.

Figure 3. - Continued. Wing, booms, and tail.

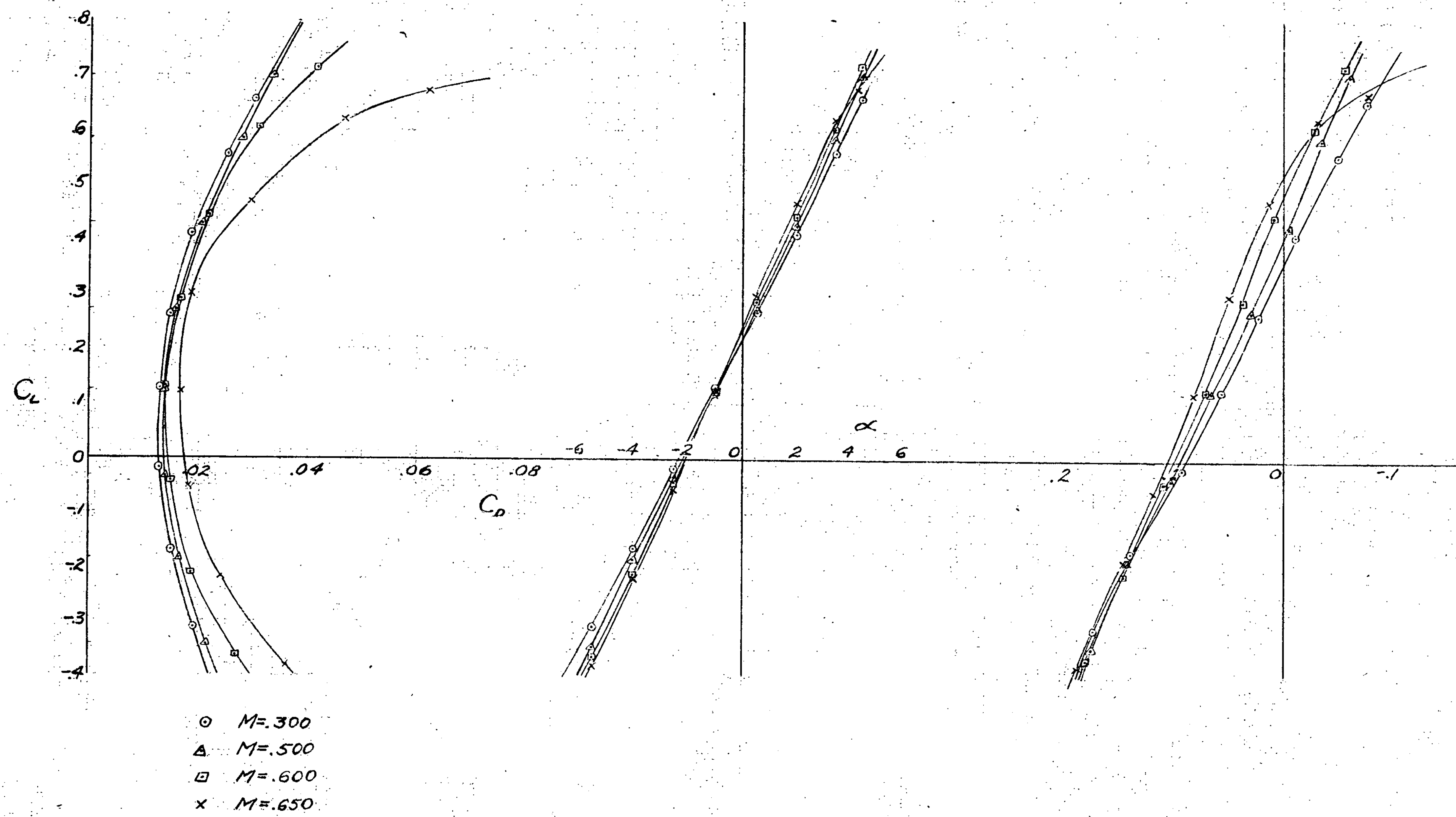

NATIONAL ADVISORY COMMITTEE FOR AERONAUTICS

(a) Basic data from Mach number 0.300 to 0.650.

Figure 3. - Wing, booms, and tail.

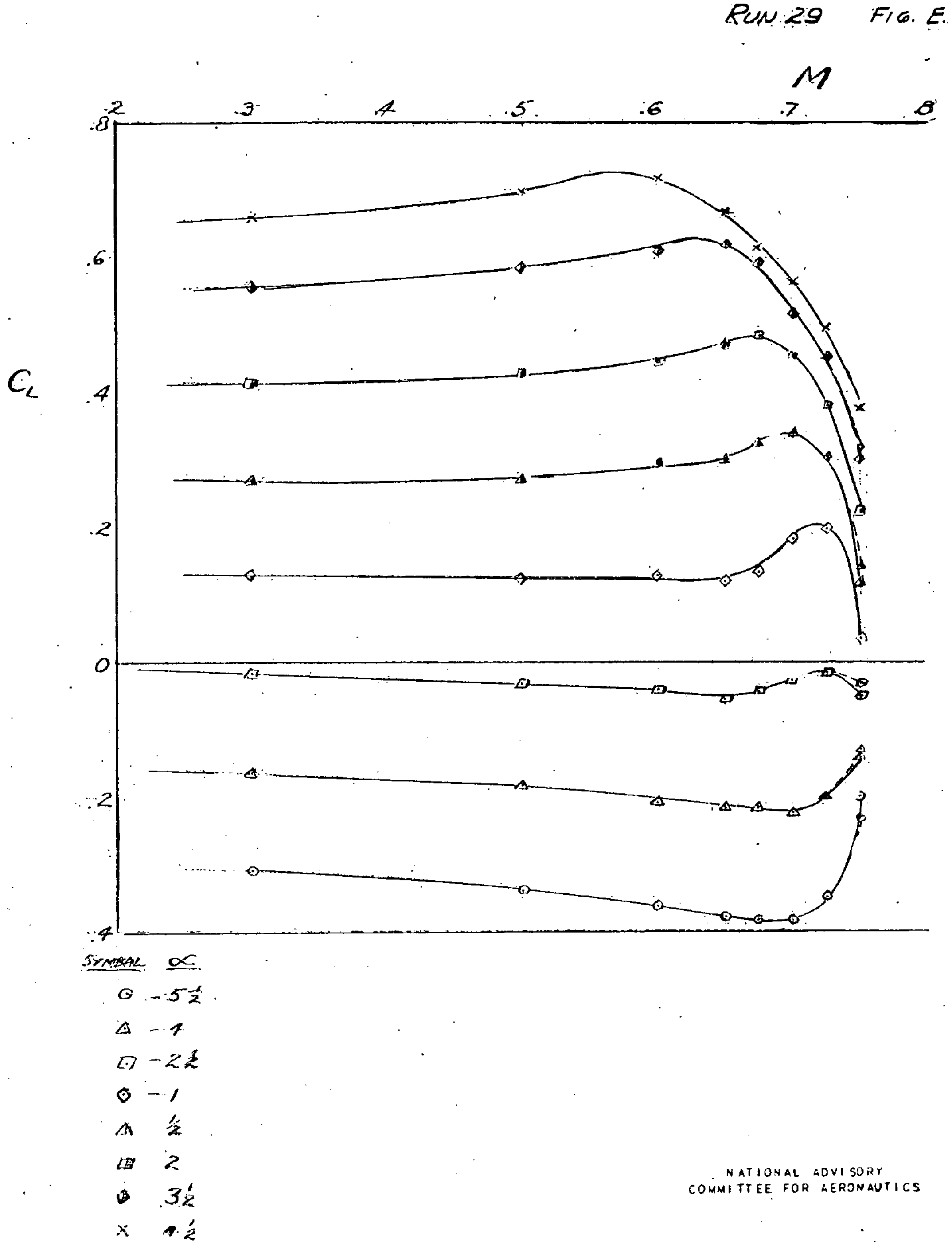

(c) Variation of C_L with Mach number at constant angles of attack.

Figure 3. - Continued. Wing, booms, and tail.

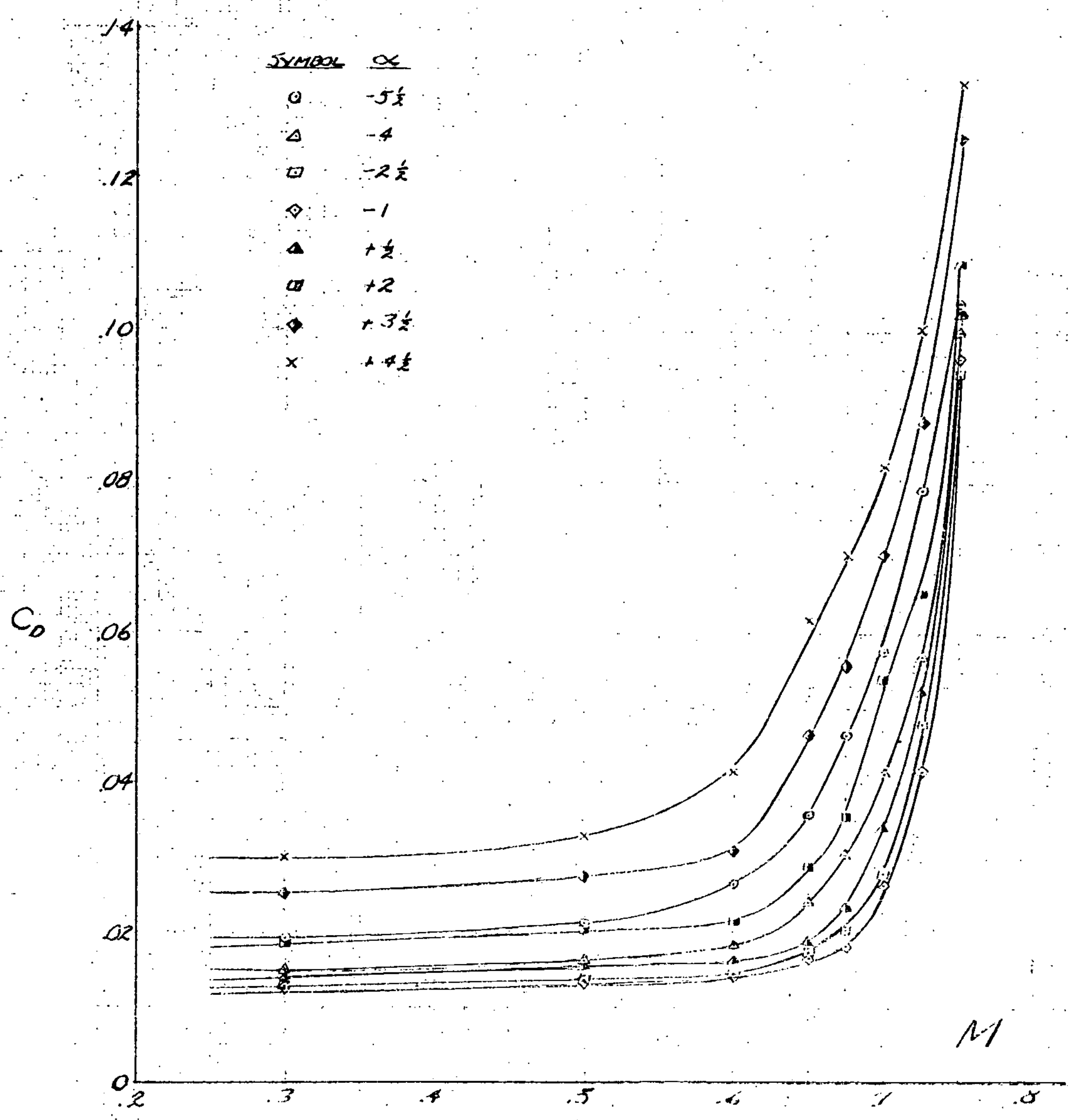

NATIONAL ADVISORY
COMMITTEE FOR AERONAUTICS

(d) Variation of C_D with Mach number at constant angles of attack.

Figure 3. - Continued. Wing, booms, and tail.

RUN 29 FIG K

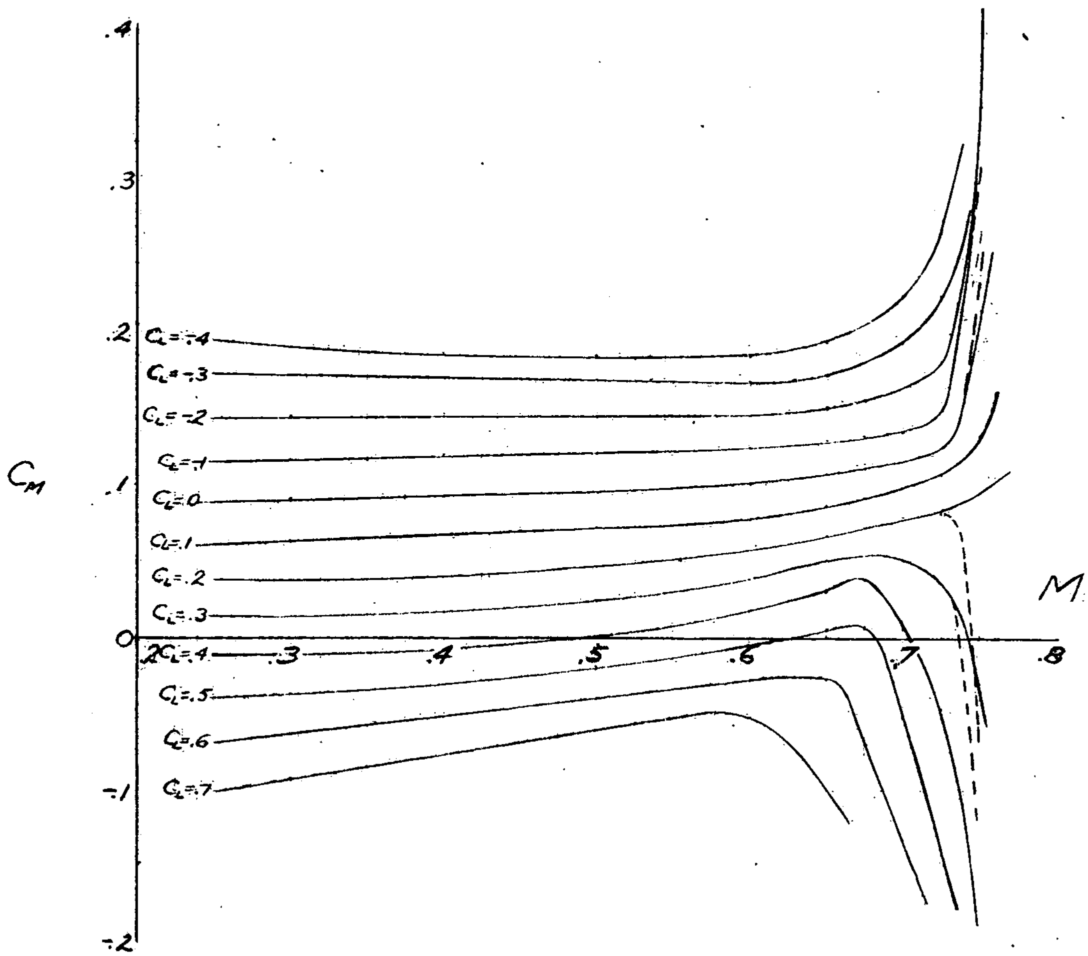

NATIONAL ADVISORY
COMMITTEE FOR AERONAUTICS

(e) Variation of C_M with Mach number at constant lift coefficients.

Figure 3. - Concluded. Wing, booms, and tail.

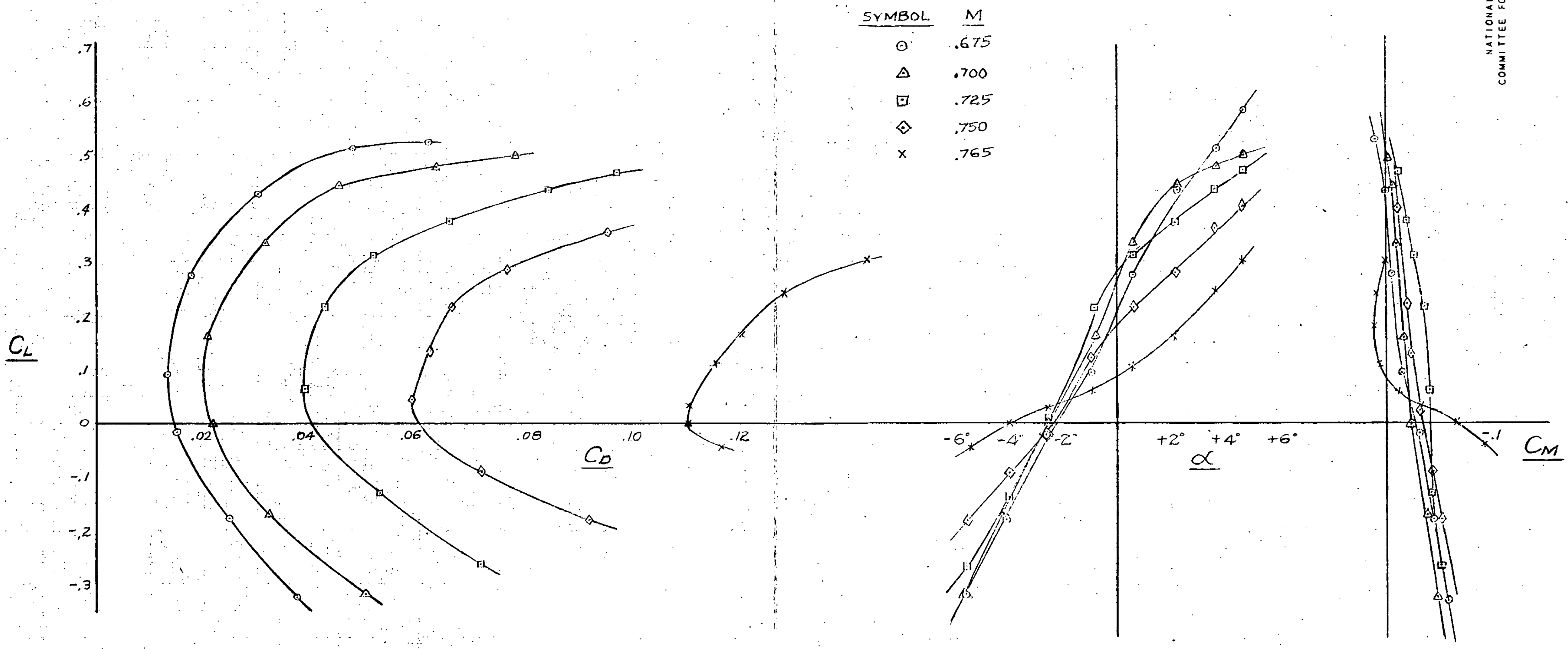

(b) Basic data from Mach number 0.675 to 0.765.

Figure 4. - Continued. Wing and booms.

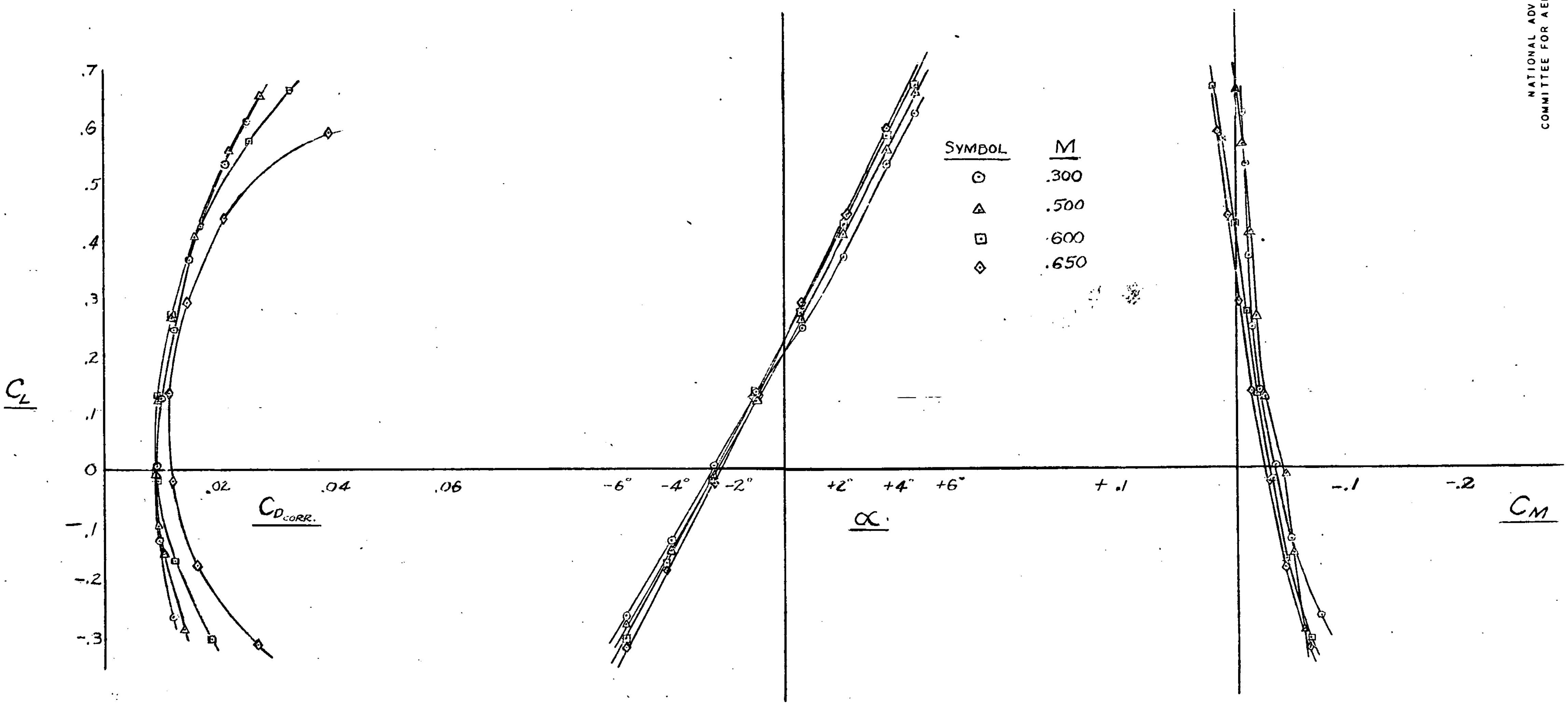

NATIONAL ADVISORY COMMITTEE FOR AERONAUTICS

(a) Basic data from Mach number 0.300 to 0.650.

Figure 4. - Wing and booms.

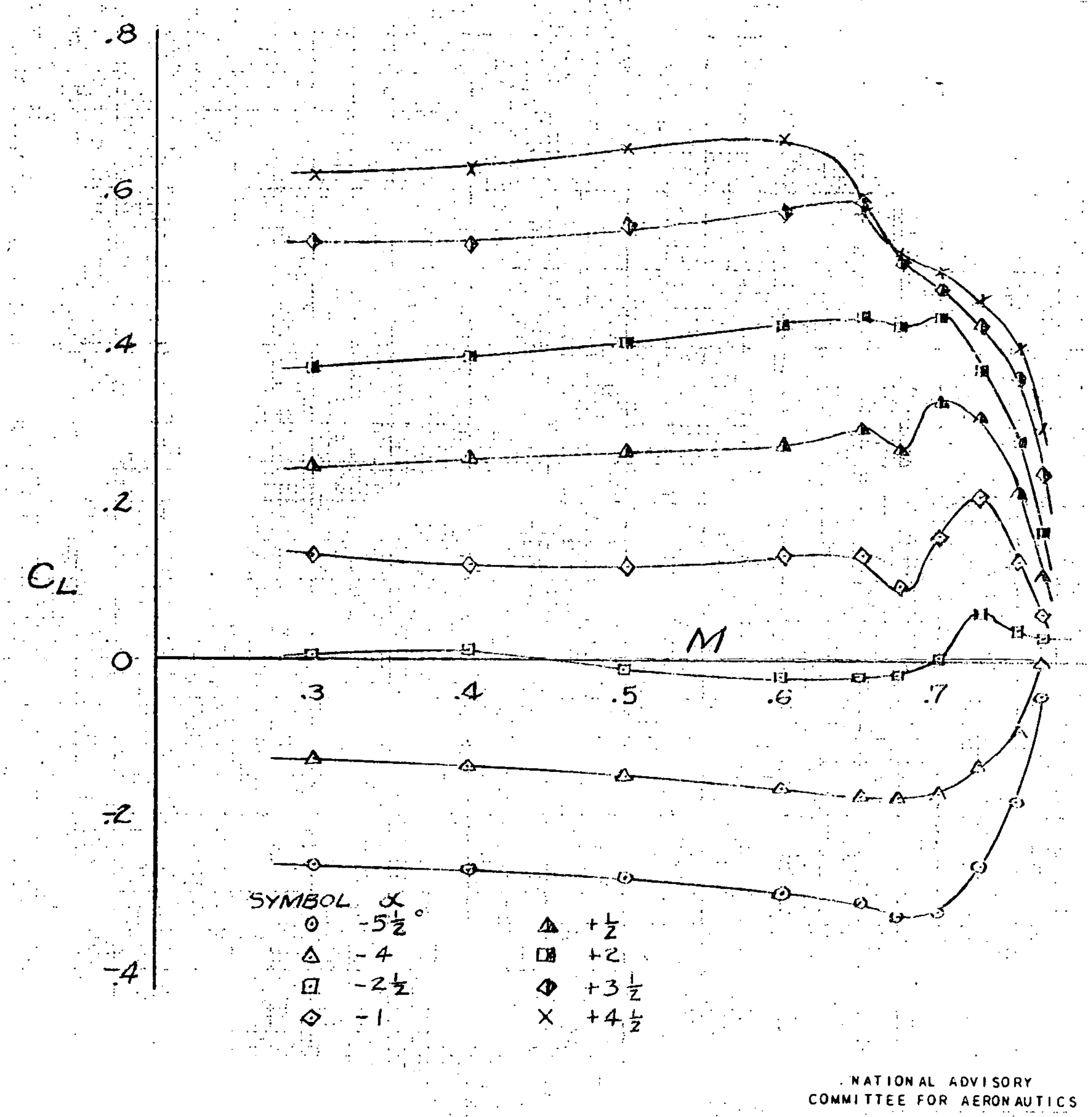

(c) Variation of C_L with Mach number at constant angles of attack.

Figure 4. - Continued. Wing and booms.

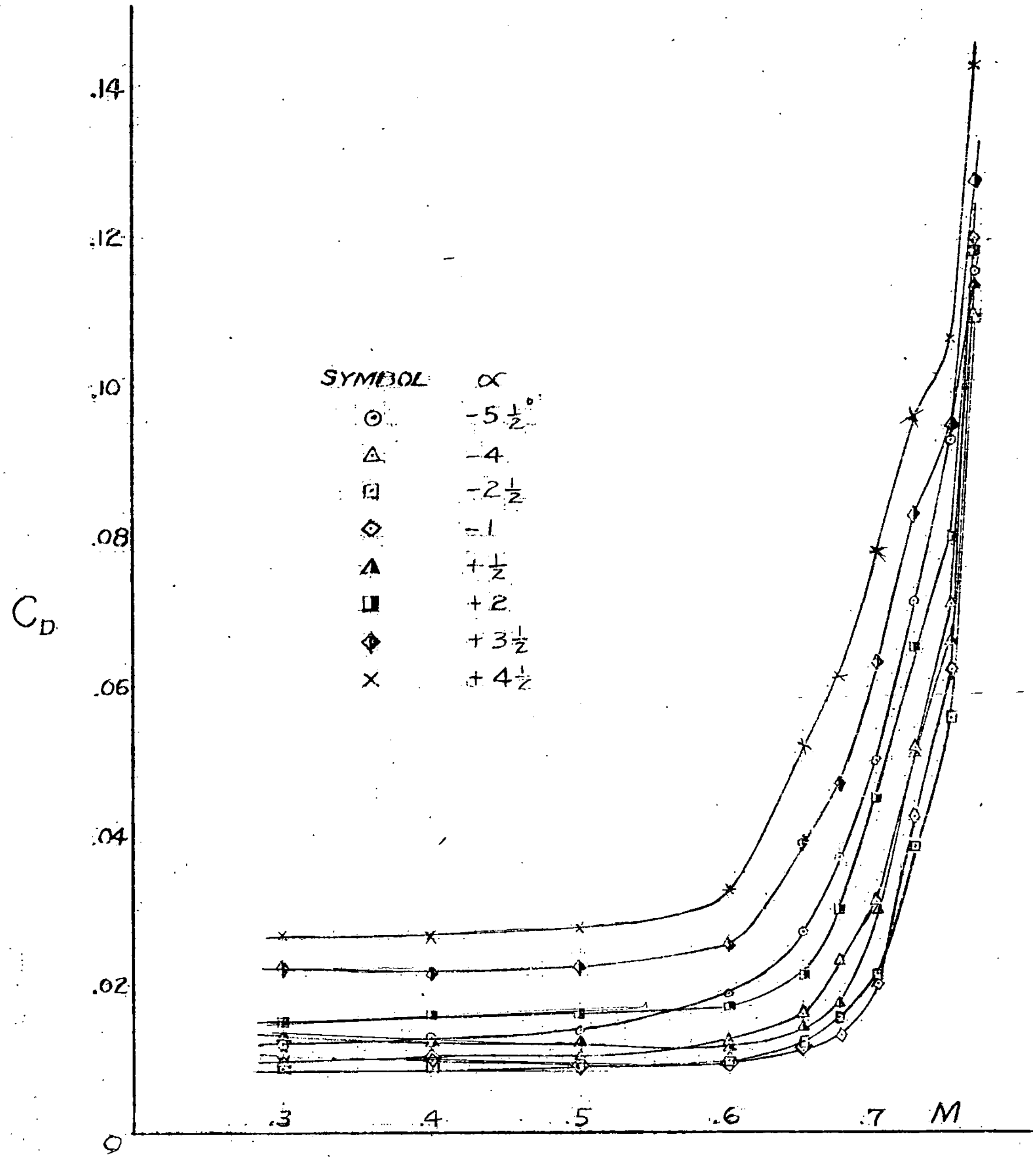

NATIONAL ADVISORY
COMMITTEE FOR AERONAUTICS

(d) Variation of C_D with Mach number at constant angles of attack.

Figure 4. - Continued. Wing and booms.

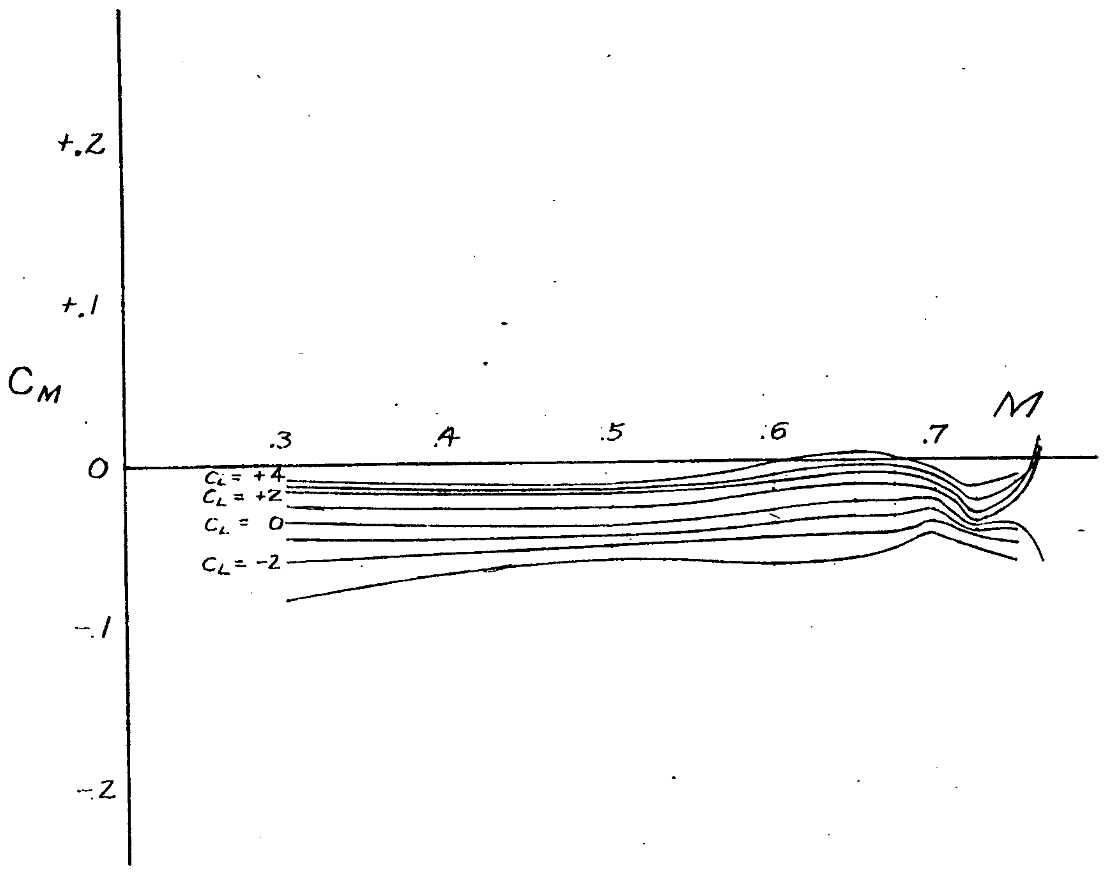

NATIONAL ADVISORY
COMMITTEE FOR AERONAUTICS

(e) Variation of C_M with Mach number at constant lift coefficients.

Figure 4. - Concluded. Wing and booms.

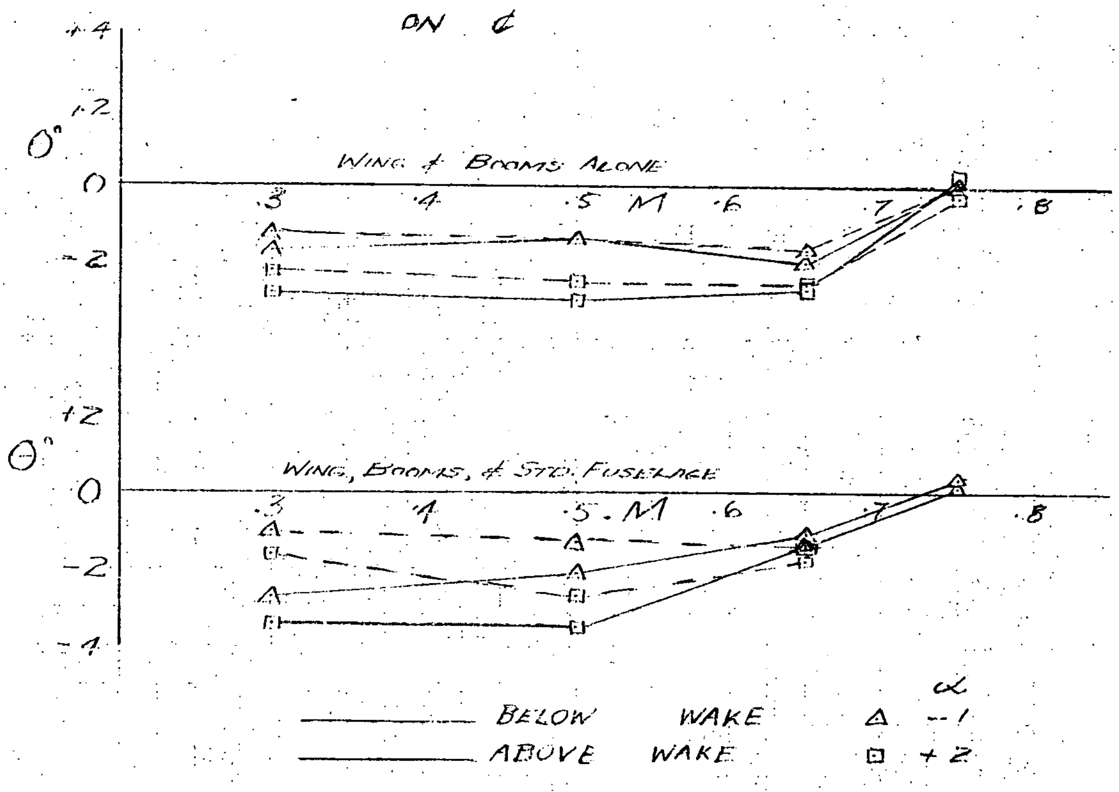

NATIONAL ADVISORY
COMMITTEE FOR AERONAUTICS

Figure 5. - Downwash angles in region of tail, wing and booms alone (runs 2 to 7) and wing, booms, and standard fuselage (runs 11 and 15).
and Standard Fuselage (Runs 11 and 15).

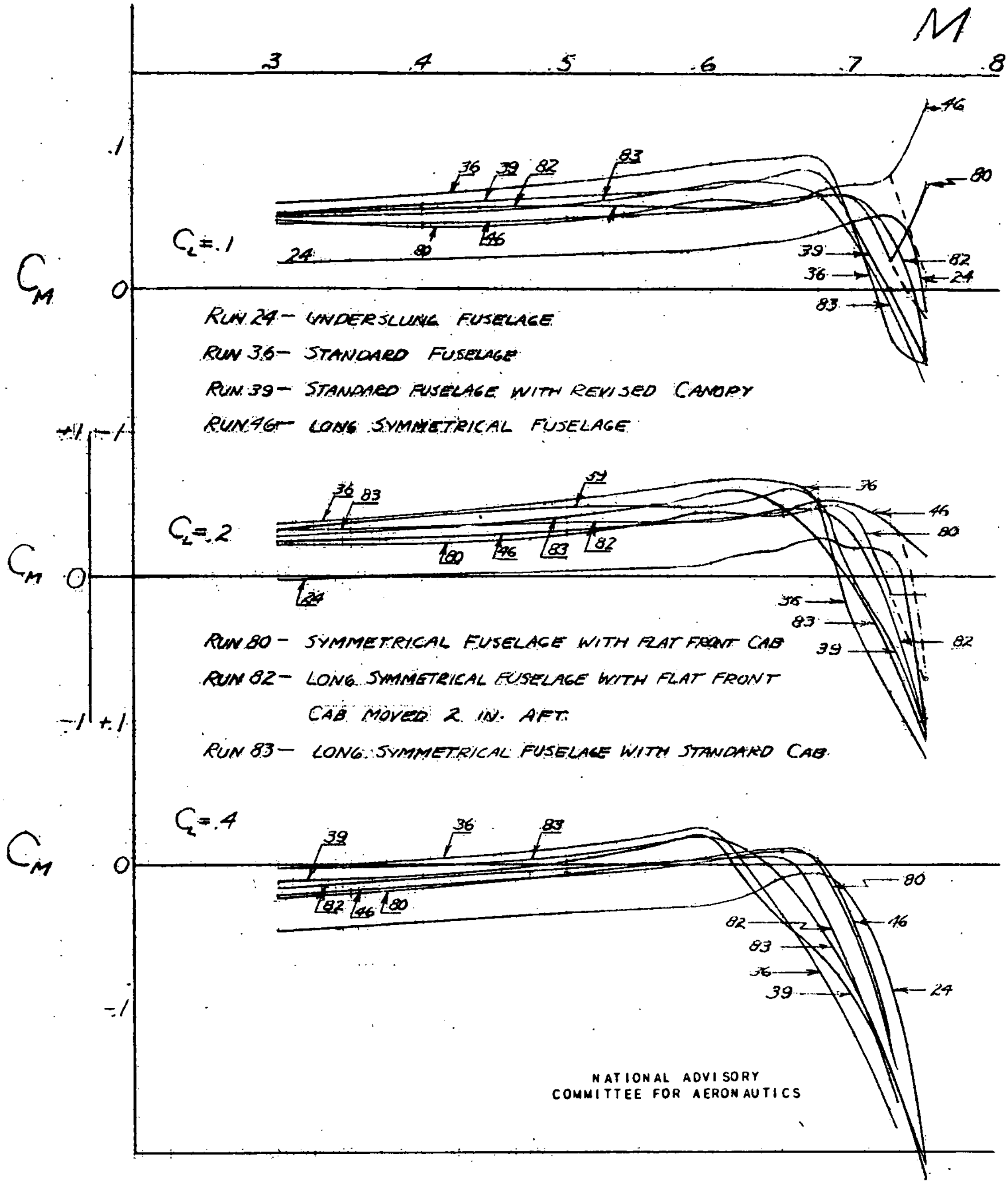

Figure 6. - Effect of fuselage shape on pitching moment at constant lift coefficients of 0.1, 0.2, and 0.4.

Page intentionally left blank

Page intentionally left blank

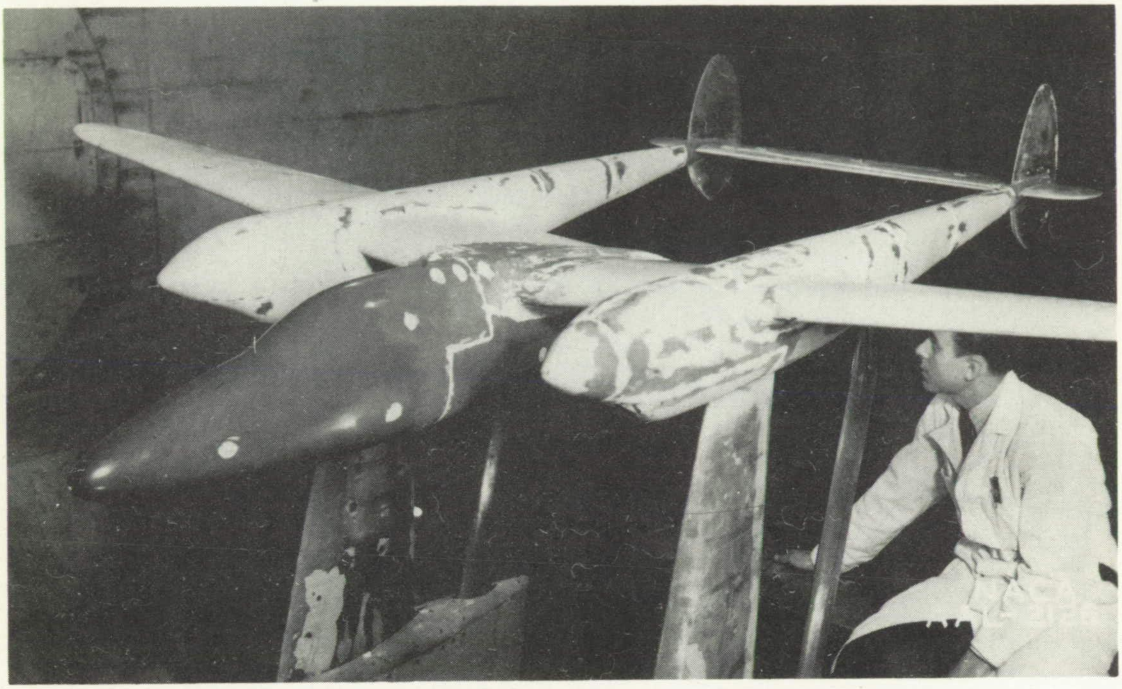

Figure 8. - Underslung elongated fuselage with tail.

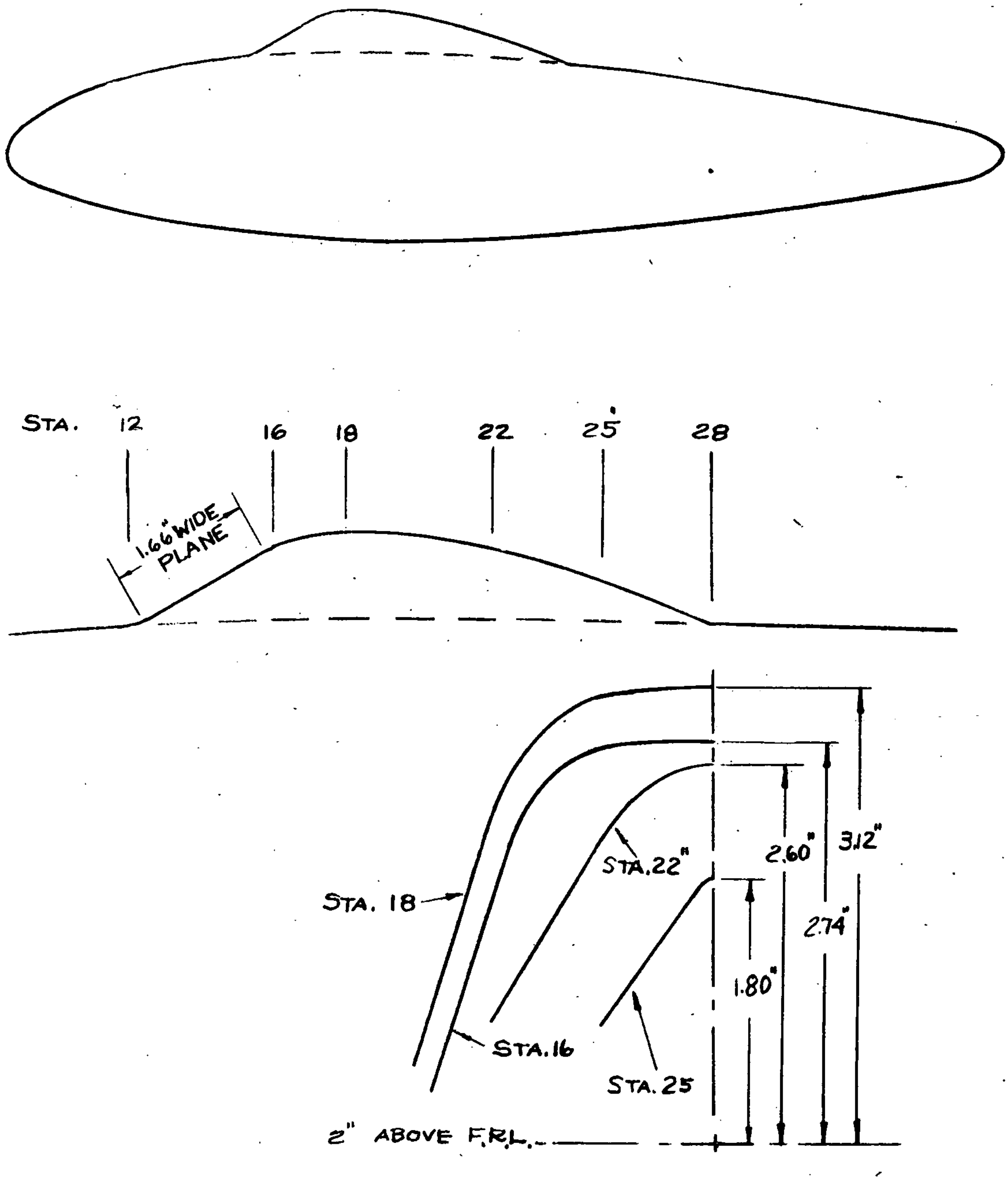

NATIONAL ADVISORY COMMITTEE FOR AERONAUTICS

Figure 9. - Flat-front cab on the long symmetrical fuselage.

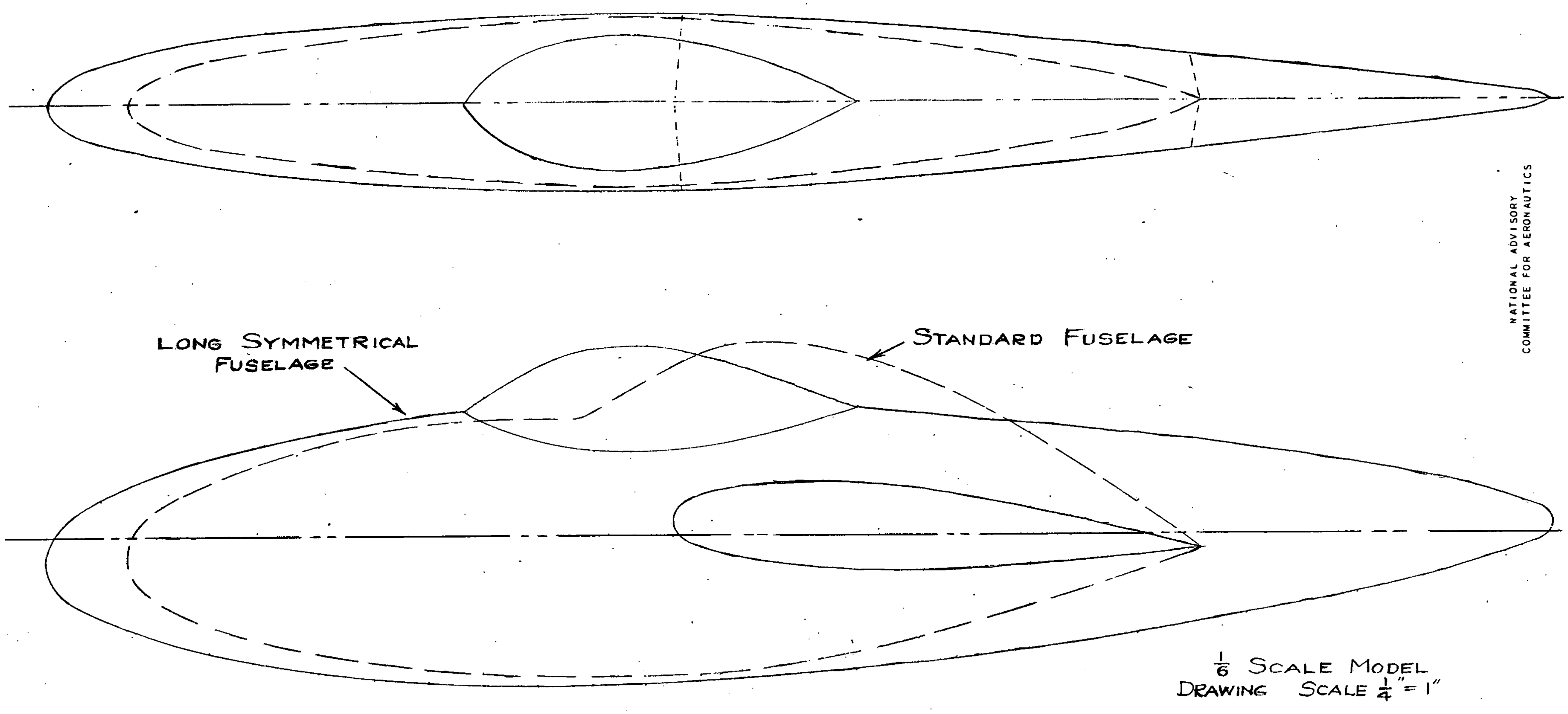

NATIONAL ADVISORY COMMITTEE FOR AERONAUTICS

Figure 7. - Relative shapes and positions of the standard and long symmetrical fuselages.

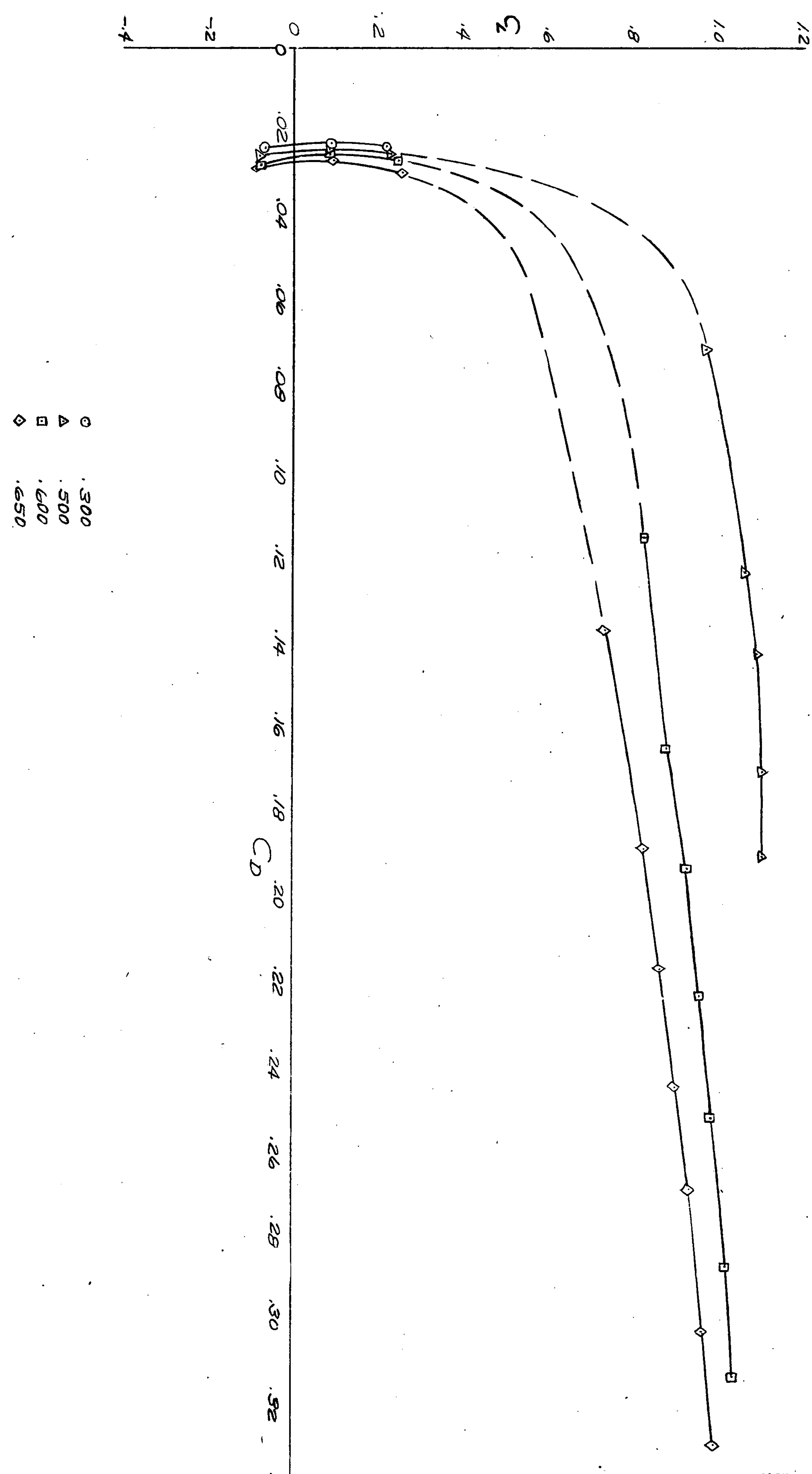

NATIONAL ADVISORY
COMMITTEE FOR AERONAUTICS

(a) Basic data from Mach number 0.300 to 0.650.

Figure 10. - Wing, booms, long symmetrical fuselage, tail and all accessories.

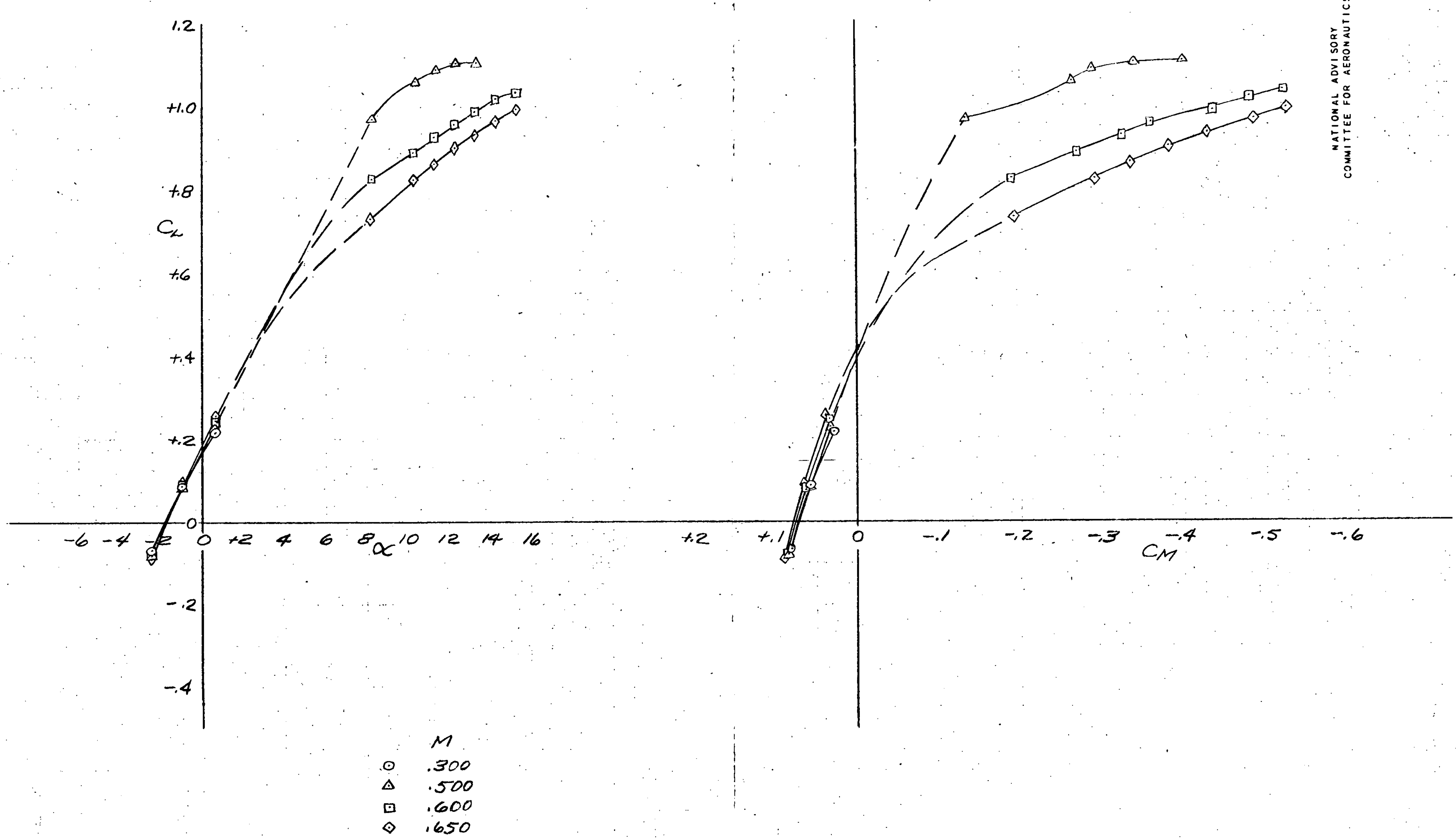

NATIONAL ADVISORY COMMITTEE FOR AERONAUTICS

(a) Concluded. Basic data from Mach number 0.300 to 0.650.

Figure 10. - Continued. Wing, booms, long symmetrical fuselage, tail and all accessories.

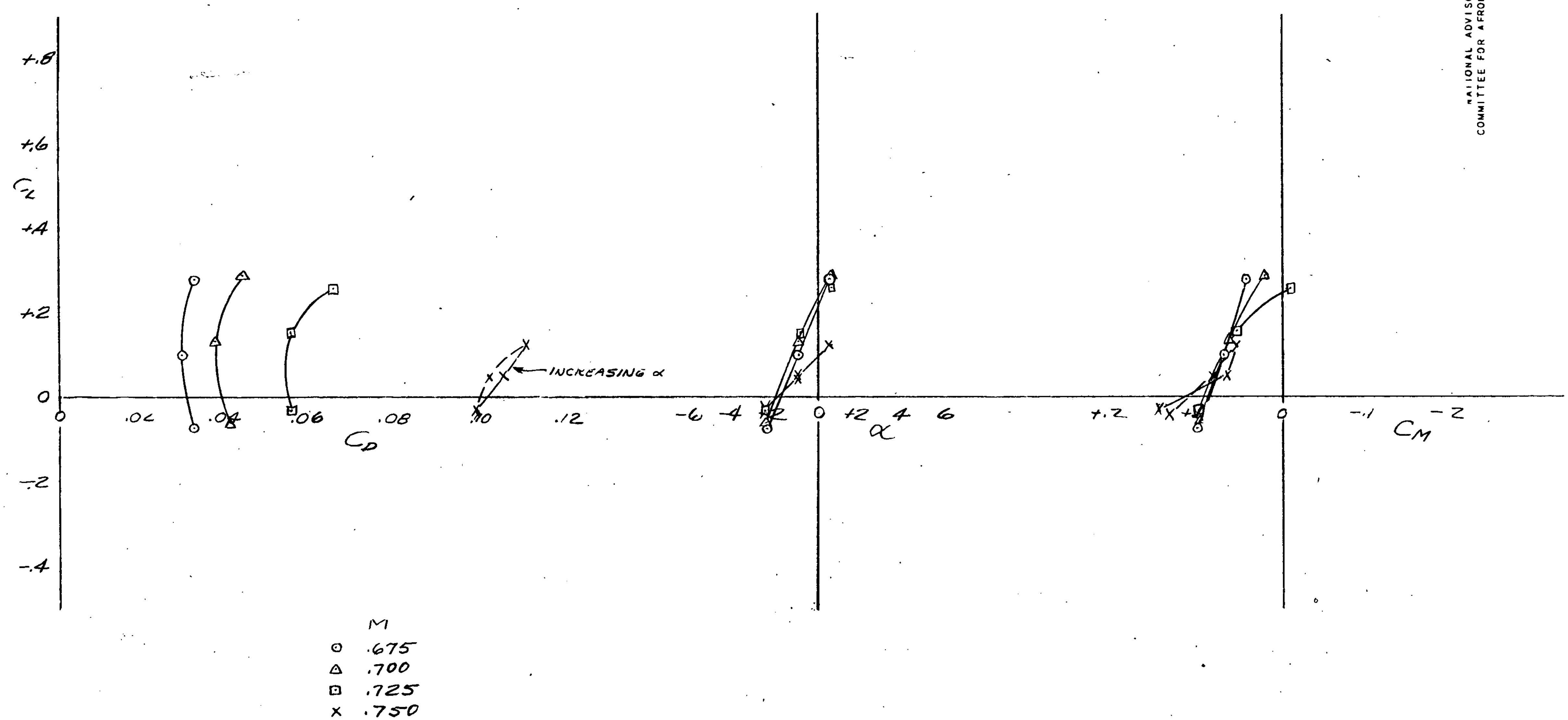

NATIONAL ADVISORY
COMMITTEE FOR AERONAUTICS

(b) Basic data from Mach number 0.675 to 0.750.

Figure 10. - Continued. Wing, booms, long symmetrical fuselage, tail and all accessories.

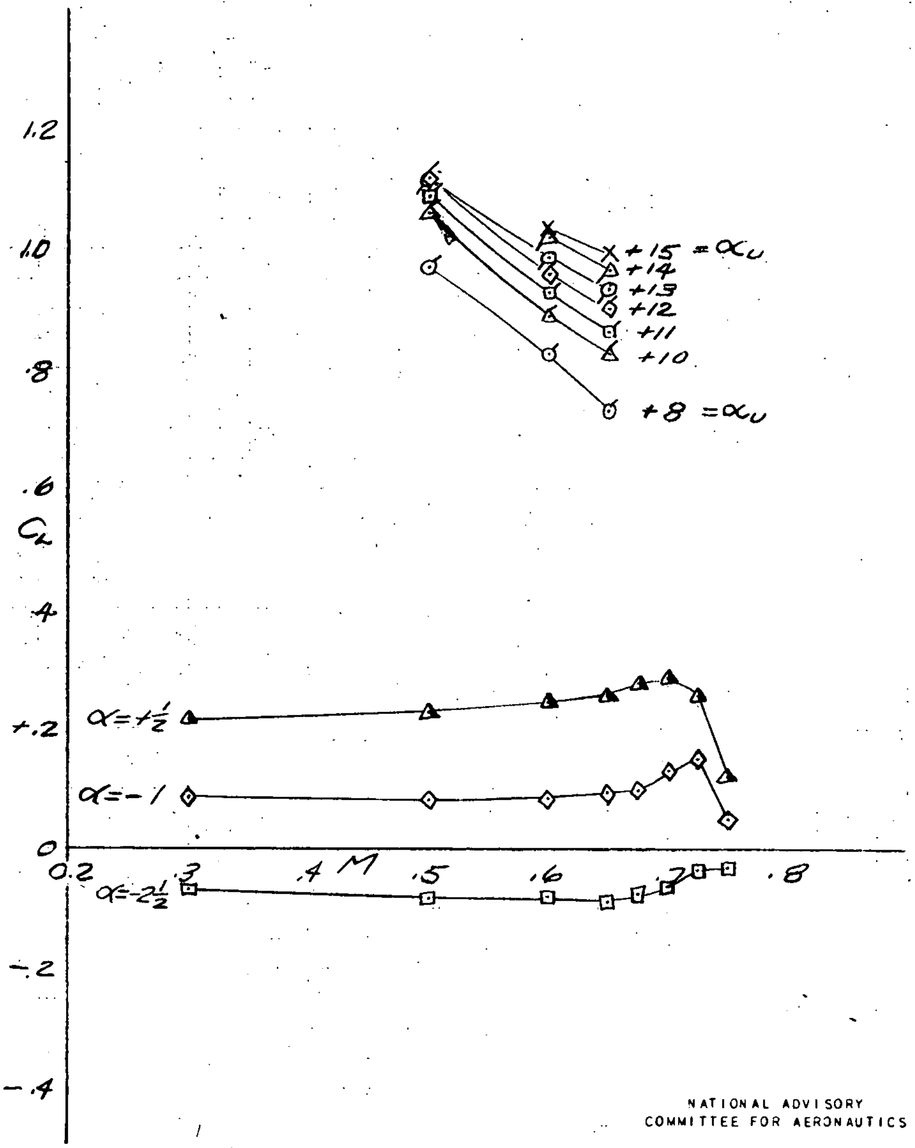

(c) Variation of C_L with Mach number at constant angles of attack.

Figure 10. - Continued. Wing, booms, long symmetrical fuselage, tail and all accessories.

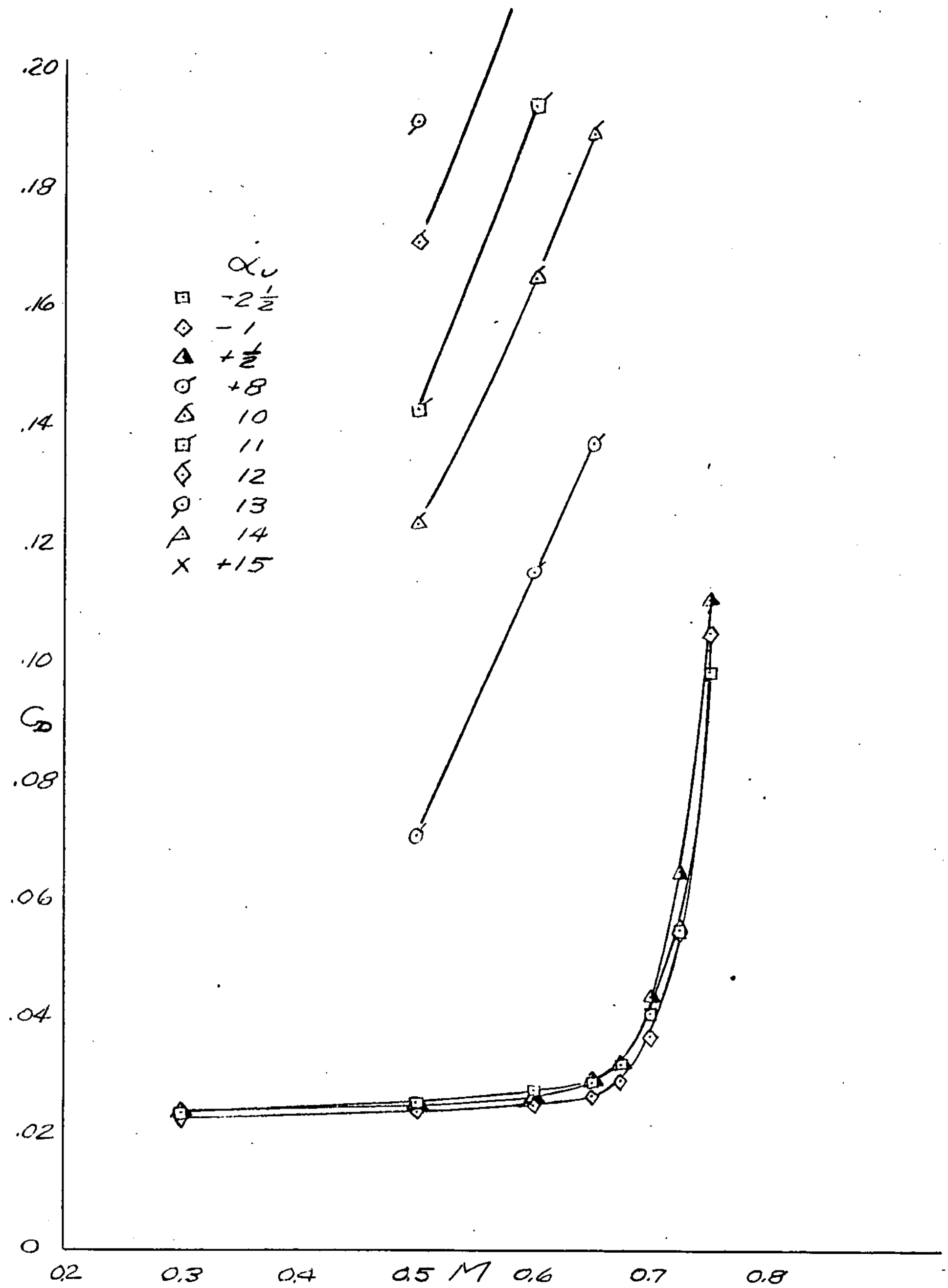

NATIONAL ADVISORY
COMMITTEE FOR AERONAUTICS

(d) Variation of C_D with Mach number at constant angles of attack.

Figure 10. - Continued. Wing, booms, long symmetrical fuselage, tail and all accessories.

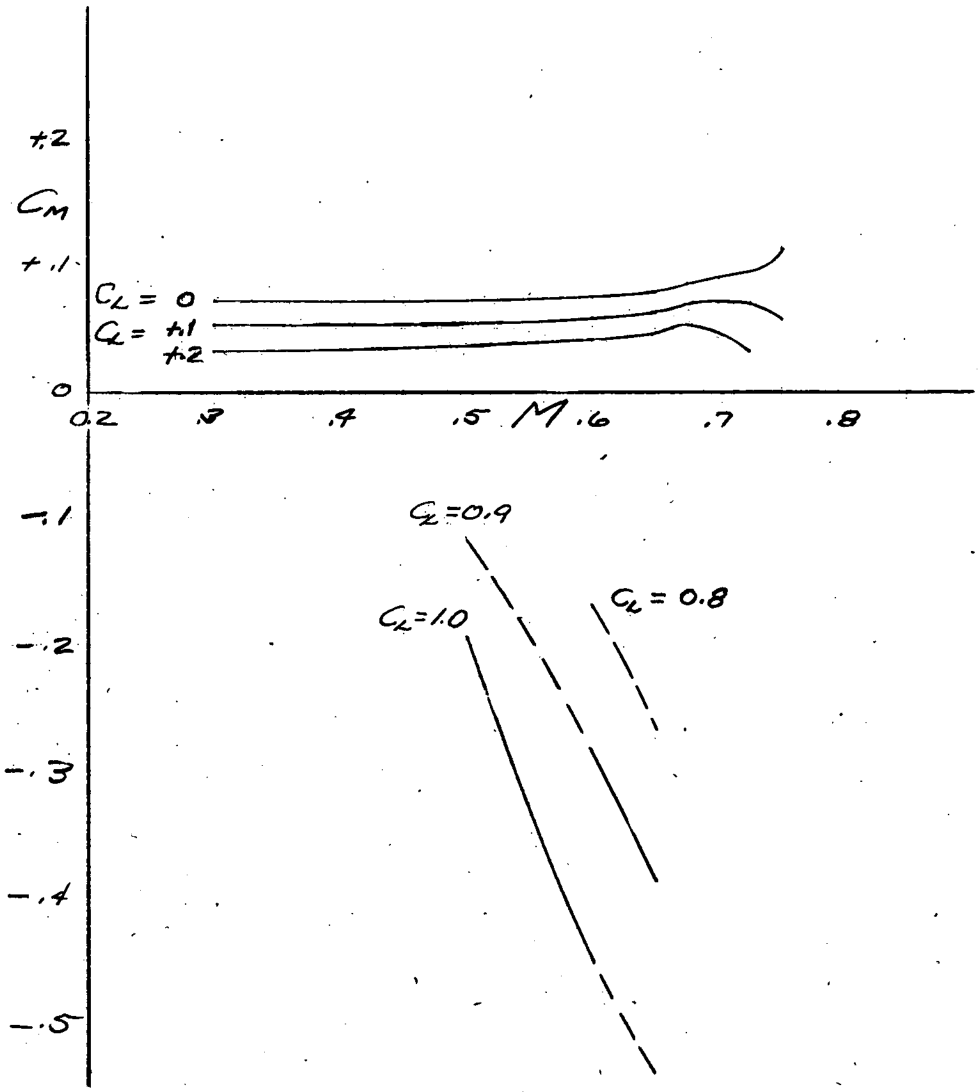

NATIONAL ADVISORY
COMMITTEE FOR AERONAUTICS

(e) Variation of C_M with Mach number at constant lift coefficients.

Figure 10. - Concluded. Wing, booms, long symmetrical fuselage, tail, and all accessories.

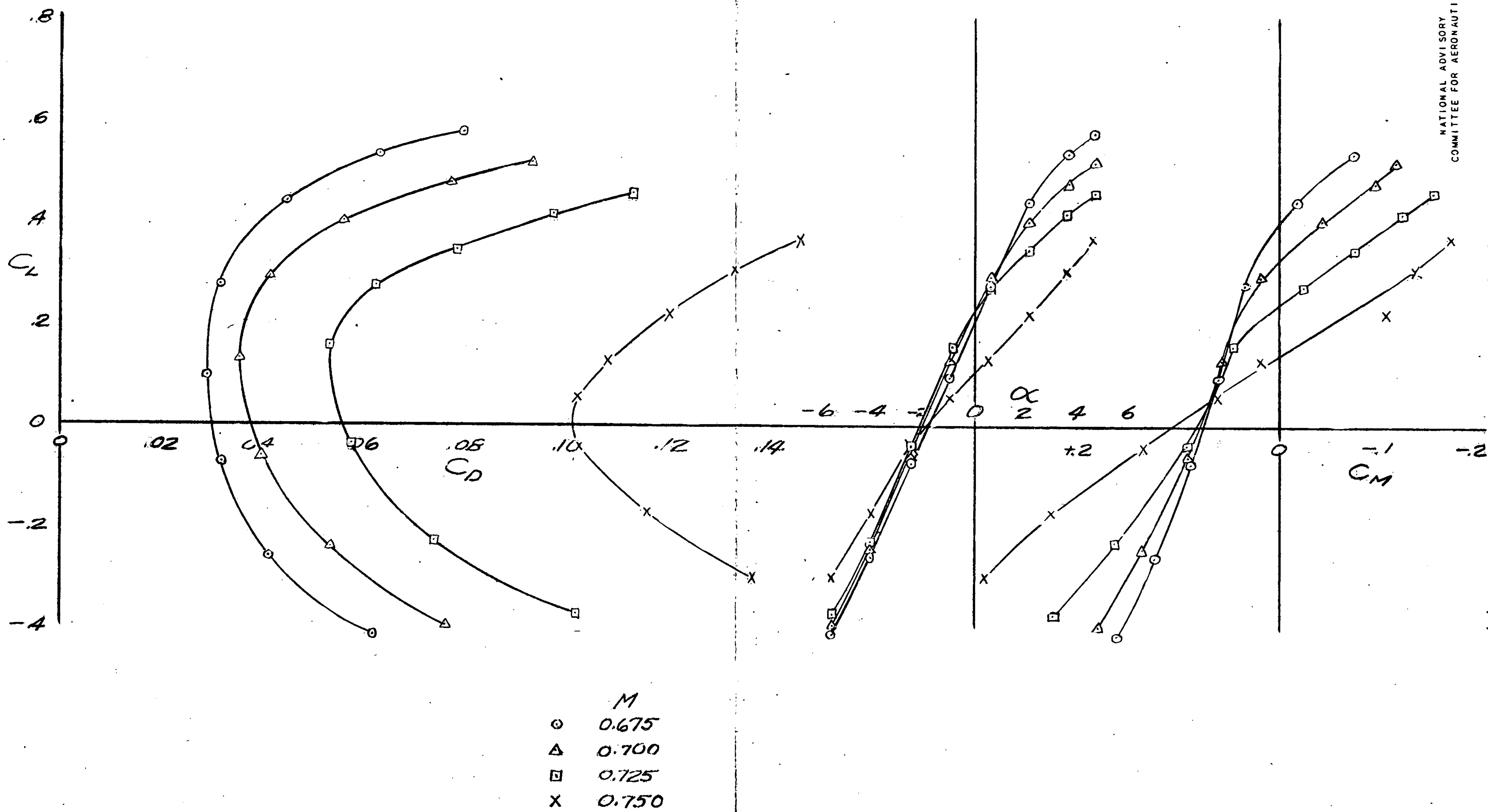

NATIONAL ADVISORY
COMMITTEE FOR AERONAUTICS

(b) Basic data from Mach number 0.675 to 0.750.

Figure 11. - Continued. Wing, booms, long symmetrical fuselage, tail, all accessories, and modified Prestone scoops.

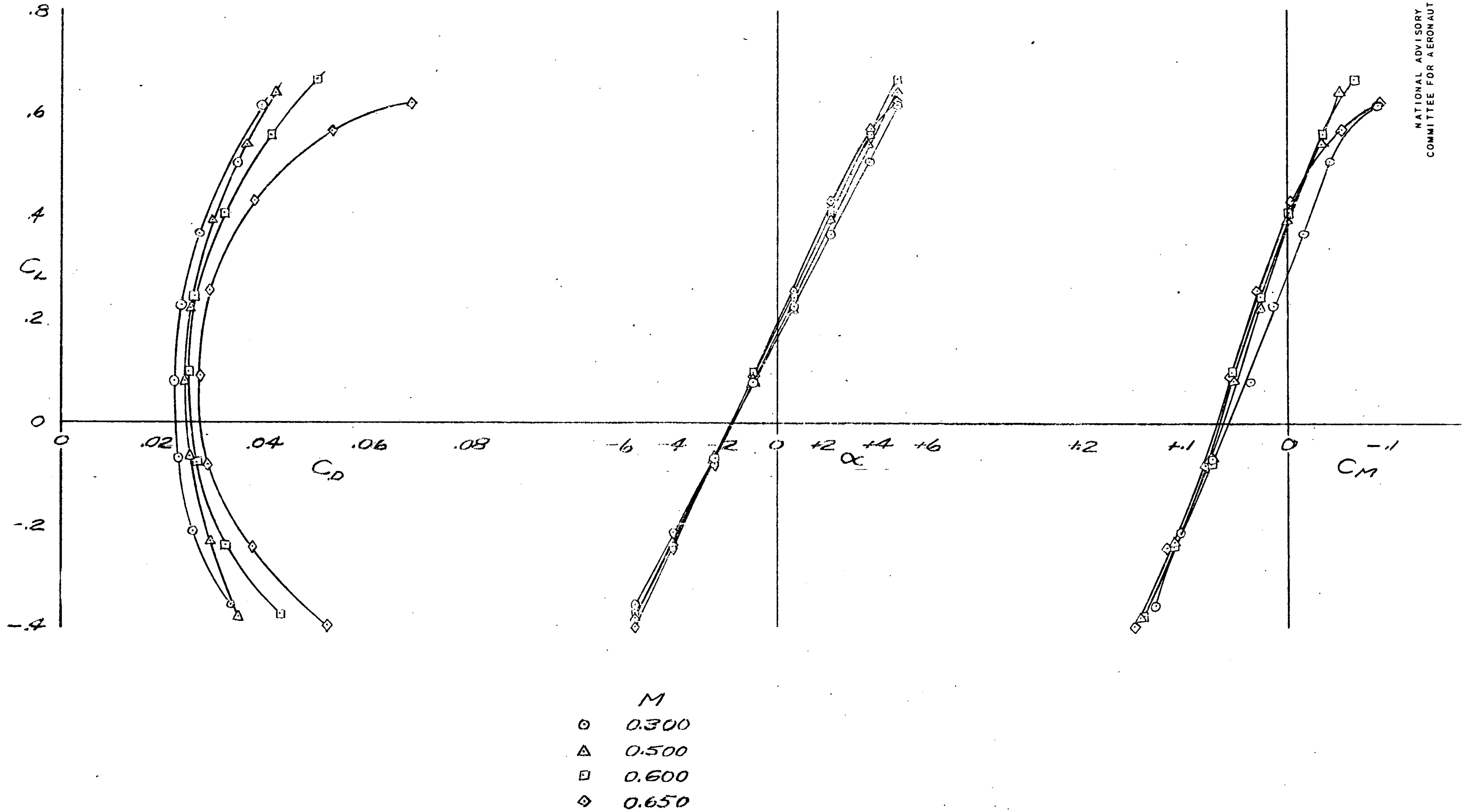

NATIONAL ADVISORY
COMMITTEE FOR AERONAUTICS

(a) Basic data from Mach number 0.300 to 0.650.

Figure 11. - Wing, booms, long symmetrical fuselage, tail, all accessories, and modified Prestone scoops.

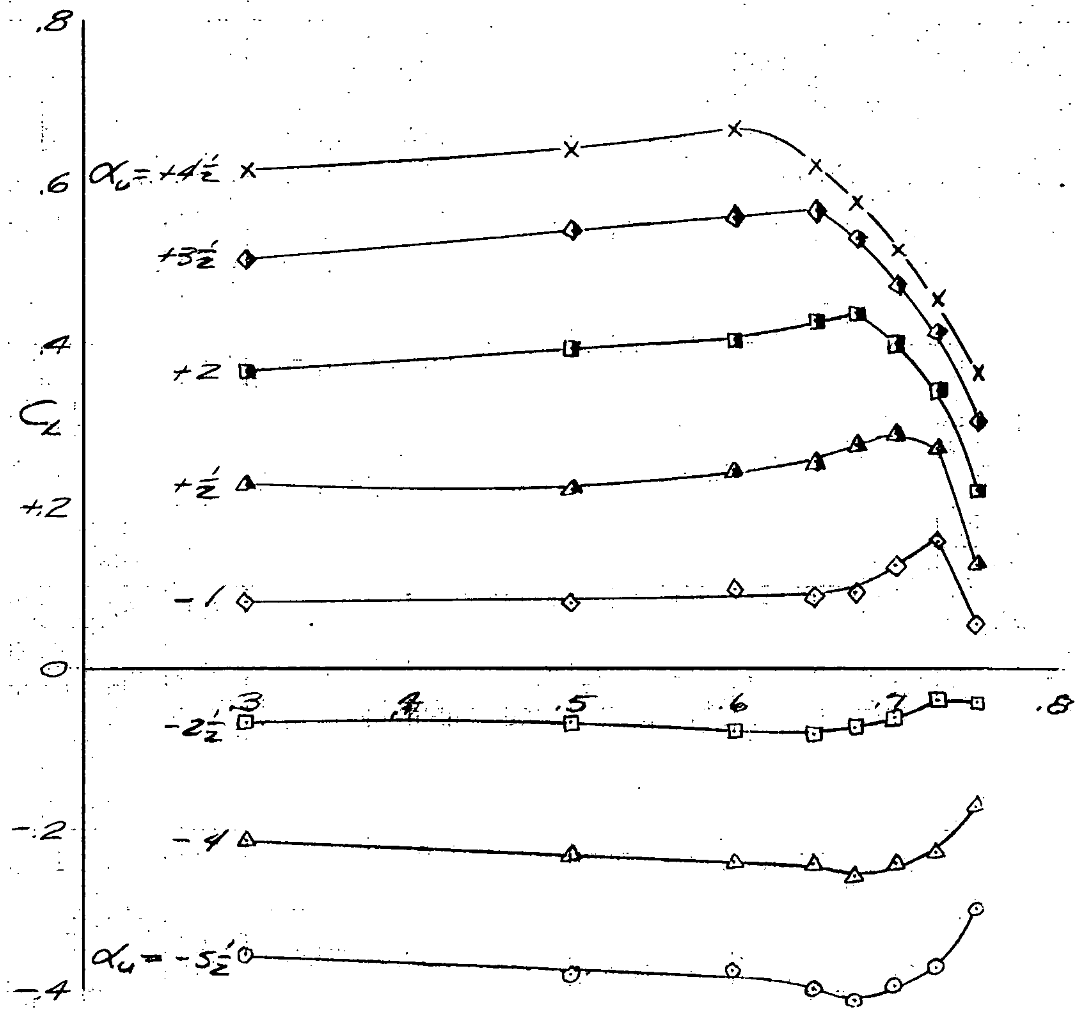

(c) Variation of C_L with Mach number at constant angles of attack.

Figure 11. - Continued. Wing, booms, long symmetrical fuselage, tail, all accessories, and modified Prestone scoops.

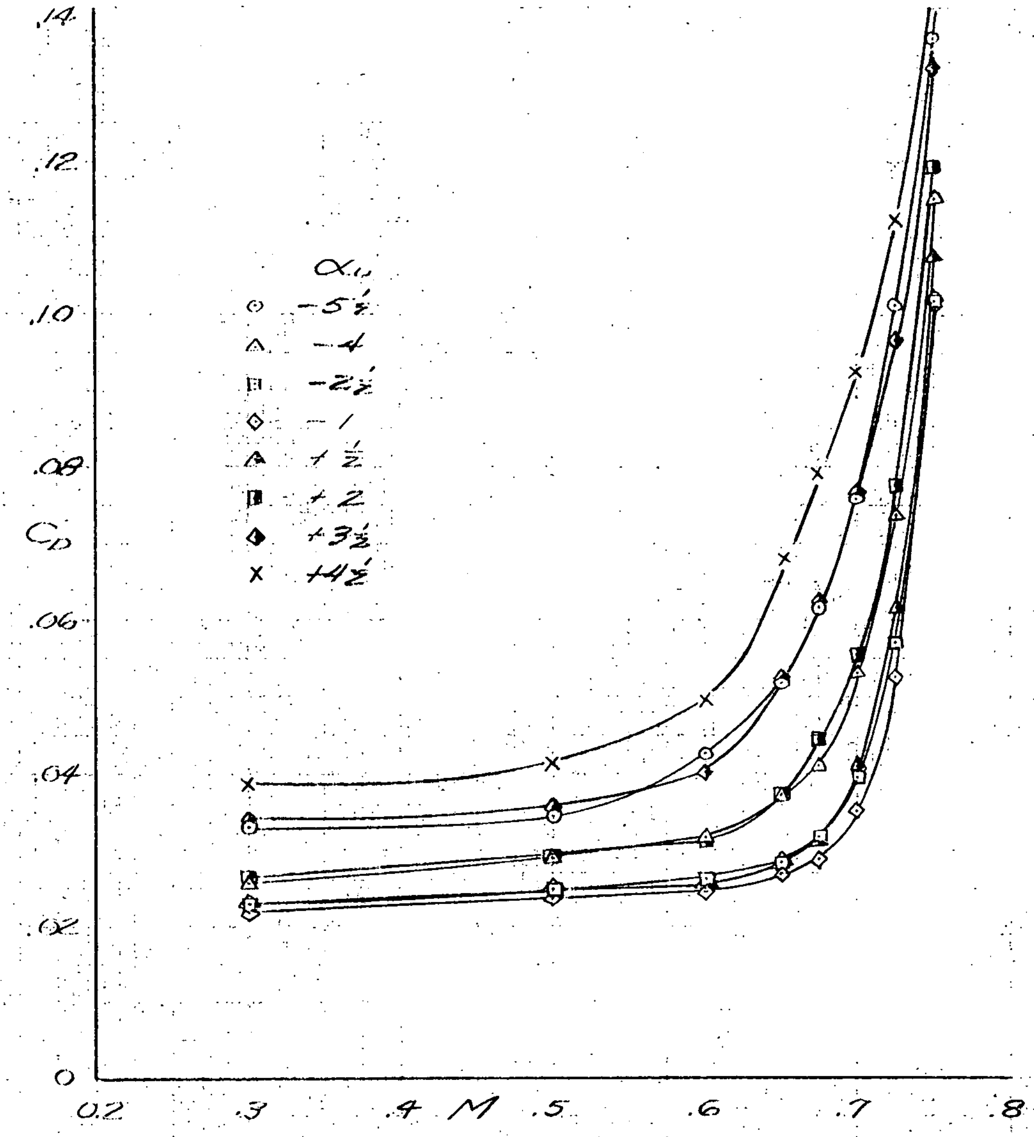

NATIONAL ADVISORY
COMMITTEE FOR AERONAUTICS

(d) Variation of C_D with Mach number at constant angles of attack.

Figure 11. - Continued. Wing, booms, long symmetrical fuselage, tail, all accessories, and modified Prestone scoops.

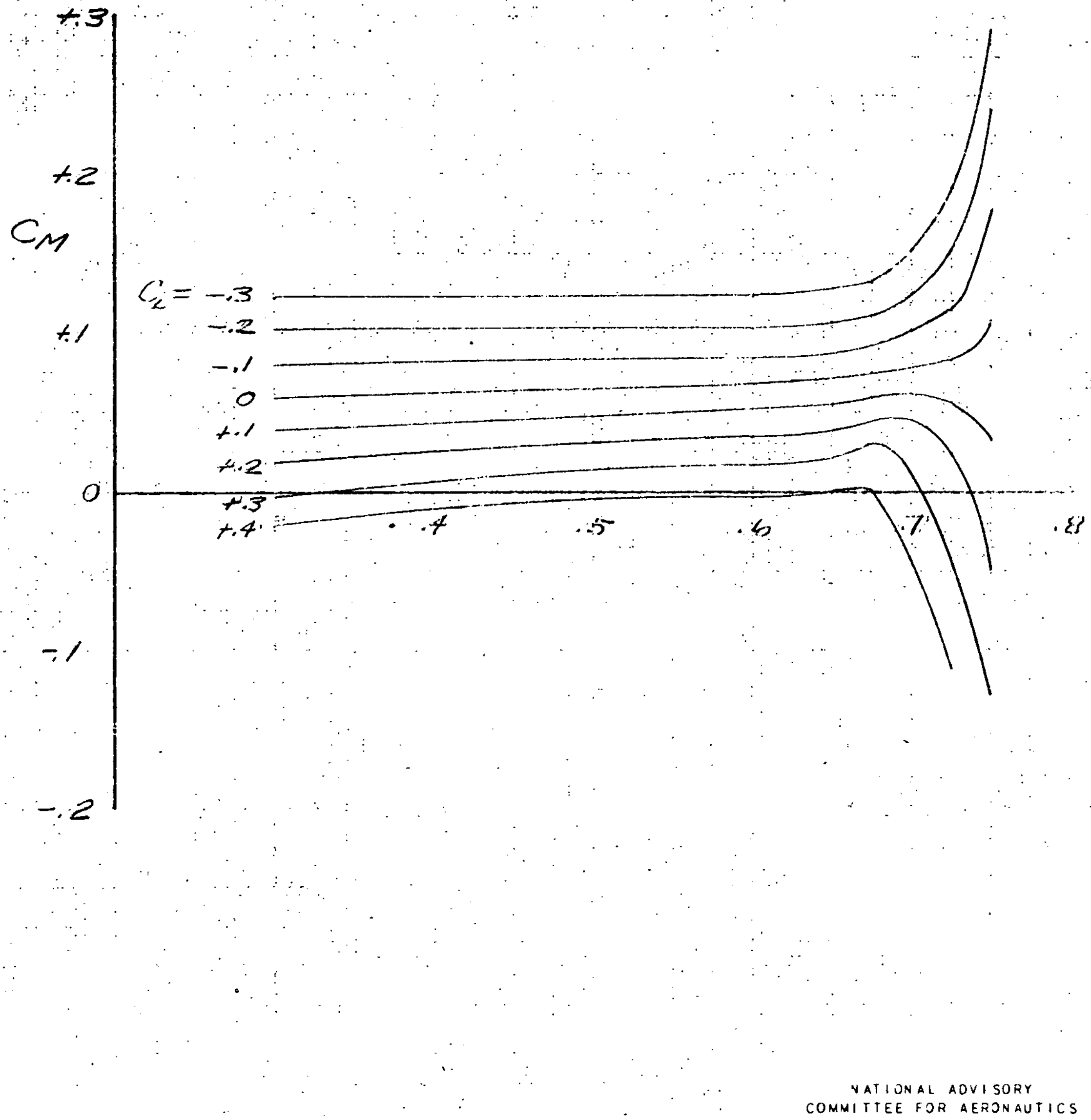

(e) Variation of C_M with Mach number at constant lift coefficients.

Figure 11. - Concluded. Wing, booms, long symmetrical fuselage, tail, all accessories, and modified Prestone scoops.

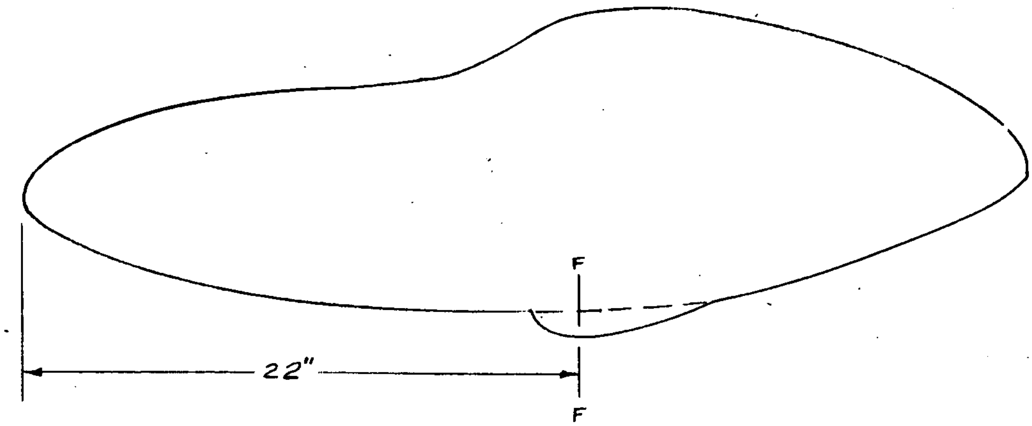

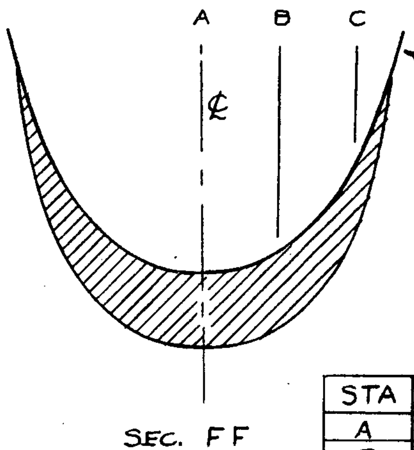

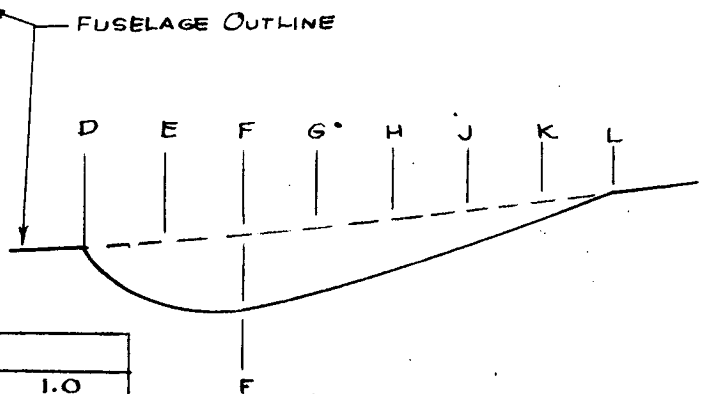

STA	
A	1.0
B	1.0
C	1.0
D	0
E	0.85
FF	1.0
G	0.85
H	0.65
J	0.40
K	0.20
L	0

DIMENSIONS ARE INCHES FROM FUSELAGE SURFACE. STATIONS ARE 1" APART

NATIONAL ADVISORY COMMITTEE FOR AERONAUTICS

Figure 12. - Bump on bottom of standard fuselage with revised canopy.

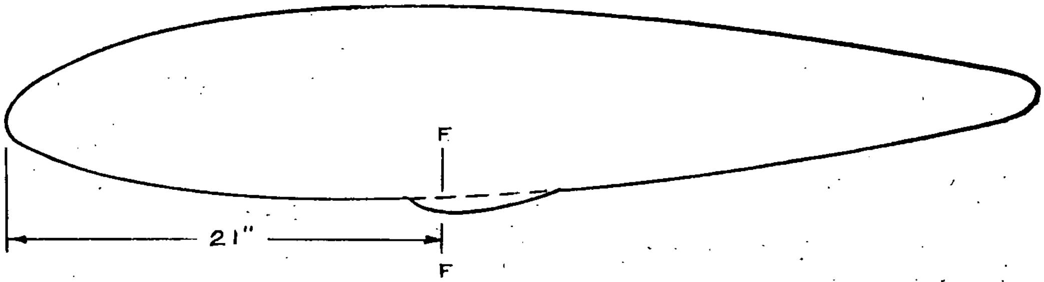

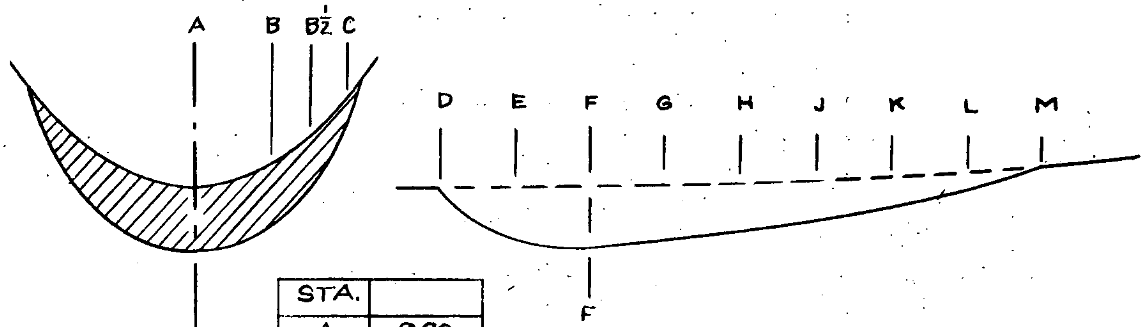

STA.	
A	0.80
B	0.80
B½	0.70
C	0.50
D	0
E	0.65
FF	0.80
G	0.70
H	0.63
J	0.50
K	0.37
L	0.22
M	0

DIMENSIONS ARE INCHES FROM FUSELAGE SURFACE
STATIONS ARE 1" APART

NATIONAL ADVISORY
COMMITTEE FOR AERONAUTICS

Figure 13. - Bump on bottom of long symmetrical fuselage without cab.

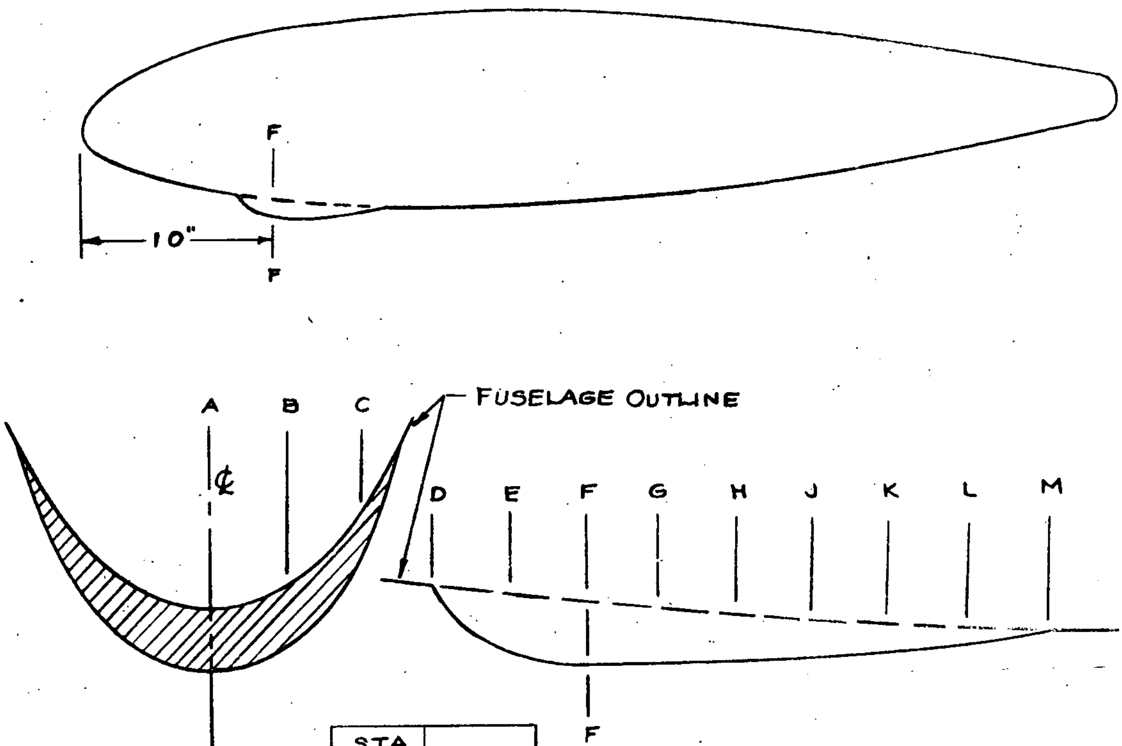

STA.	
A	0.80
B	0.80
C	0.60
D	0
E	0.75
FF	0.80
G	0.70
H	0.60
J	0.47
K	0.37
L	0.25
M	0

DIMENSIONS ARE INCHES FROM FUSELAGE SURFACE. STATIONS ARE 1" APART

NATIONAL ADVISORY COMMITTEE FOR AERONAUTICS

Figure 14. - Bump forward on long symmetrical fuselage without cab.

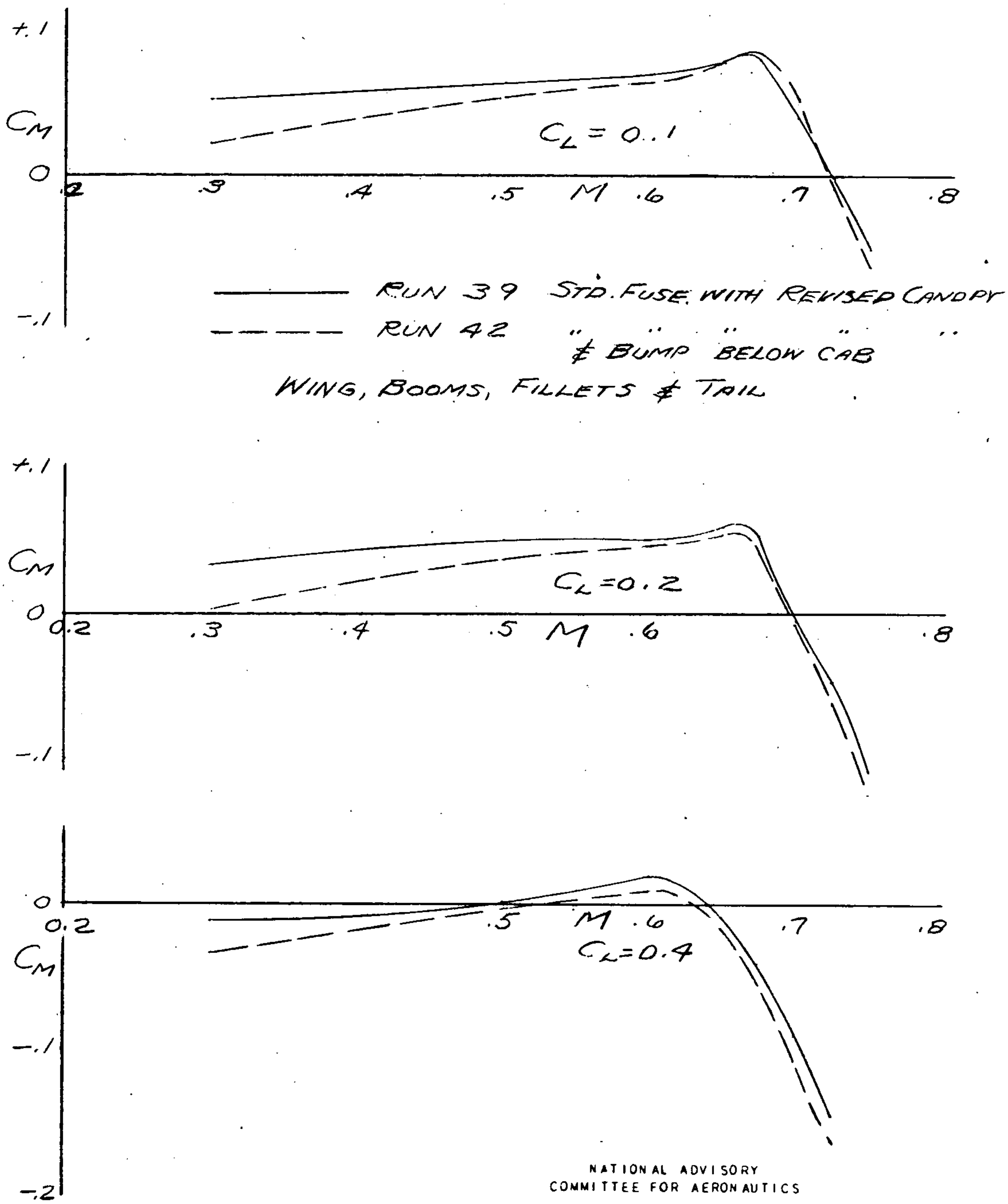

Figure 15. - Standard fuselage with revised canopy. Comparison curves showing effect of bump on bottom of fuselage. (See fig. 12.)

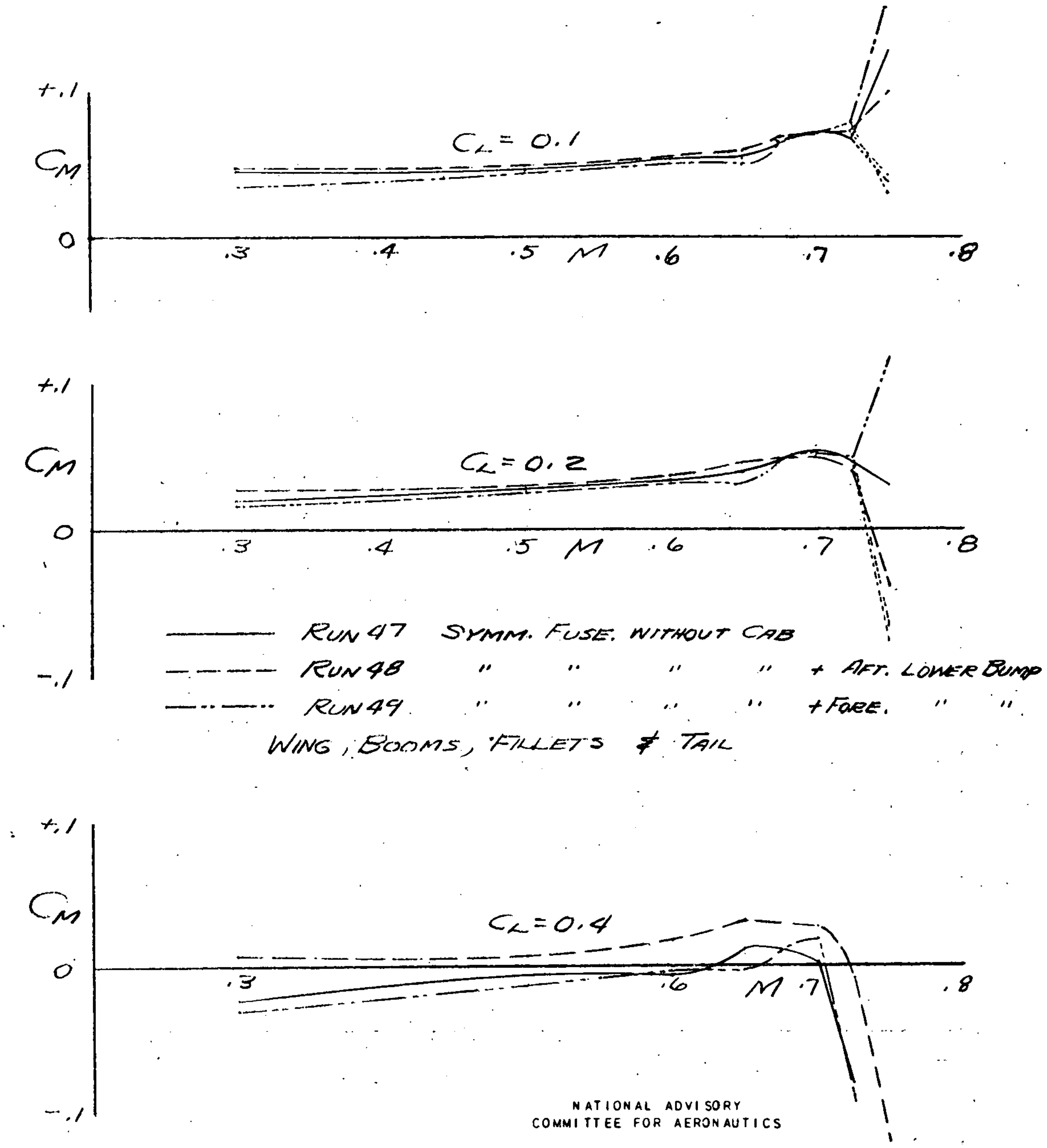

Figure 16. - Symmetrical fuselage without cab. Comparison curves showing effect of bump on bottom of fuselage. (See figs. 13 and 14.)

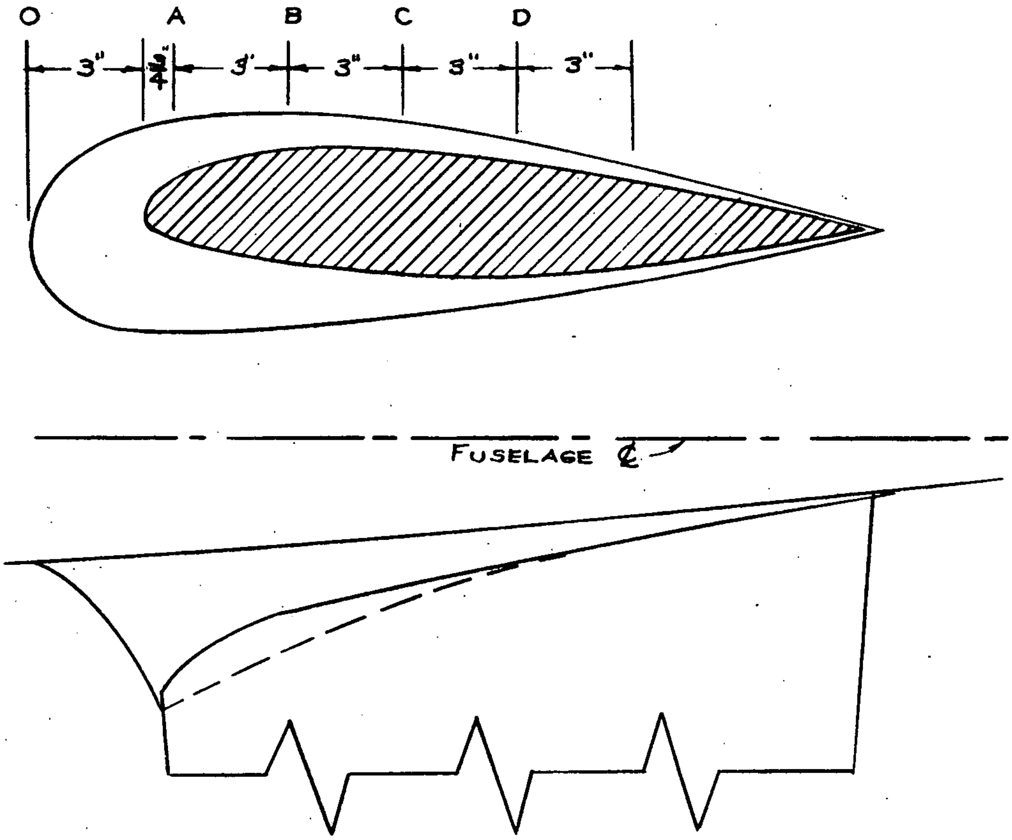

STA.	UPPER FILLET		LOWER FILLET	
	VERT.	HORIZ.	VERT.	HORIZ.
O	—	0	—	0
A	1.7	3.4	2.5	4.1
B	1.1	1.6	1.5	3.1
C	1.1	1.5	0.9	1.5
D	0.7	0.8	0.7	1.1
E	0.5	0.5	0.5	0.5

NATIONAL ADVISORY
COMMITTEE FOR AERONAUTICS

Figure 17. - Symmetrical fuselage. Leading-edge fillet with leading edge turned down.

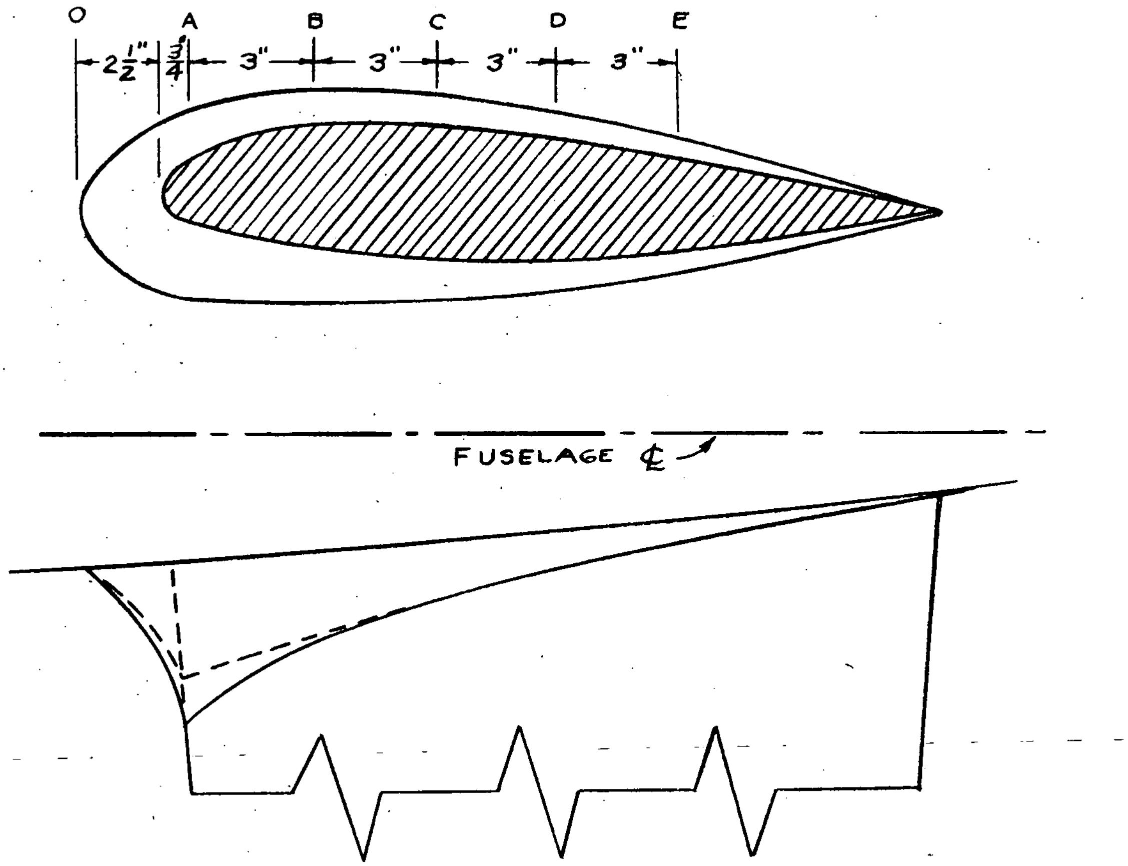

STA	UPPER FILLET		LOWER FILLET	
	VERT.	HORIZ.	VERT.	HORIZ
O	0	0	0	0
A	1.2	3.7	1.9	2.5
B	1.1	2.1	1.3	1.9
C	1.1	1.5	0.9	1.3
D	0.7	0.8	0.7	1.1
E	0.5	0.5	0.5	0.6

DIMENSIONS ARE INCHES FROM WING AND FUSELAGE SURFACES

NATIONAL ADVISORY COMMITTEE FOR AERONAUTICS

Figure 18. - Symmetrical fuselage. Leading-edge fillet with leading edge extended straight forward.

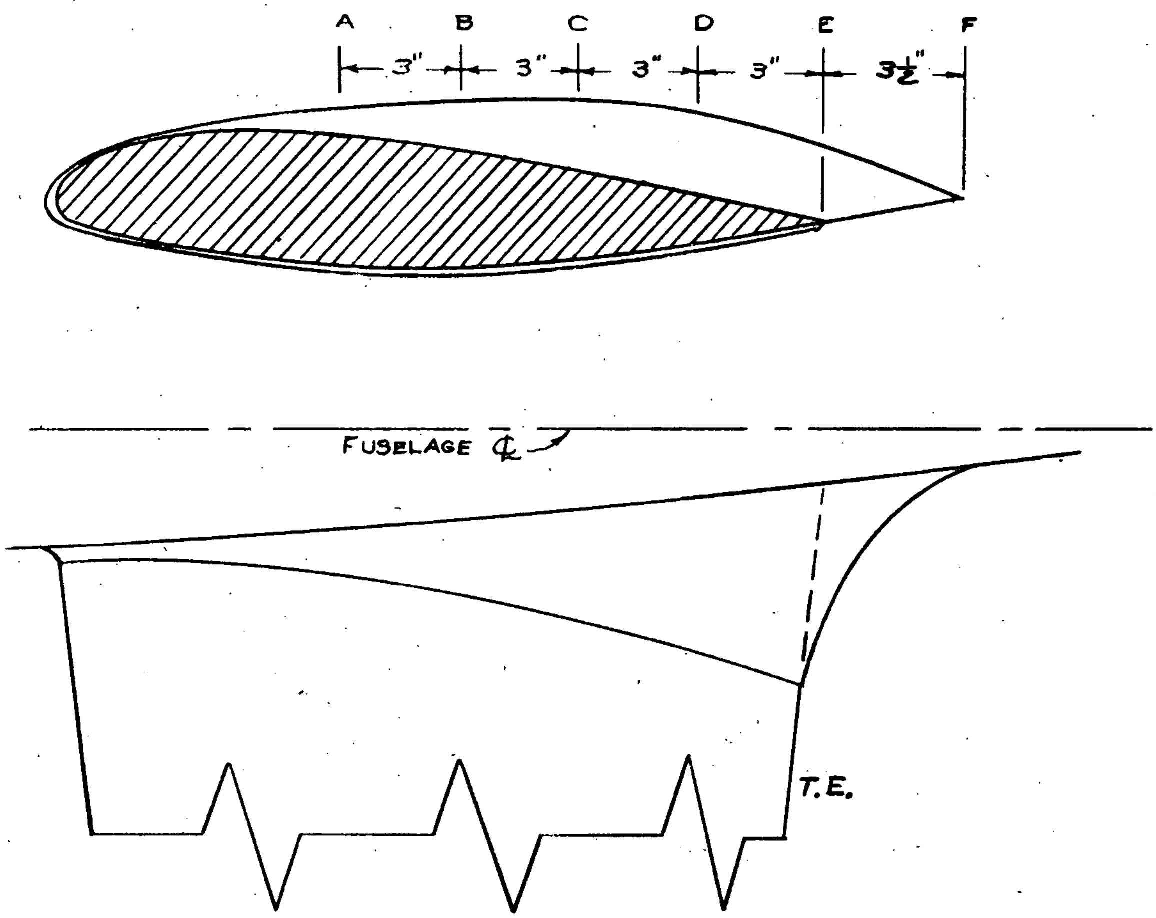

STA.	FILLET	
	VERTICAL	HORIZONTAL
A	0.6	1.1
B	1.1	1.8
C	1.6	2.7
D	1.9	3.7
E	2.1	5.0
F	—	0

DIMENSIONS ARE INCHES FROM WING & FUSELAGE SURFACES

NATIONAL ADVISORY COMMITTEE FOR AERONAUTICS

Figure 19. - Symmetrical fuselage with expanding fillet to the rear.

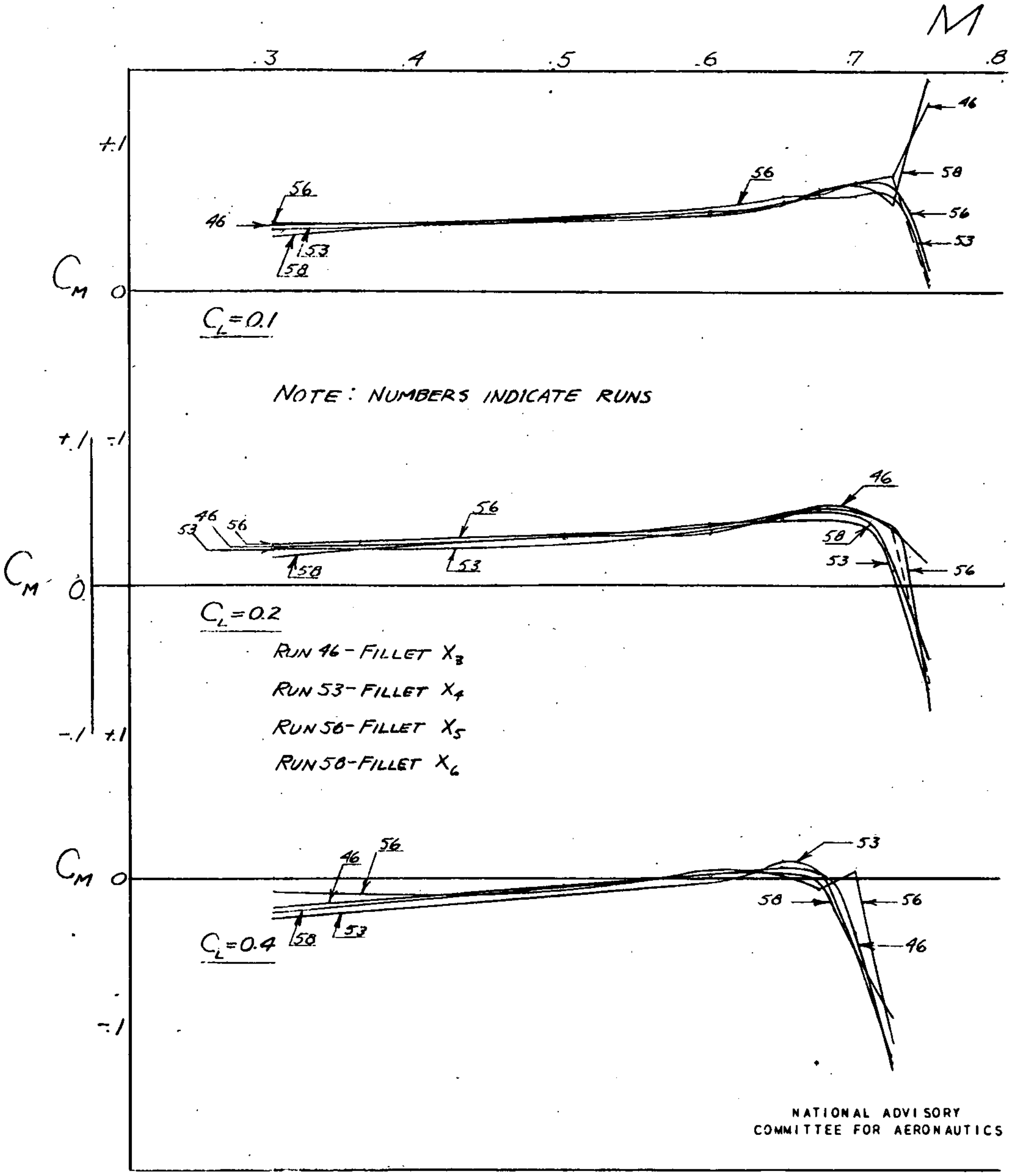

Figure 20. - Comparison of effects of various fillets on symmetrical fuselage.

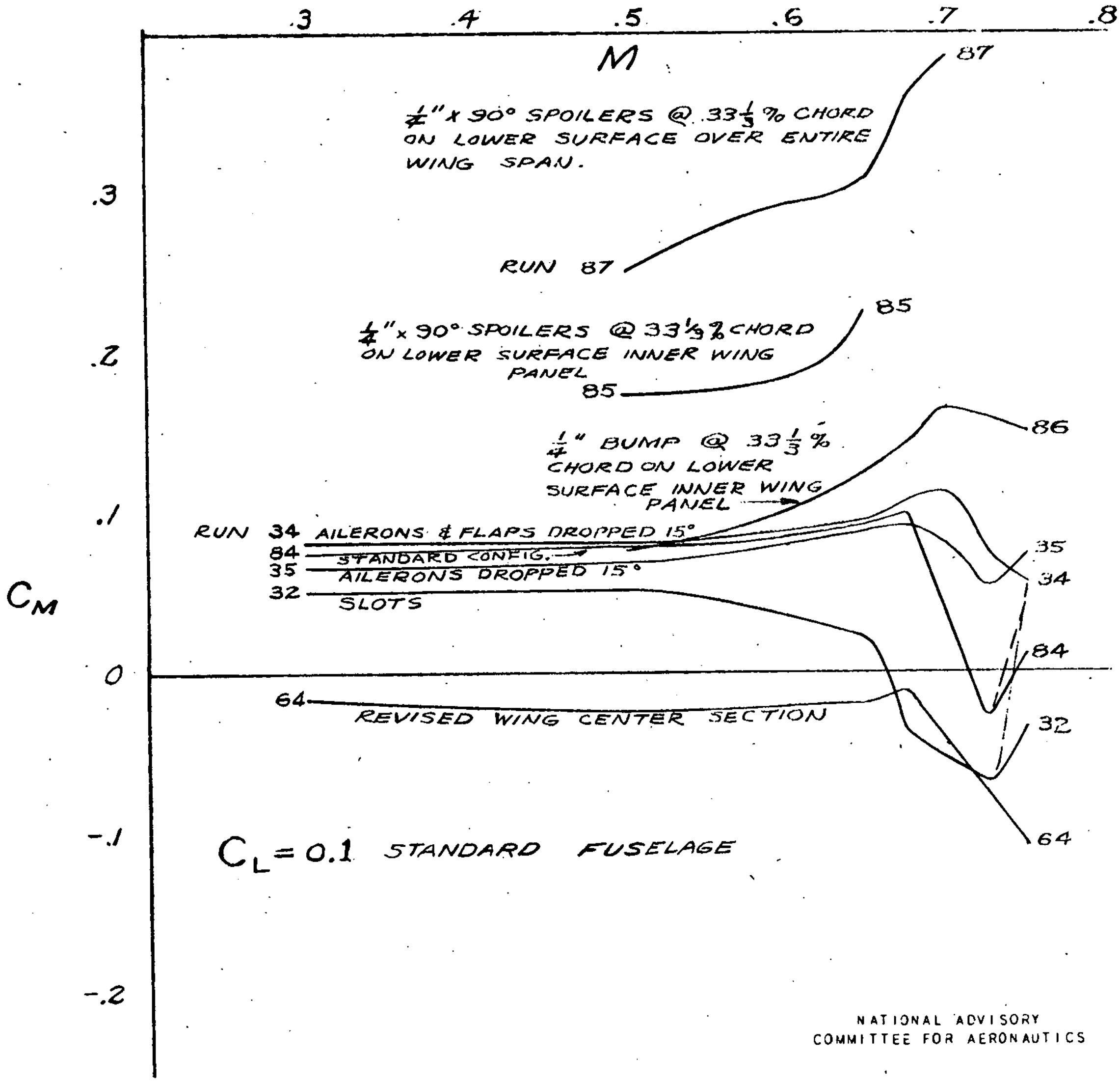

(a) $C_L = 0.1$.

Figure 21. - Effect of wing spoilers and wing bumps on pitching moments.

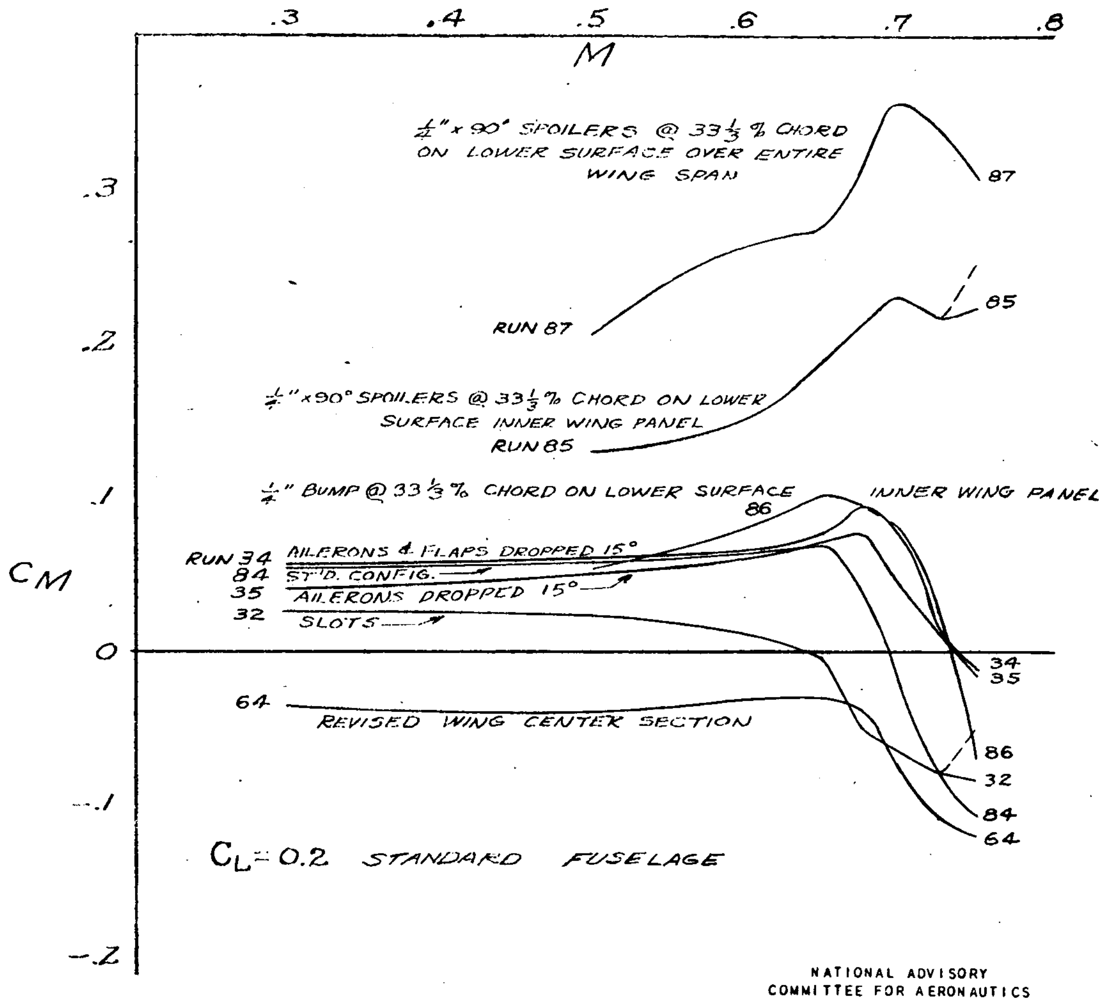

(b) $C_L = 0.2$.

Figure 21. - Continued. Effect of wing spoilers and wing bumps on pitching moments.

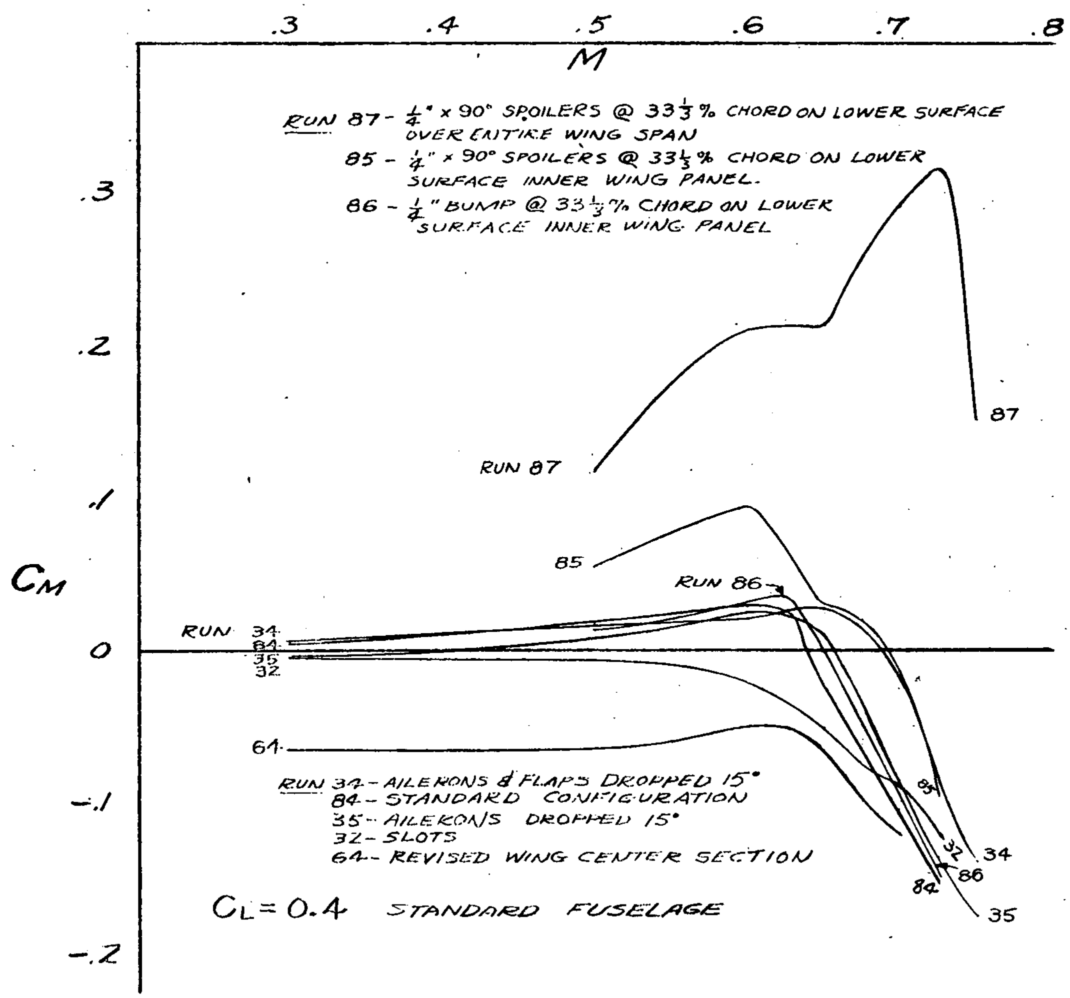

NATIONAL ADVISORY
COMMITTEE FOR AERONAUTICS

(c) $C_L = 0.4$.

Figure 21. - Concluded. Effect of wing spoilers and wing bumps on pitching moments.

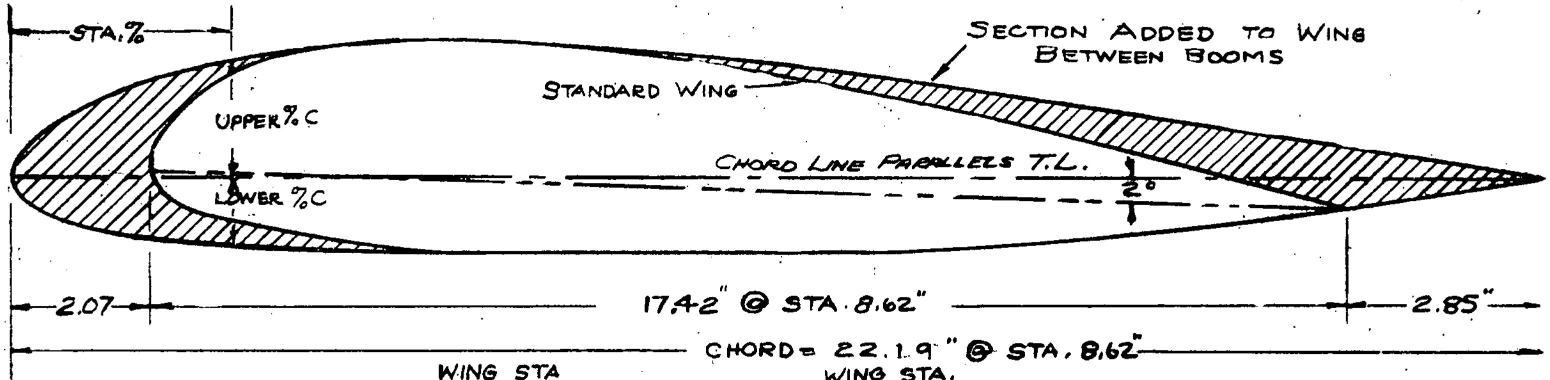

WING STA 4.69"

STA.%	UPPER	LOWER
0	0	0
1.25	1.954	2.49
2.5	3.08	3.19
5.0	4.34	3.92
7.5	5.25	4.34
10	5.99	4.60
15	7.12	4.98
20	7.78	5.16
25	7.99	5.30
30	7.90	5.42
40	7.38	5.38
50	6.47	5.16
60	5.38	4.73
70	4.22	3.99
80	3.08	3.18
90	1.65	1.78
95	0.91	0.91
100	0.09	0.09

CHORD = 23.02"

WING STA. 10.13"

STA.%	UPPER	LOWER
0	-.93	.93
1.25	1.58	3.07
2.5	2.42	3.73
5.0	3.63	4.37
7.5	4.56	4.84
10	5.30	5.16
15	6.33	5.49
20	6.89	5.53
25	7.17	5.72
30	7.22	5.59
40	6.80	5.40
50	6.10	5.16
60	5.07	4.66
70	4.01	4.09
80	2.79	3.07
90	1.49	1.87
95	0.79	0.98
100	0.09	0.05

CHORD = 21.98"

NATIONAL ADVISORY
COMMITTEE FOR AERONAUTICS

Figure 22. - Wing glove mounted over standard wing between booms.

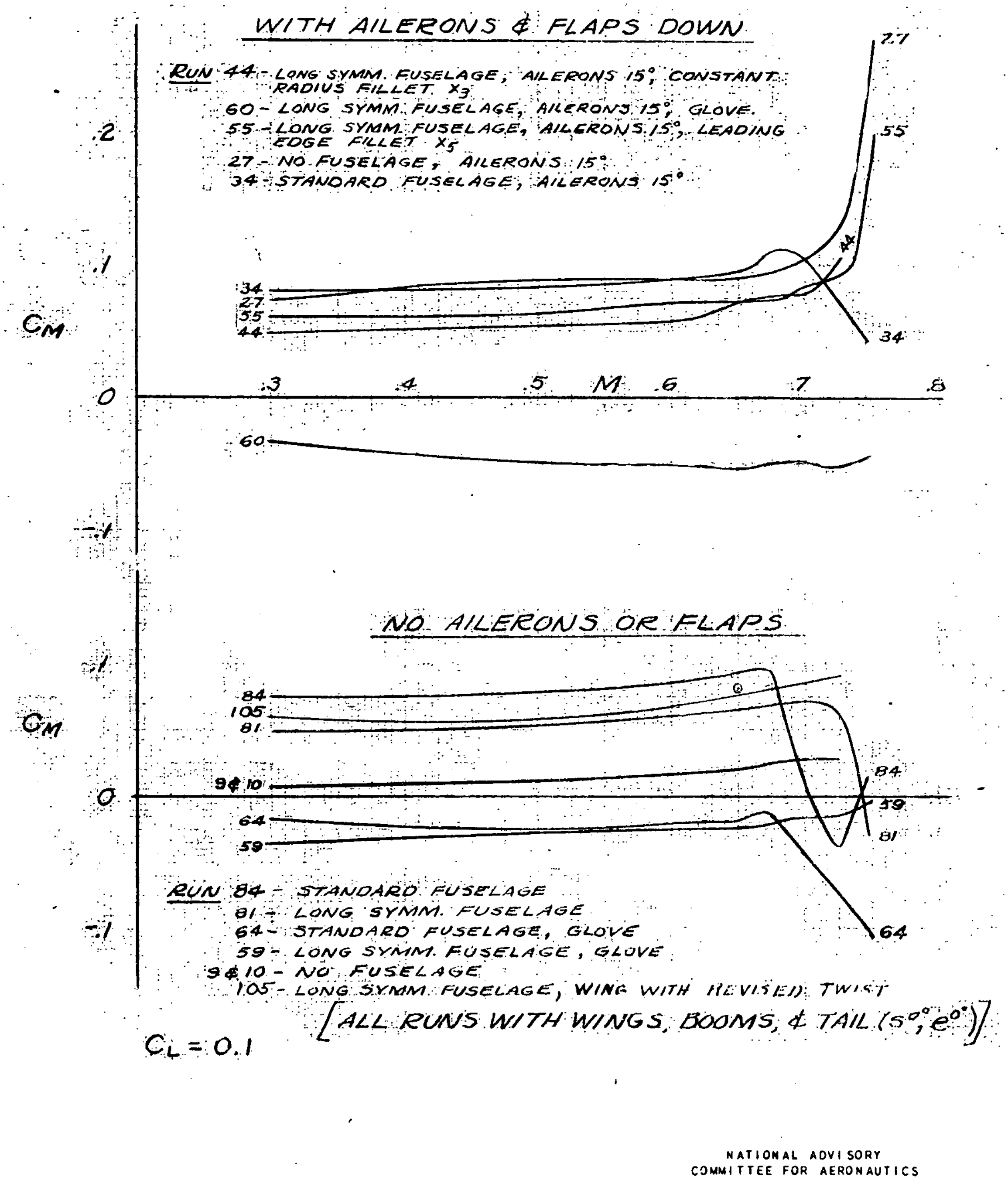

(a) $C_L = 0.1$.

Figure 23. - Comparison curves of configurations tried with and without ailerons and flaps.

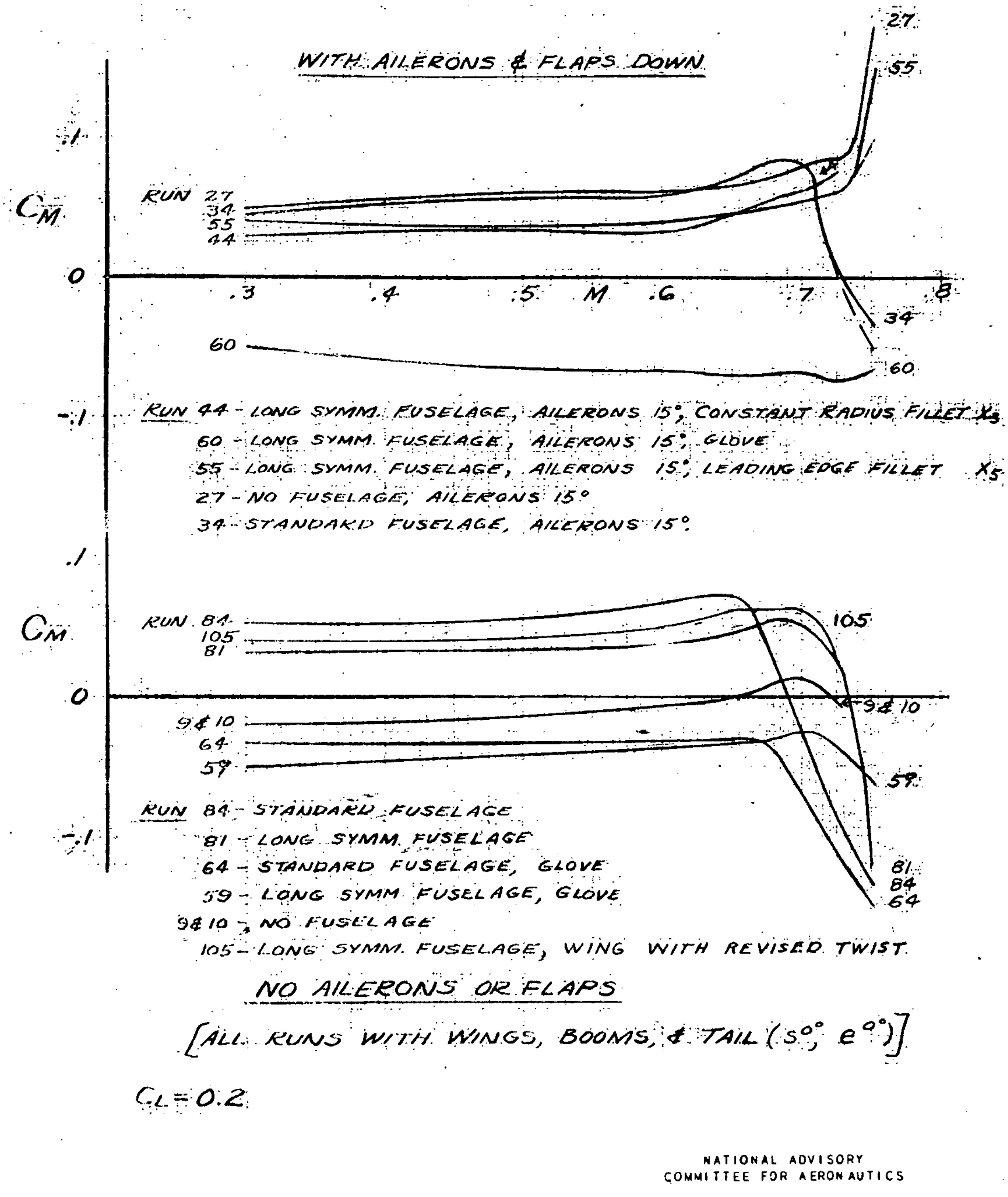

(b) $C_L = 0.2$.

Figure 23. - Continued. Comparison curves of configurations tried with and without ailerons and flaps.

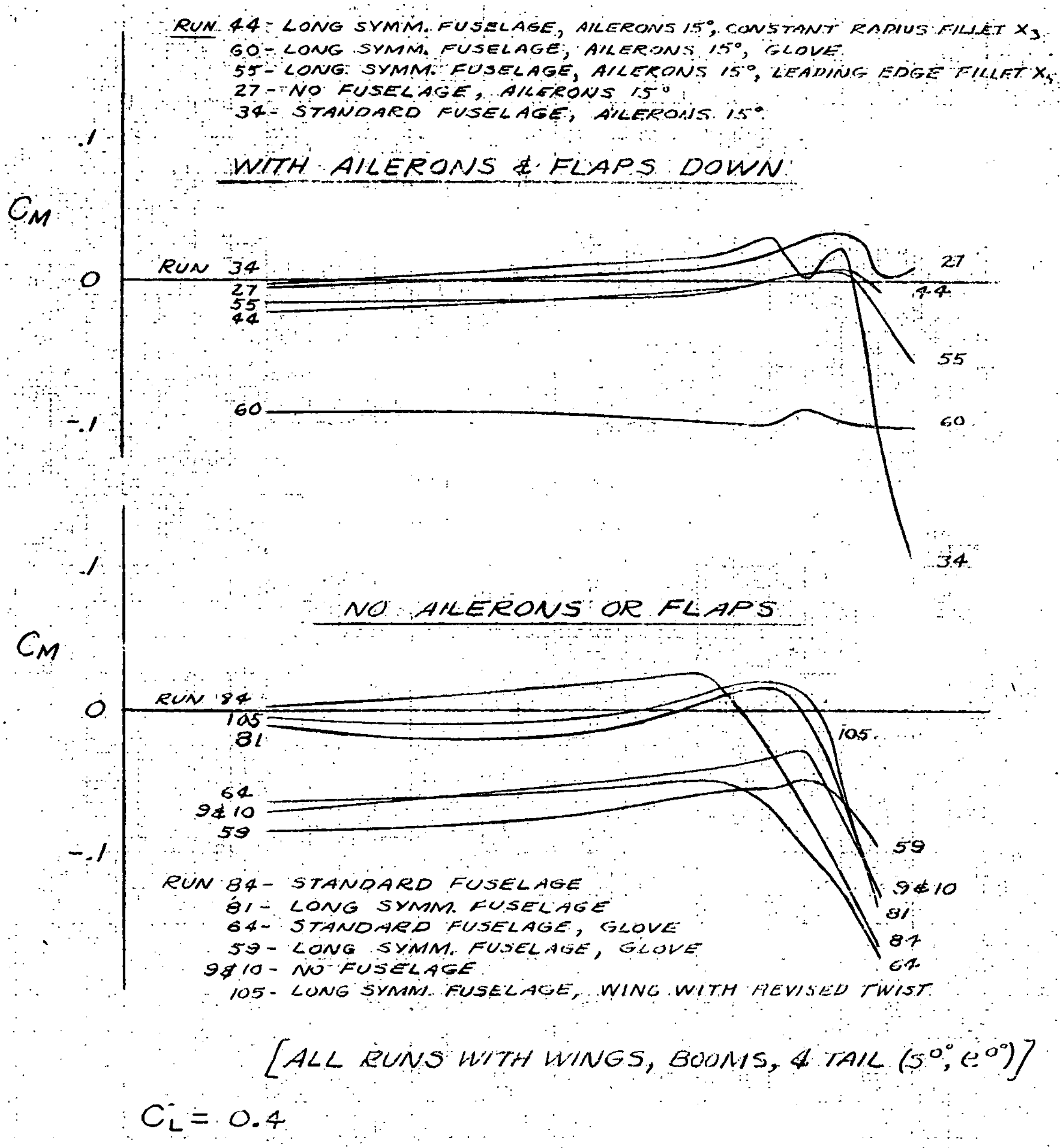

NATIONAL ADVISORY
COMMITTEE FOR AERONAUTICS

(c) $C_L = 0.4$.

Figure 23. - Concluded. Comparison curves of configurations tried with and without ailerons and flaps.

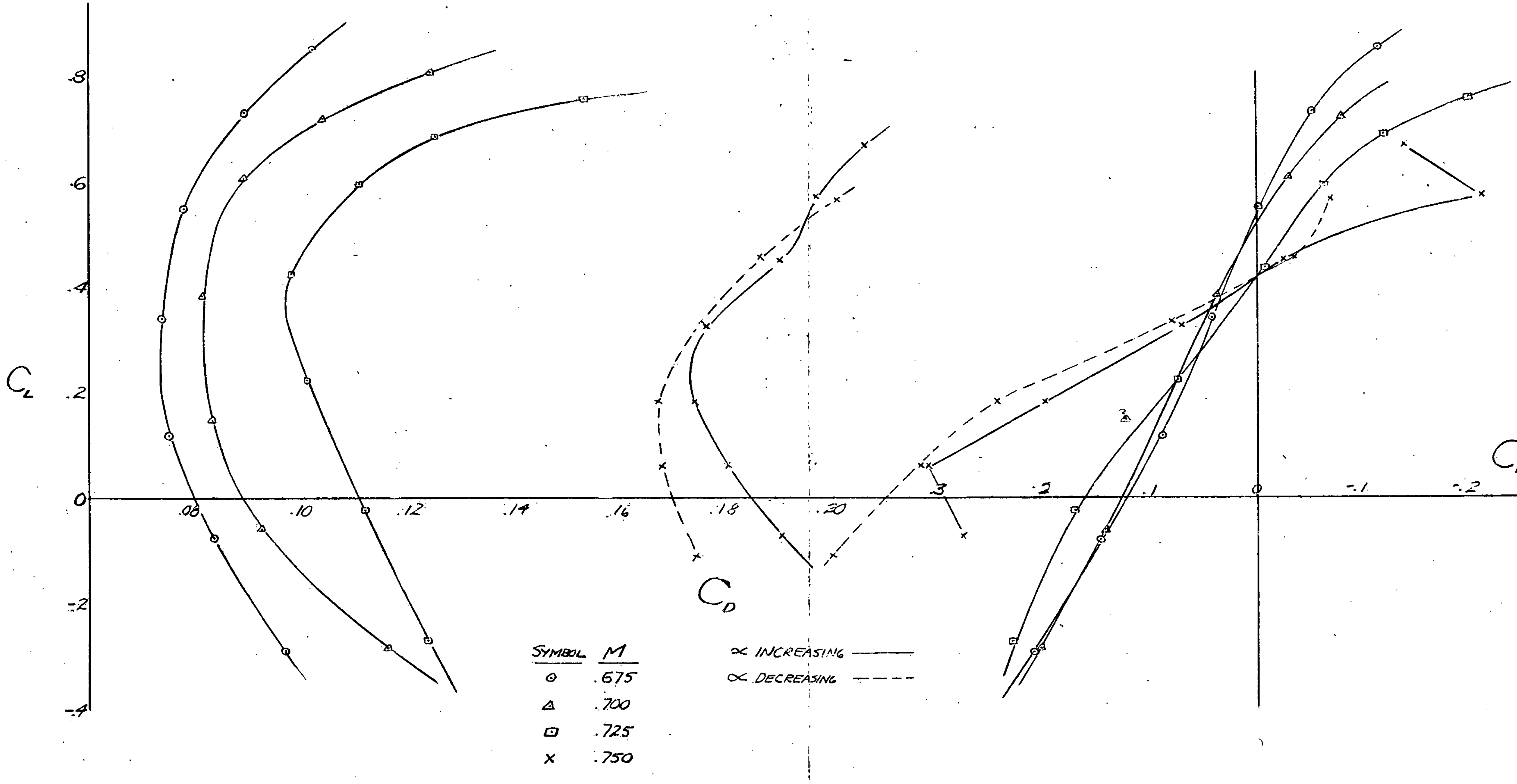

NATIONAL ADVISORY
COMMITTEE FOR AERONAUTICS

(b) Basic data from Mach number 0.675 to 0.750.

Figure 24. - Continued. Wing, booms, tail, ailerons and flaps drooped 15° from wing tip to booms.

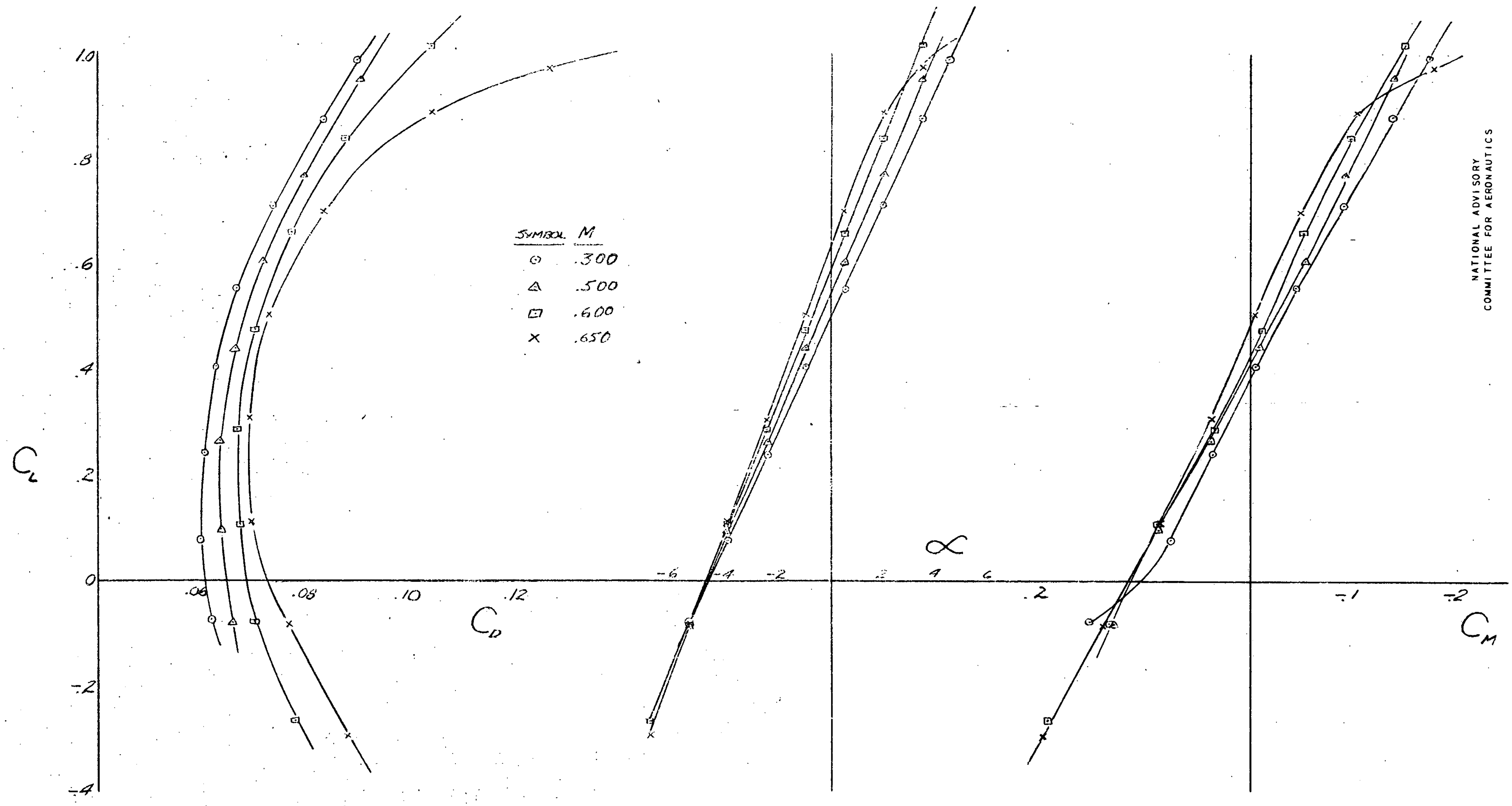

NATIONAL ADVISORY COMMITTEE FOR AERONAUTICS

(a) Basic data from Mach number 0.300 to 0.650.

Figure 24. - Wing, booms, tail, ailerons and flaps drooped 15° from wing tip to booms.

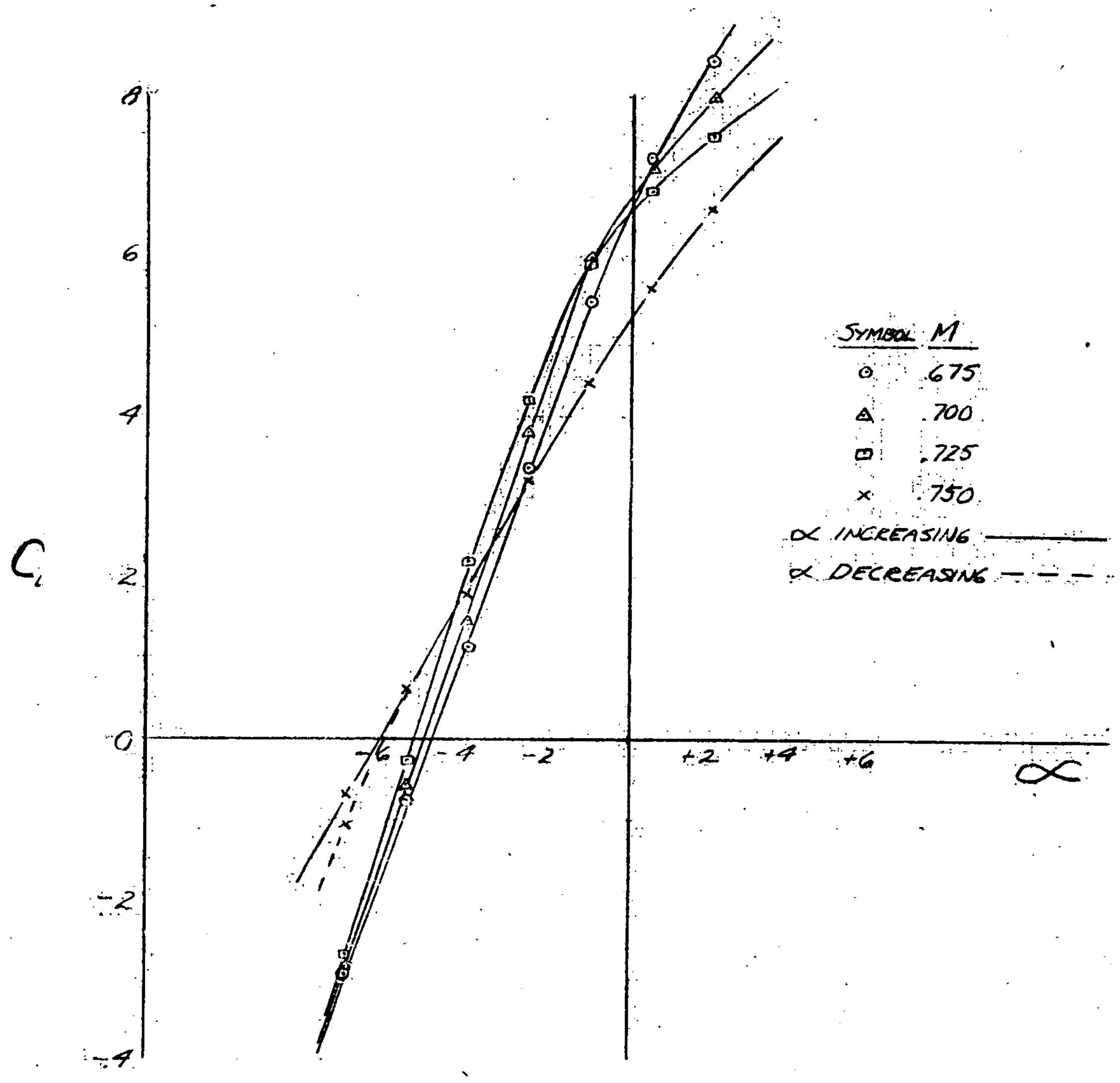

NATIONAL ADVISORY
COMMITTEE FOR AERONAUTICS

(b) Concluded. Basic data from Mach number 0.675 to 0.750.

Figure 24. - Continued. Wing, booms, tail, ailerons and flaps drooped 15° from wing tip to booms.

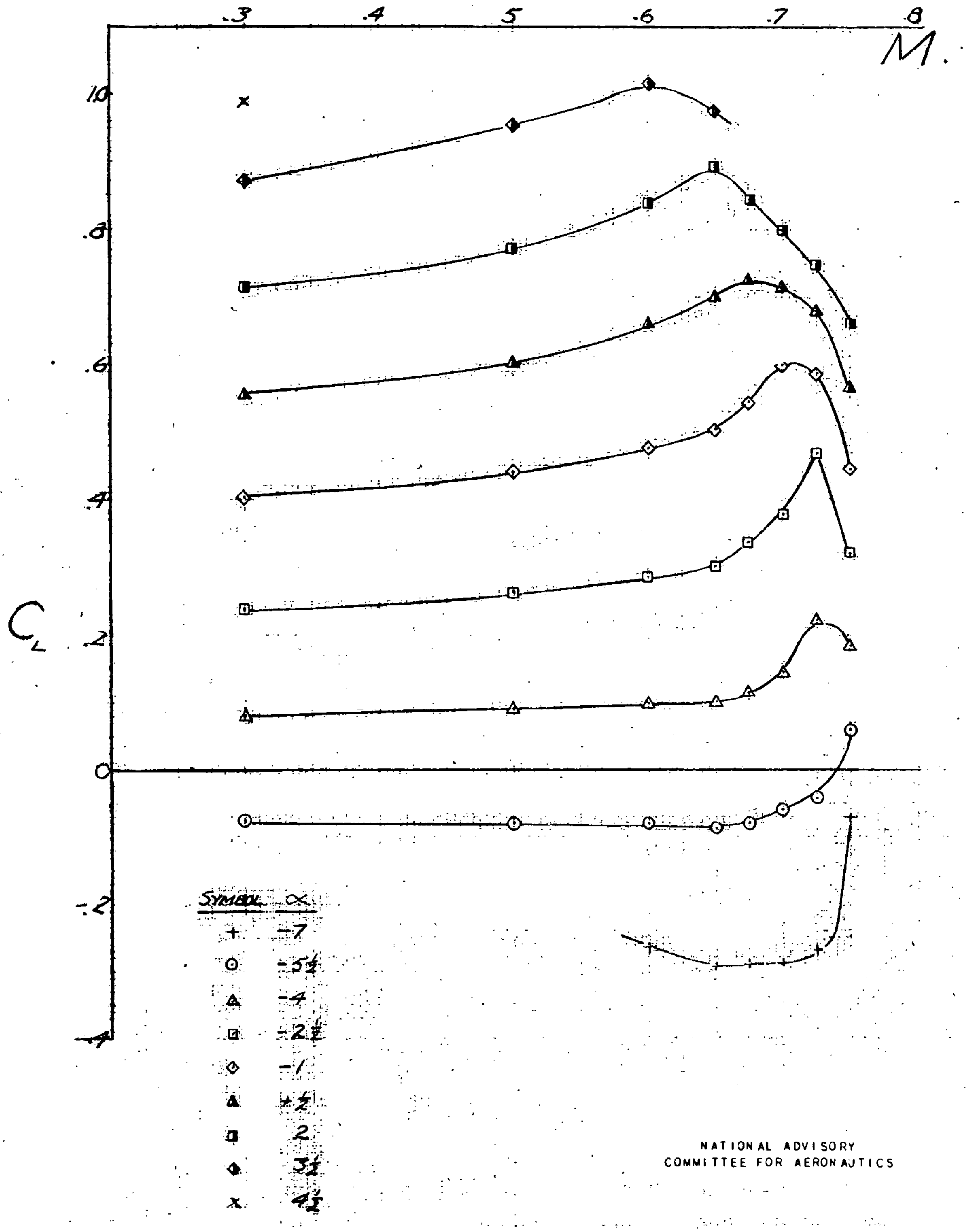

(c) Variation of C_L with Mach number at constant angles of attack.

Figure 24. - Continued. Wing, booms, tail, ailerons and flaps dropped 15° from wing tip to booms.

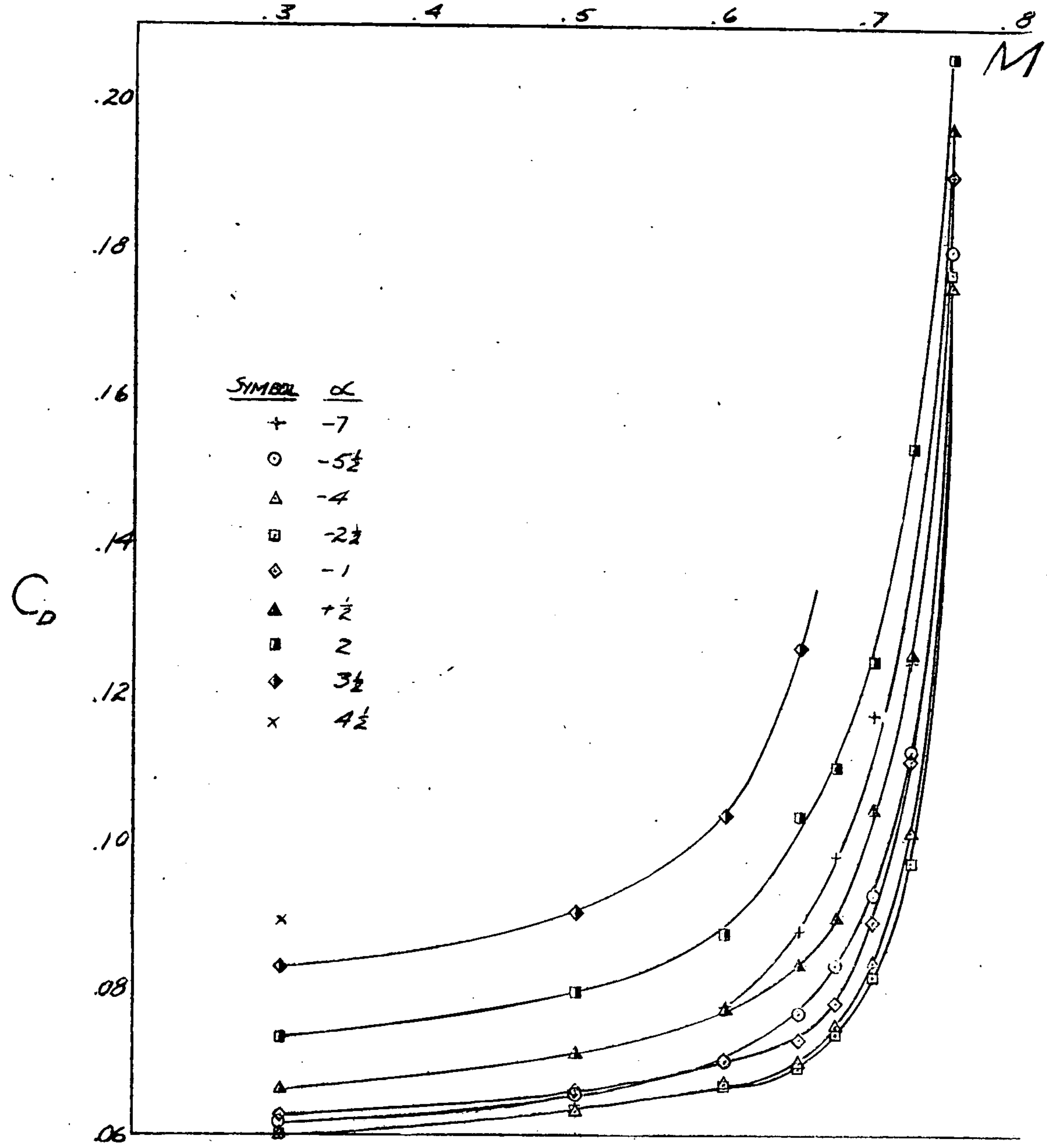

NATIONAL ADVISORY COMMITTEE FOR AERONAUTICS

(d) Variation of C_D with Mach number at constant angles of attack.

Figure 24. - Continued. Wing, booms, tail, ailerons and flaps drooped 15° from wing tip to booms.

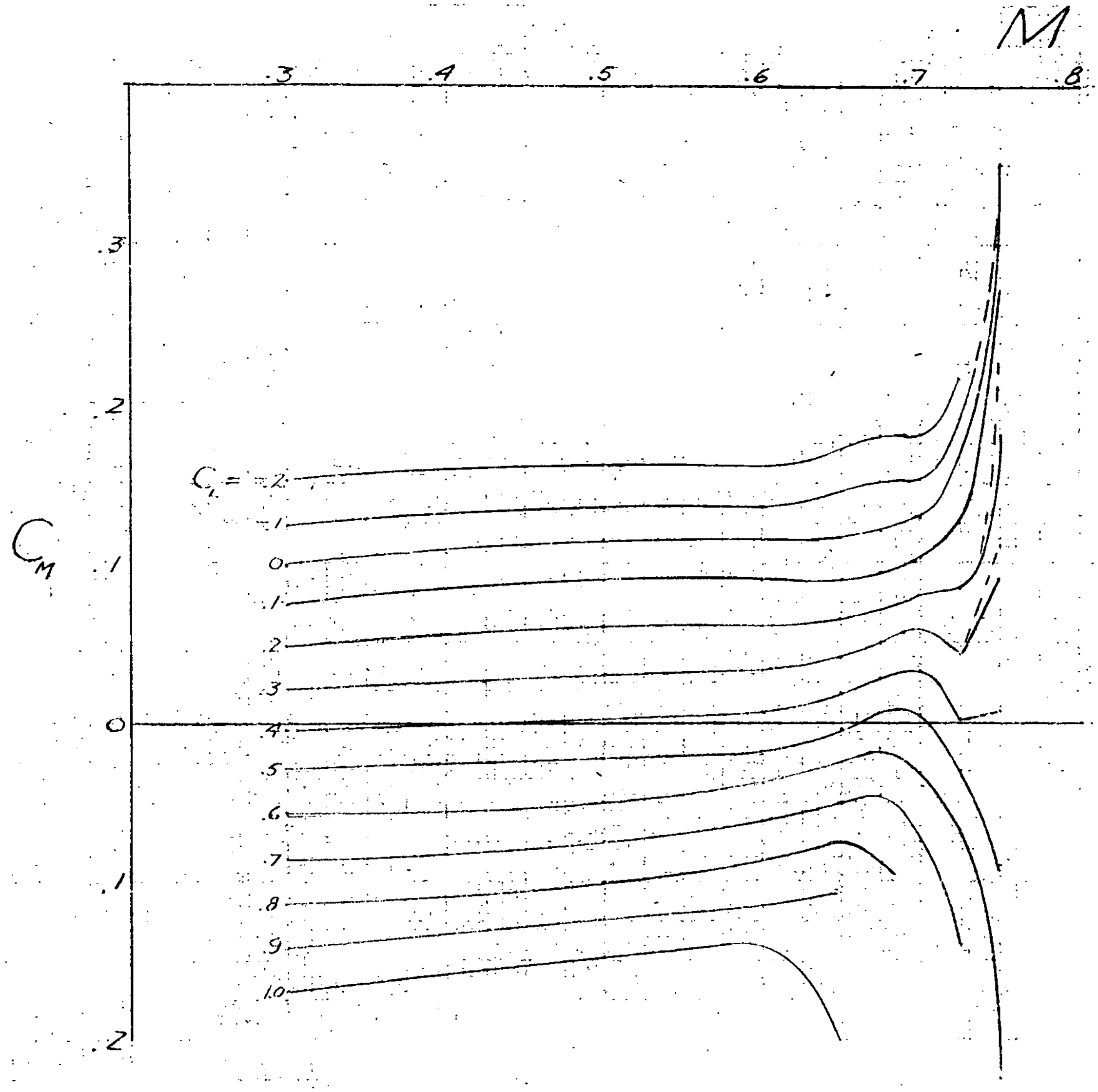

NATIONAL ADVISORY
COMMITTEE FOR AERONAUTICS

(e) Variation of C_M with Mach number at constant lift coefficients.

Figure 24. - Concluded. Wing, booms, tail, ailerons and flaps drooped 15° from wing tip to booms.

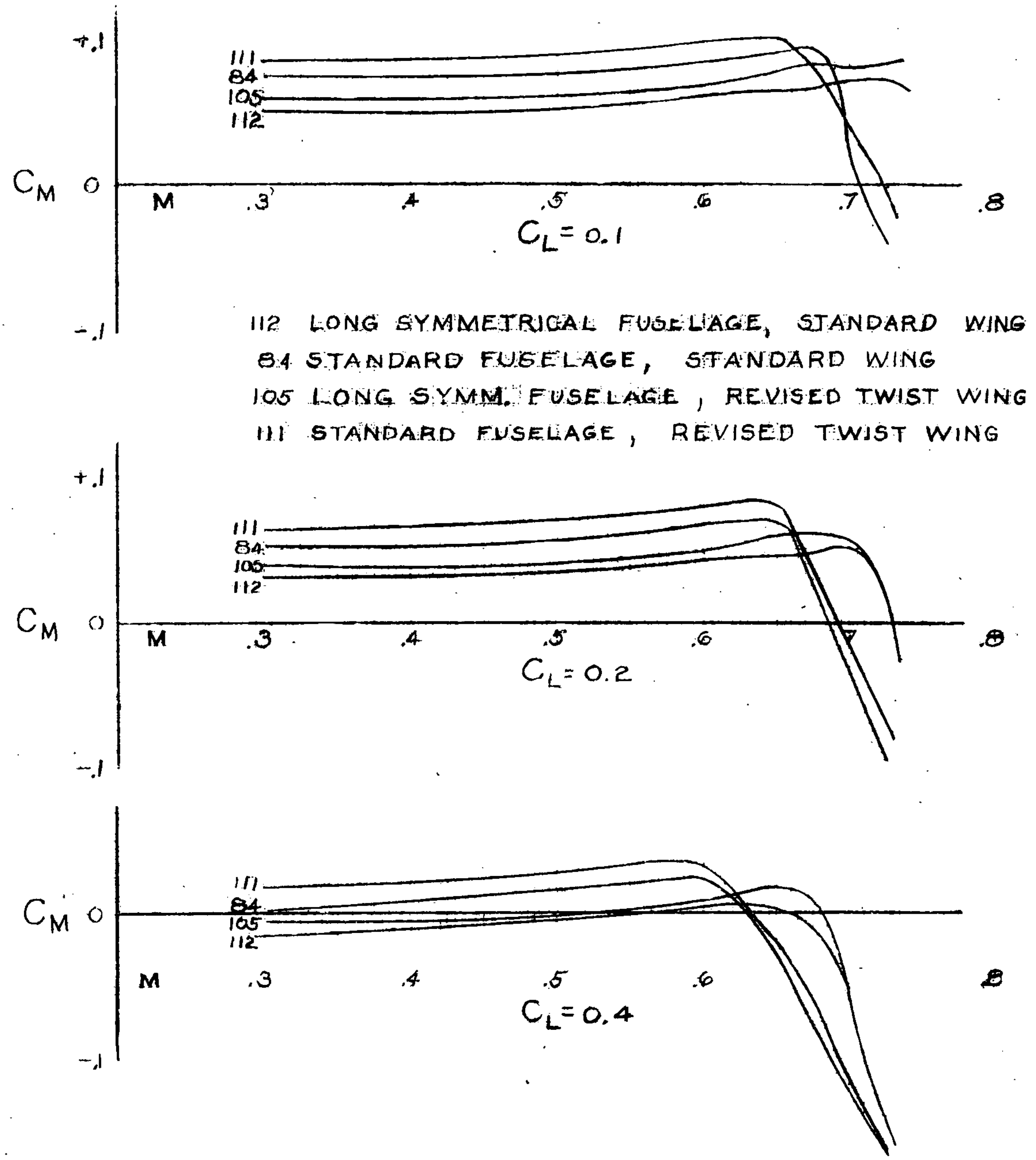

NATIONAL ADVISORY
COMMITTEE FOR AERONAUTICS

Figure 25. - Effect of the 3° change in wing twist.

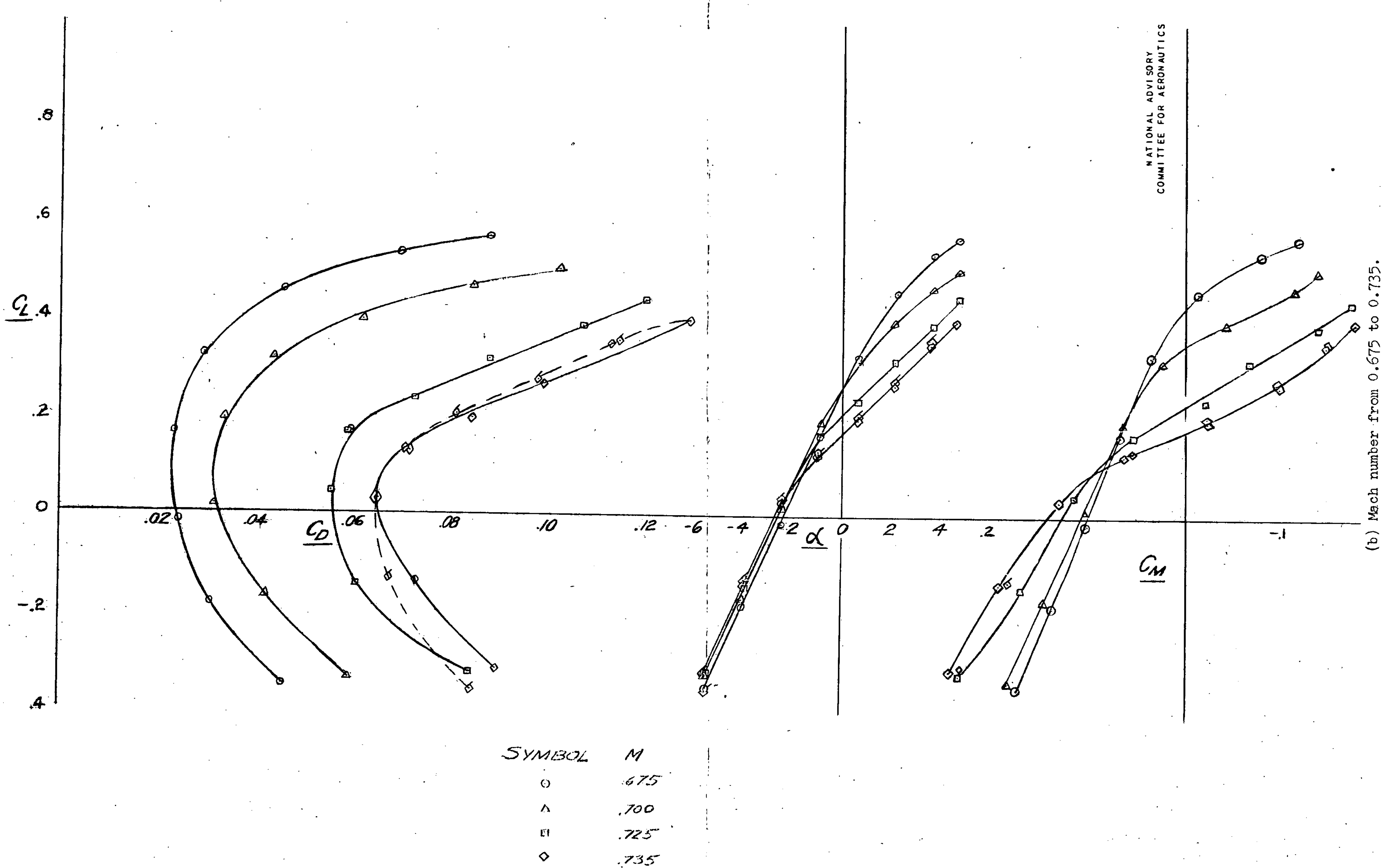

(b) Mach number from 0.675 to 0.735.

Figure 26. - Continued. Wing with revised twist, booms, long symmetrical fuselage, constant-radius fillet, and tail. Elevator at 0°.

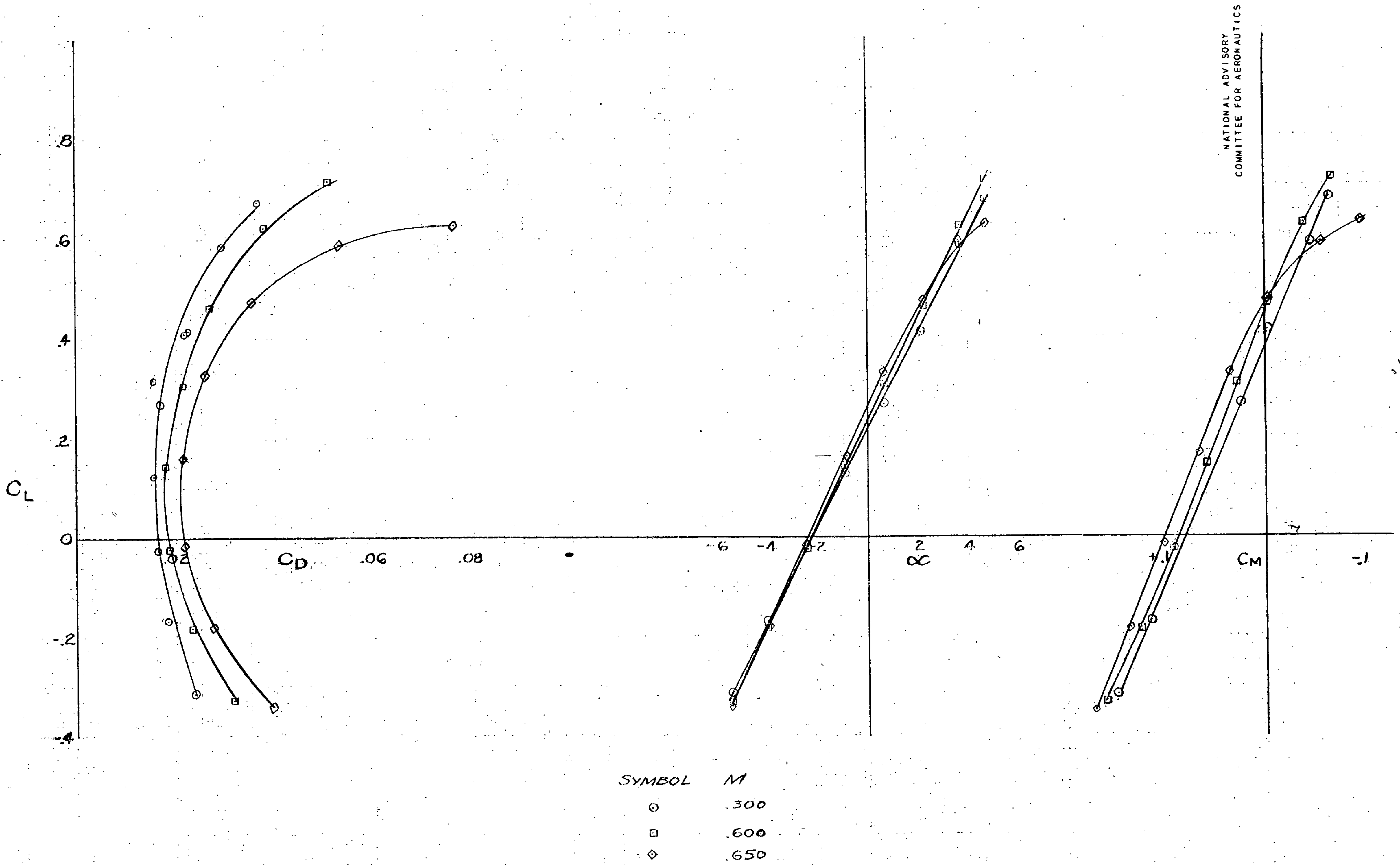

Figure 26. - Wing with revised twist, booms, long symmetrical fuselage, constant-radius fillet, and tail. Elevator at 0°.

(a) Mach number from 0.300 to 0.650.

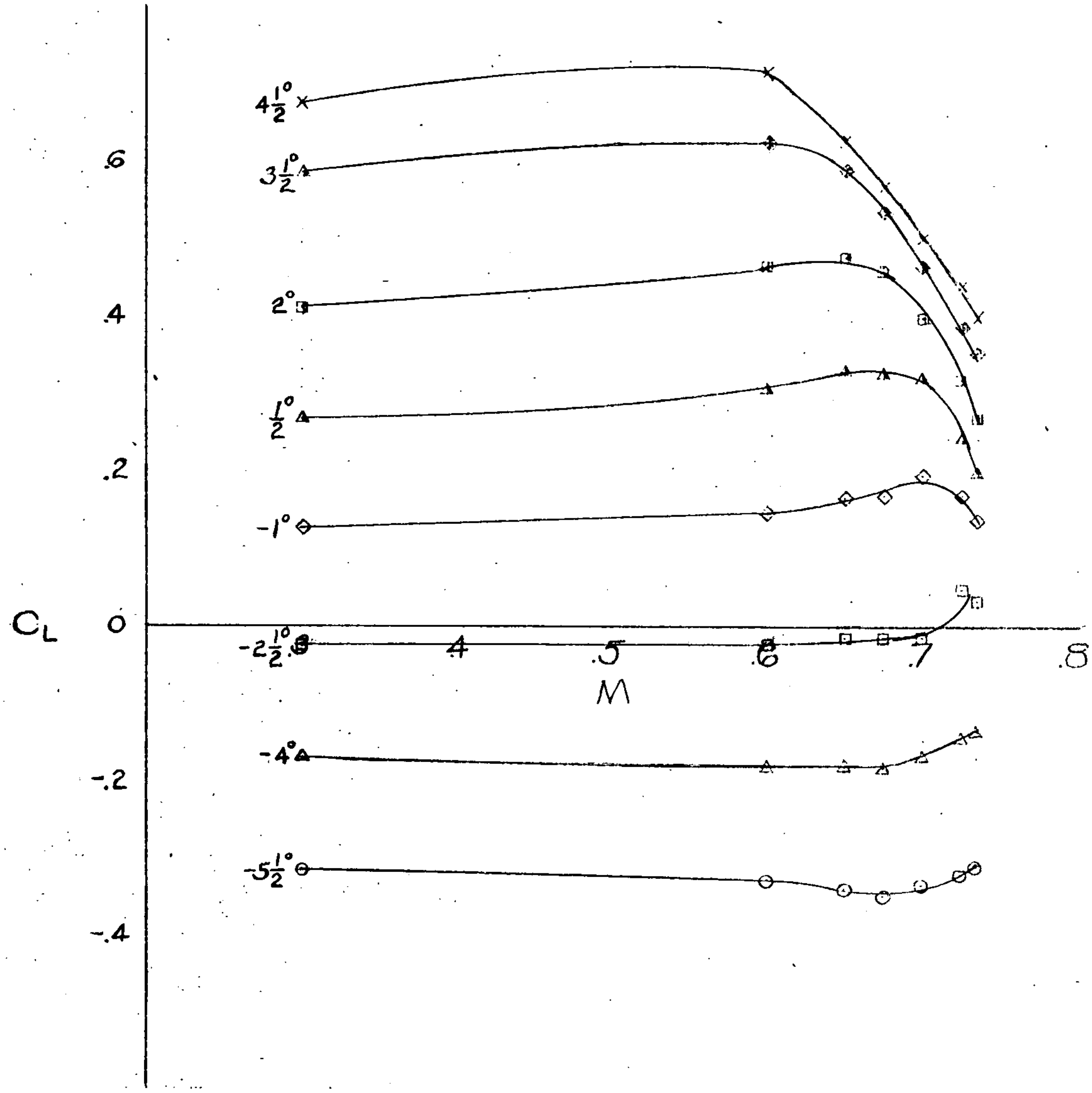

(c) Variation of C_L with Mach number at constant angles of attack.

Figure 26. - Continued. Wing with revised twist, booms, long symmetrical fuselage, constant-radius fillet, and tail. Elevator at 0°.

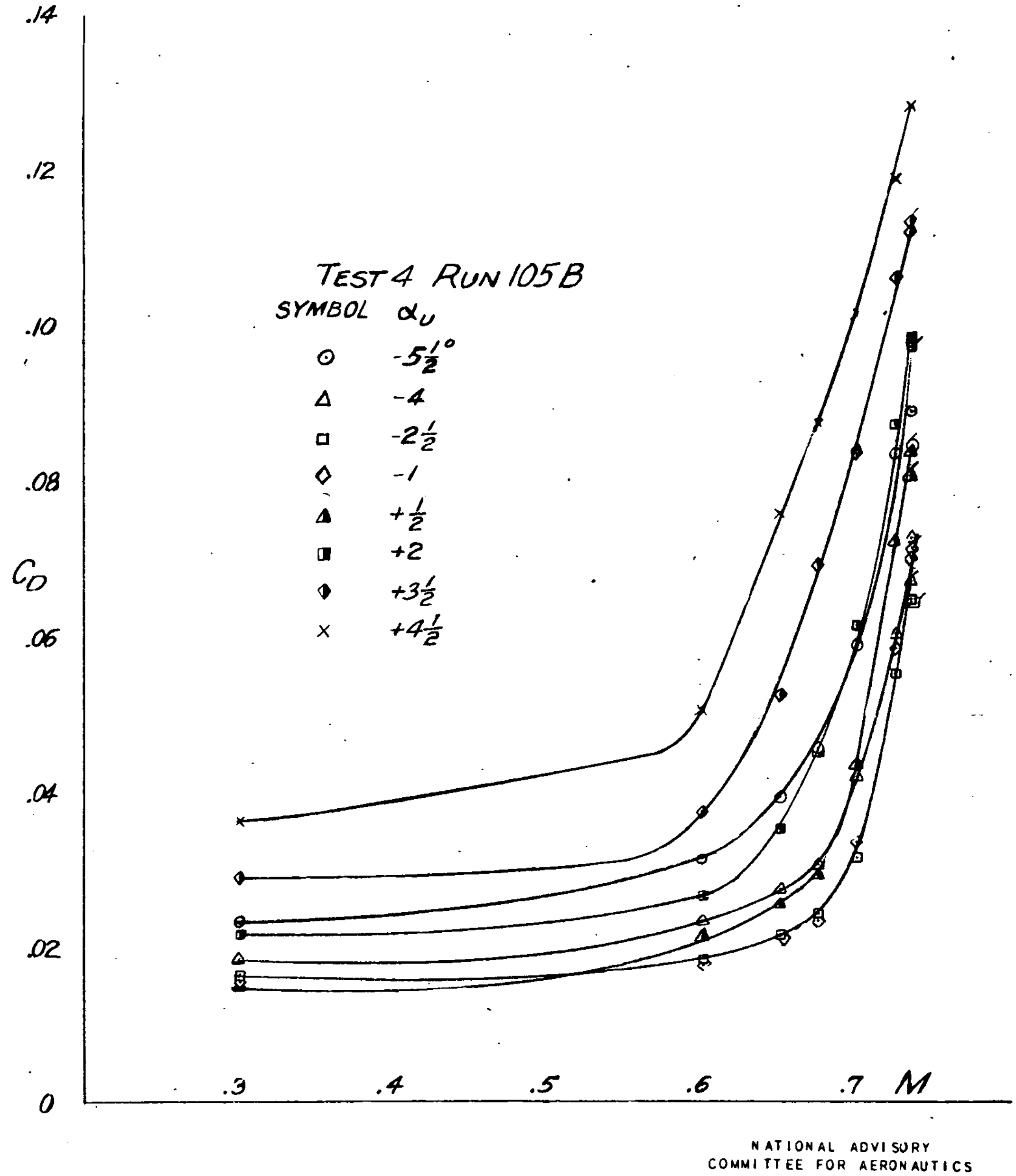

(d) Variation of C_D with Mach number at constant angles of attack.

Figure 26. - Continued. Wing with revised twist, booms, long symmetrical fuselage, constant-radius fillet, and tail. Elevator at 0°.

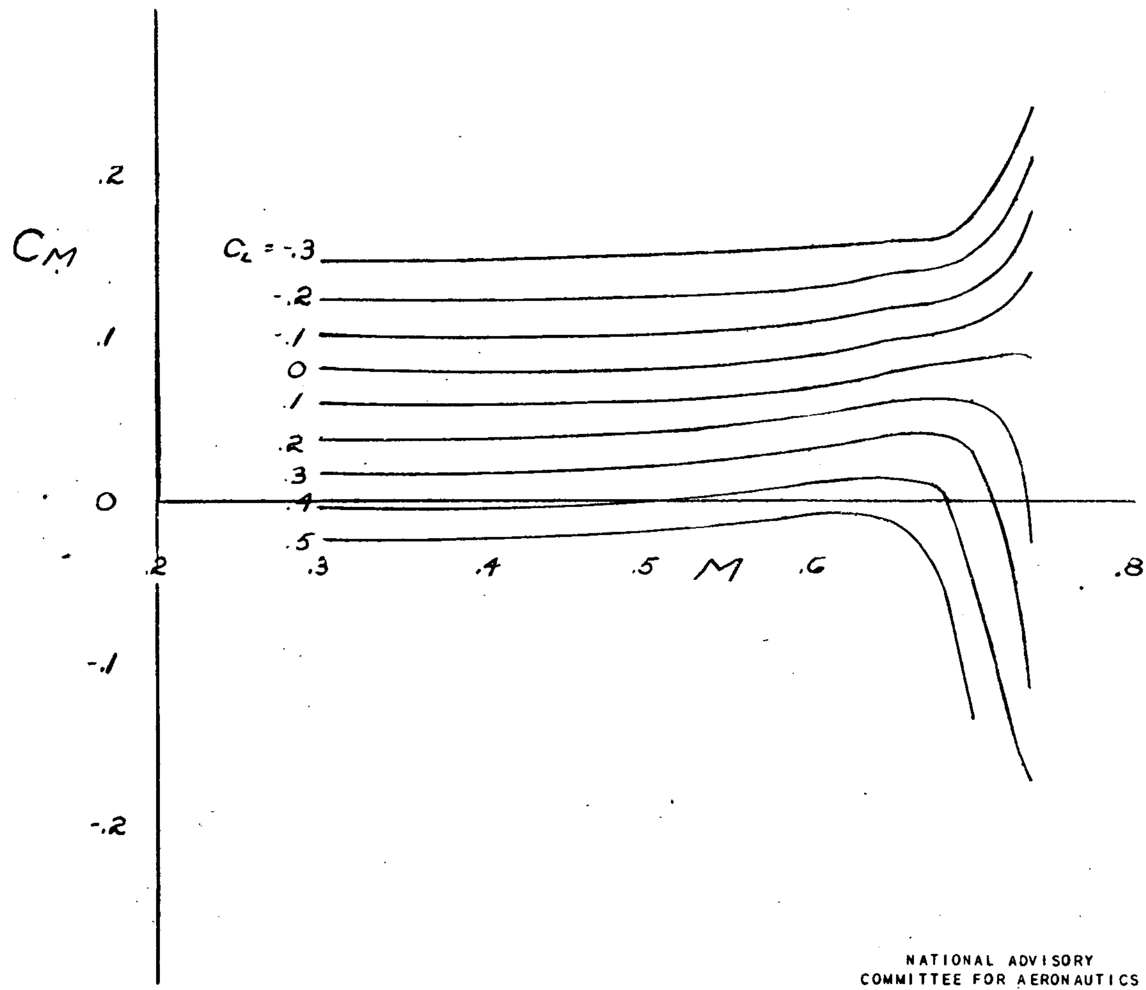

(e) Variation of C_M with Mach number at constant lift coefficients.

Figure 26. - Concluded. Wing with revised twist, booms, long symmetrical fuselage, constant-radius fillet, and tail. Elevator at 0°.

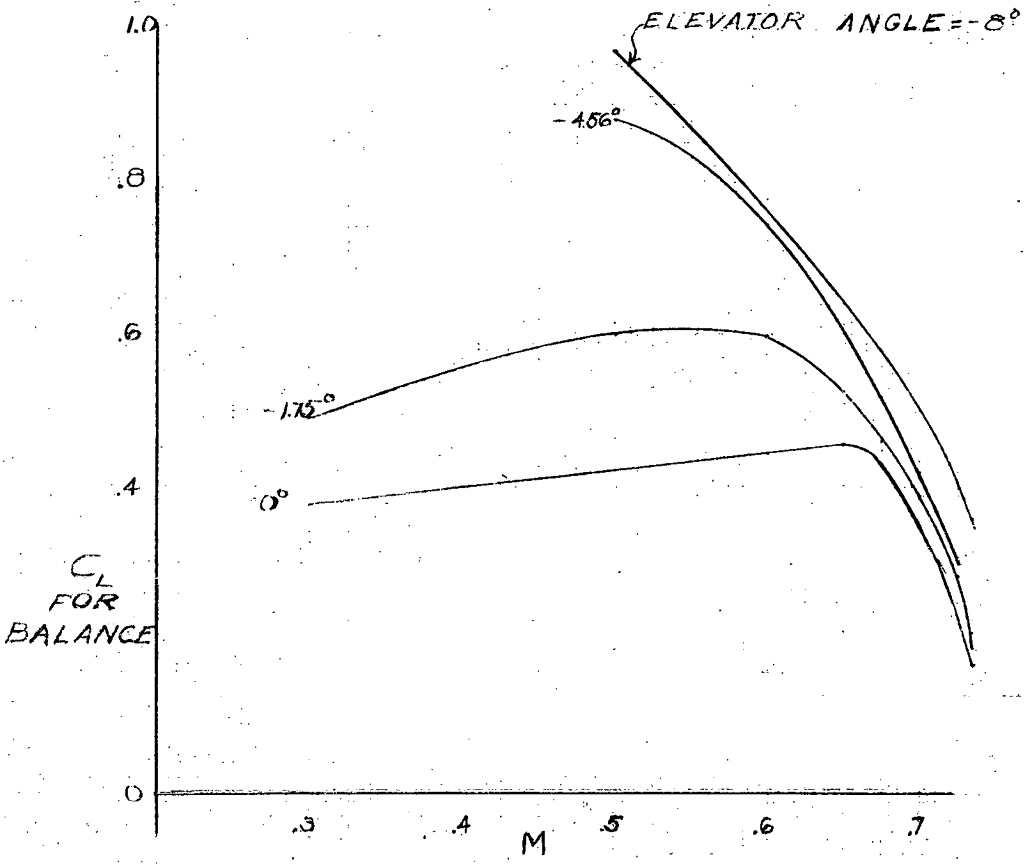

NATIONAL ADVISORY
COMMITTEE FOR AERONAUTICS

Figure 27. - Wing with revised twist; booms, long symmetrical fuselage, and tail. Lift coefficients for balance at various elevator settings.

for balance at various elevator settings.

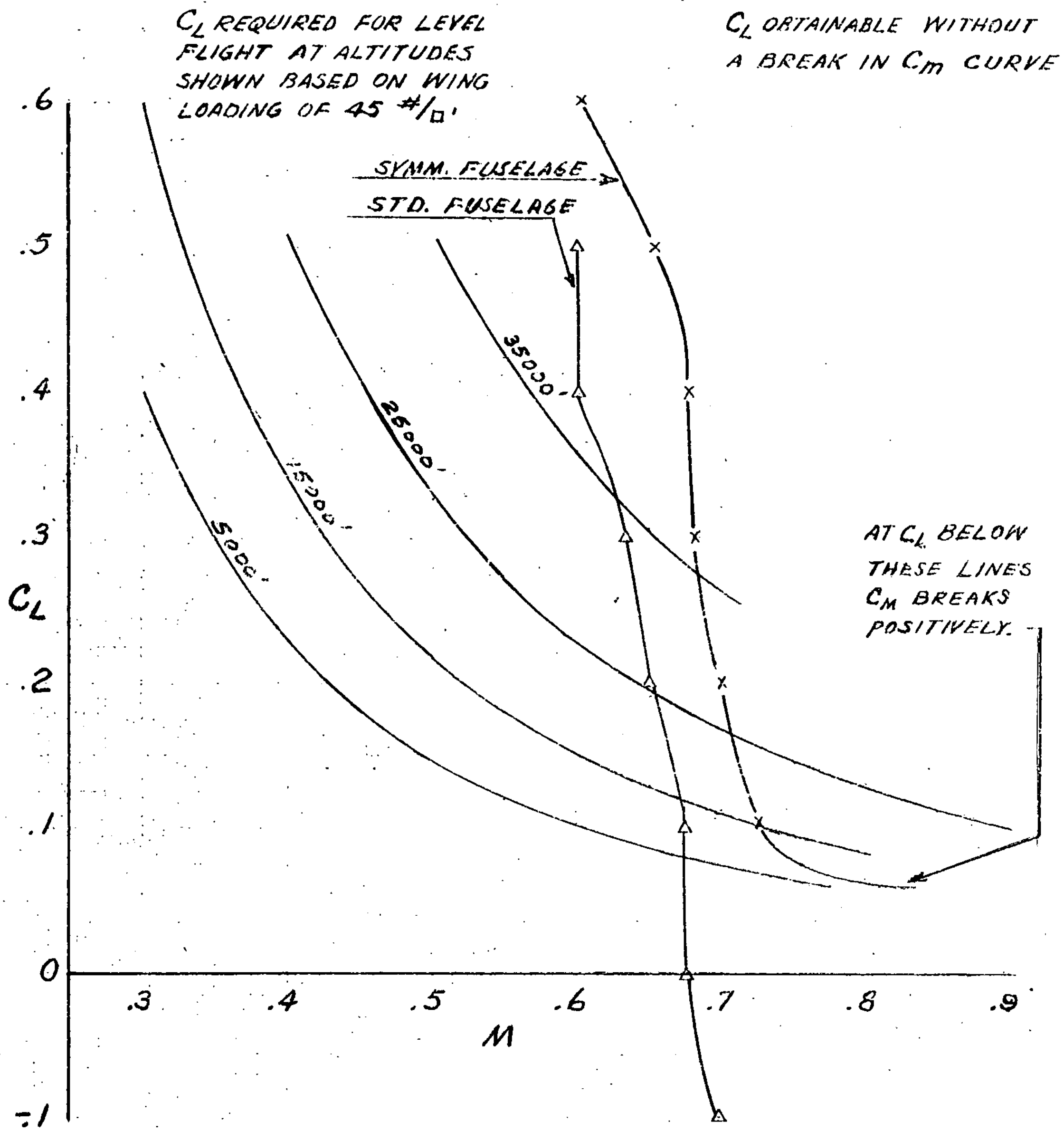

NATIONAL ADVISORY COMMITTEE FOR AERONAUTICS

Figure 28. - Maximum lift coefficient available with change in Mach number for two configurations.

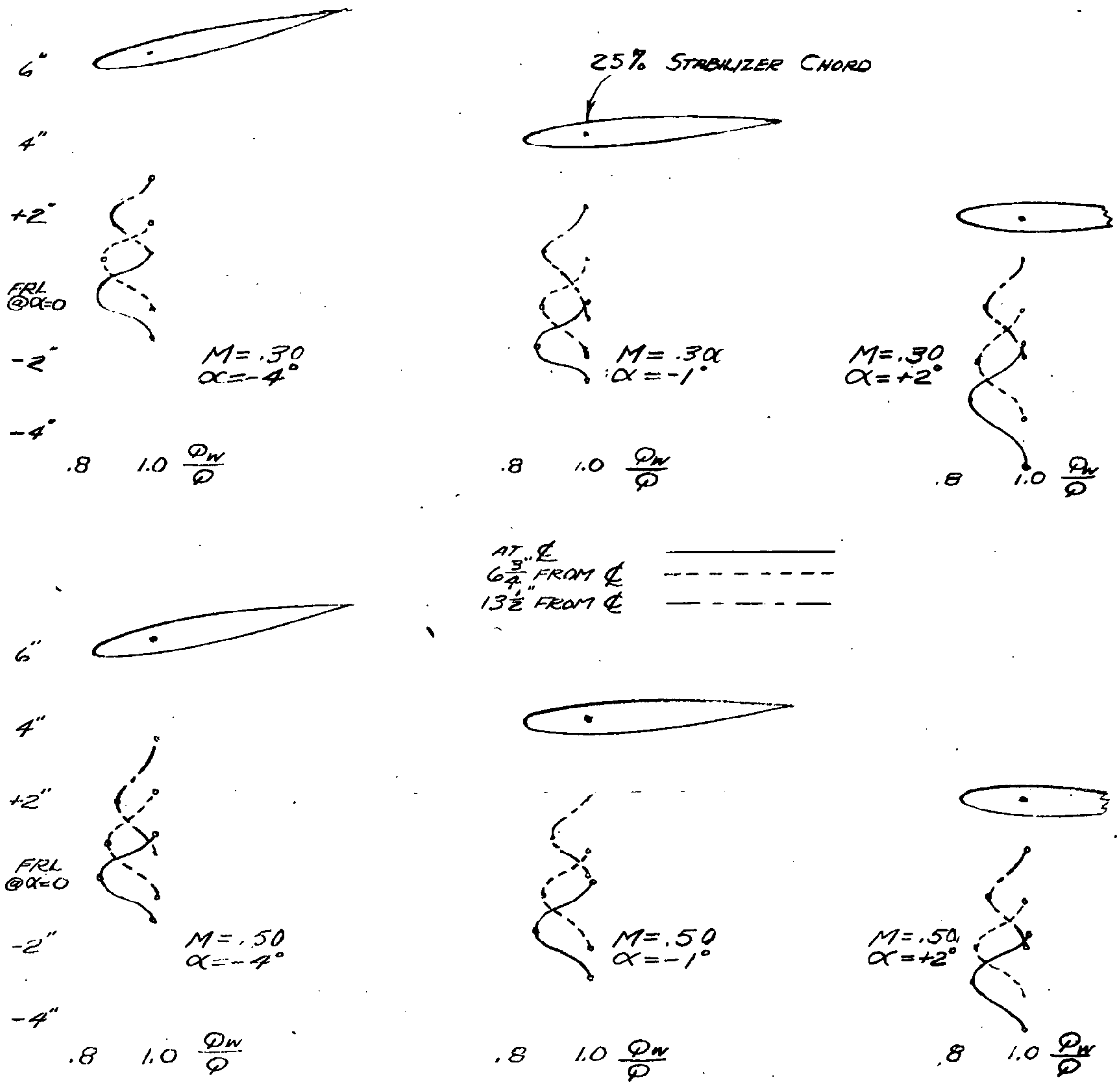

(a) Mach number, 0.30 and 0.50.

Figure 29. - Relative position of the tail and wing wake for the wing and booms alone.

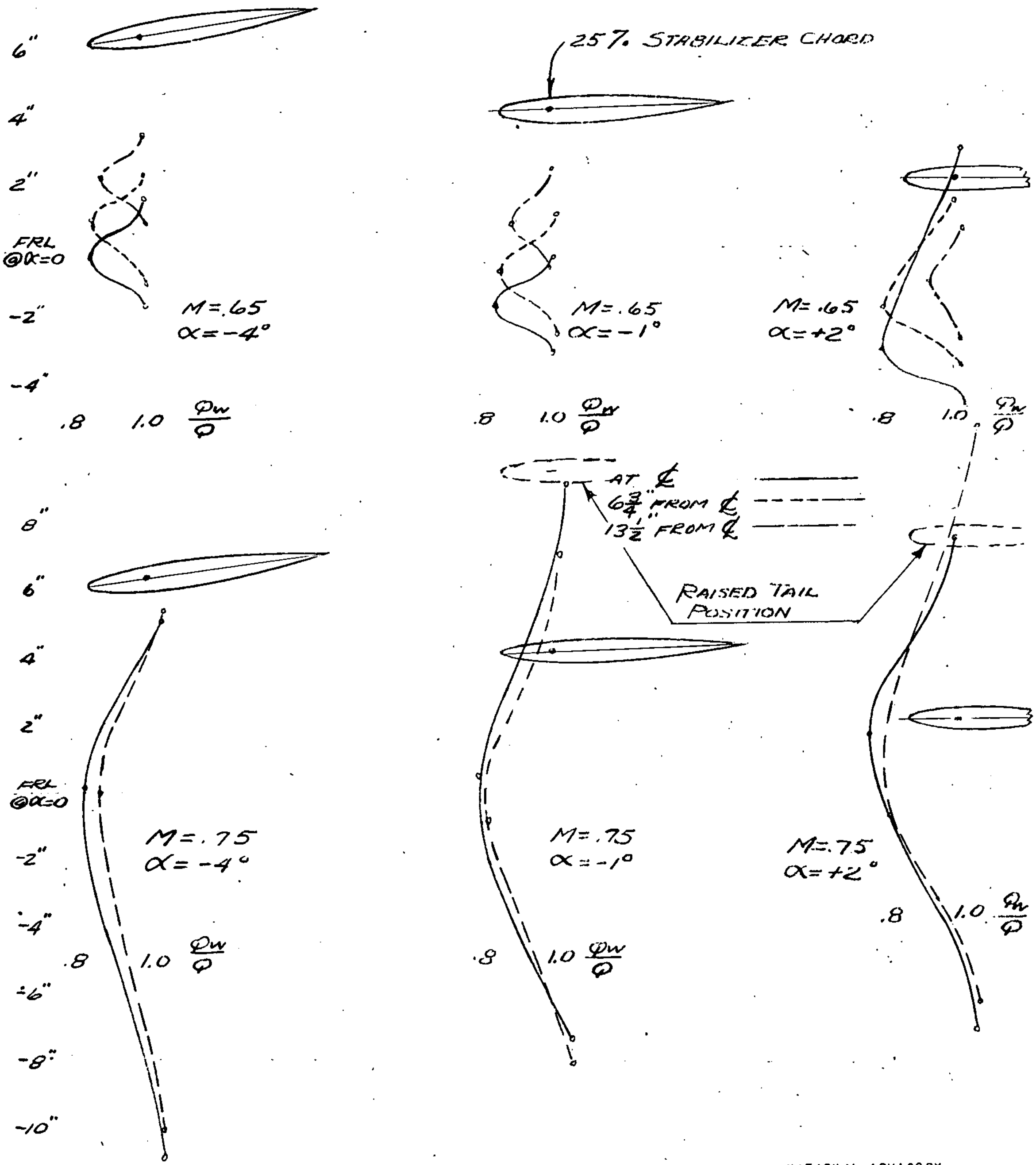

NATIONAL ADVISORY COMMITTEE FOR AERONAUTICS

(b) Mach number, 0.65 to 0.75.

Figure 29. - Concluded. Relative position of the tail and wing wake for the wing and booms alone.

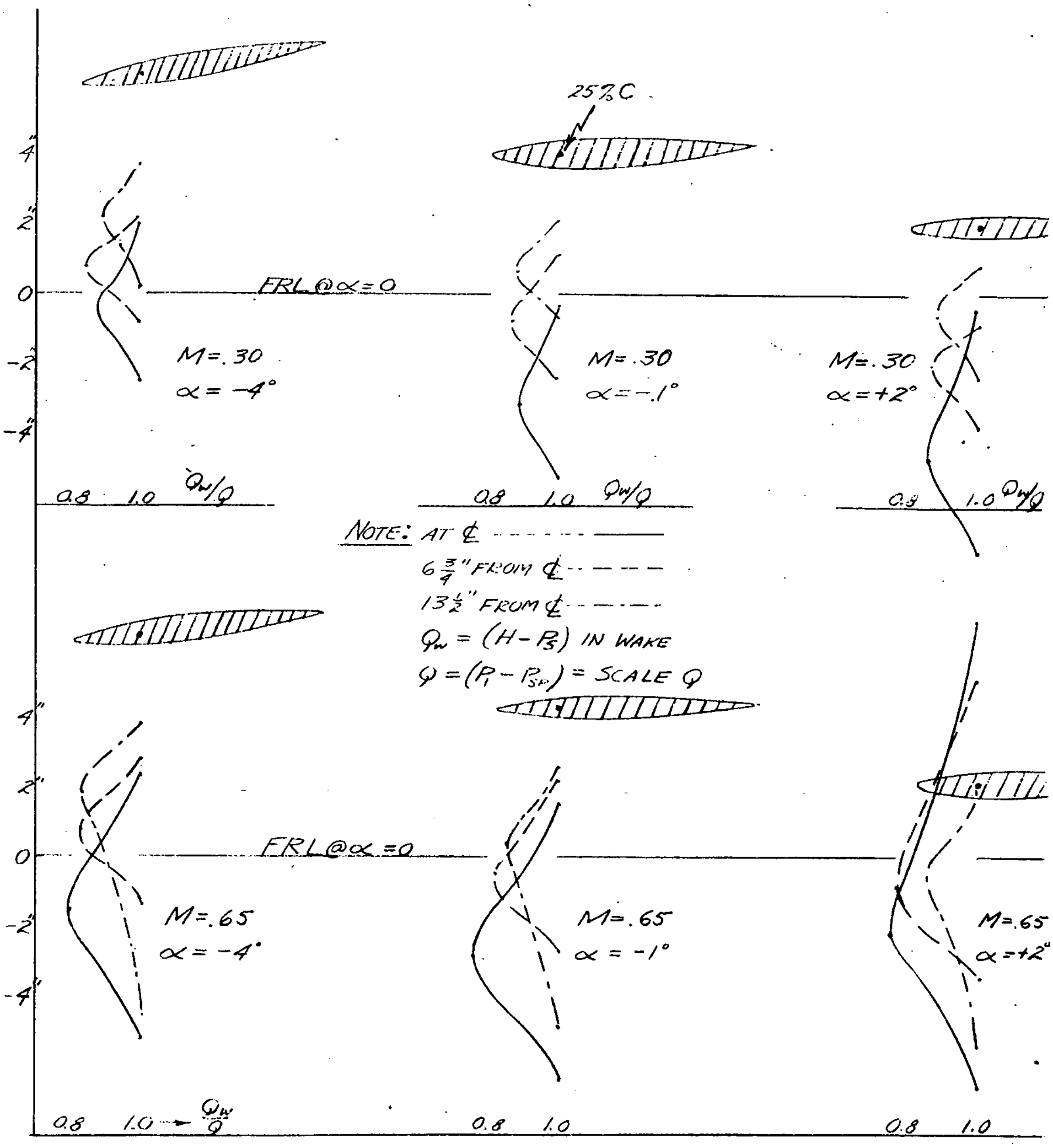

NATIONAL ADVISORY
COMMITTEE FOR AERONAUTICS

(a) Mach number, 0.30 and 0.65.

Figure 30. - Relative positions of the tail and wing wake for the wing, booms, and standard fuselage.

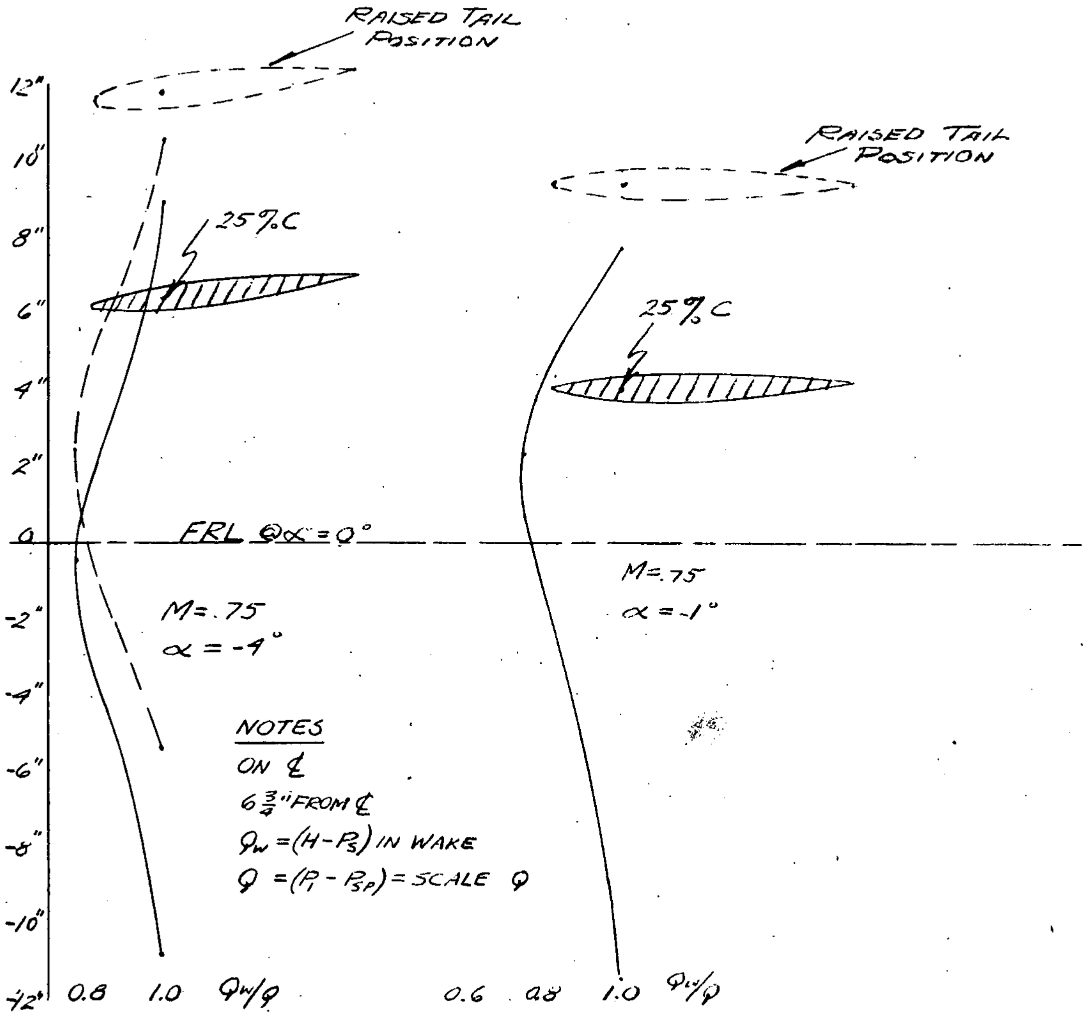

NATIONAL ADVISORY
COMMITTEE FOR AERONAUTICS

(b) Mach number, 0.75.

Figure 30. - Concluded. Relative positions of the tail and wing wake for the wing, booms, and standard fuselage.

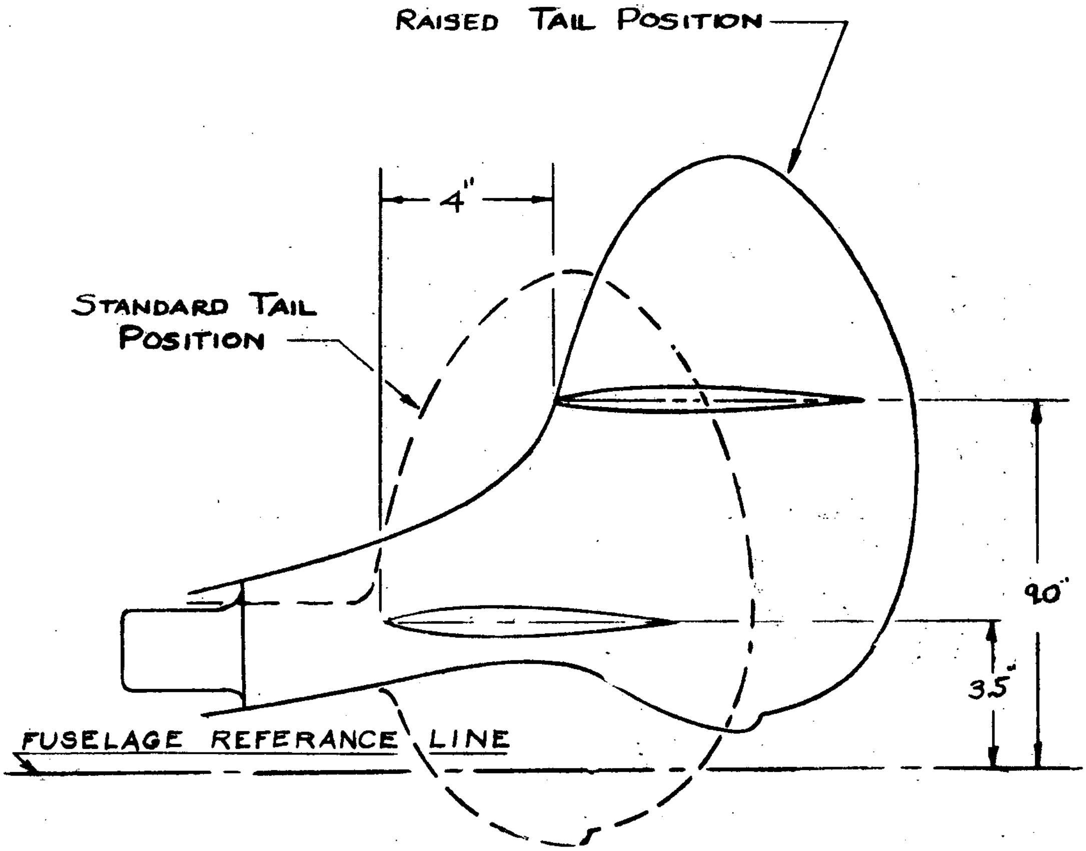

NATIONAL ADVISORY
COMMITTEE FOR AERONAUTICS

Figure 31. - Relative positions of the present standard tail and the raised tail.

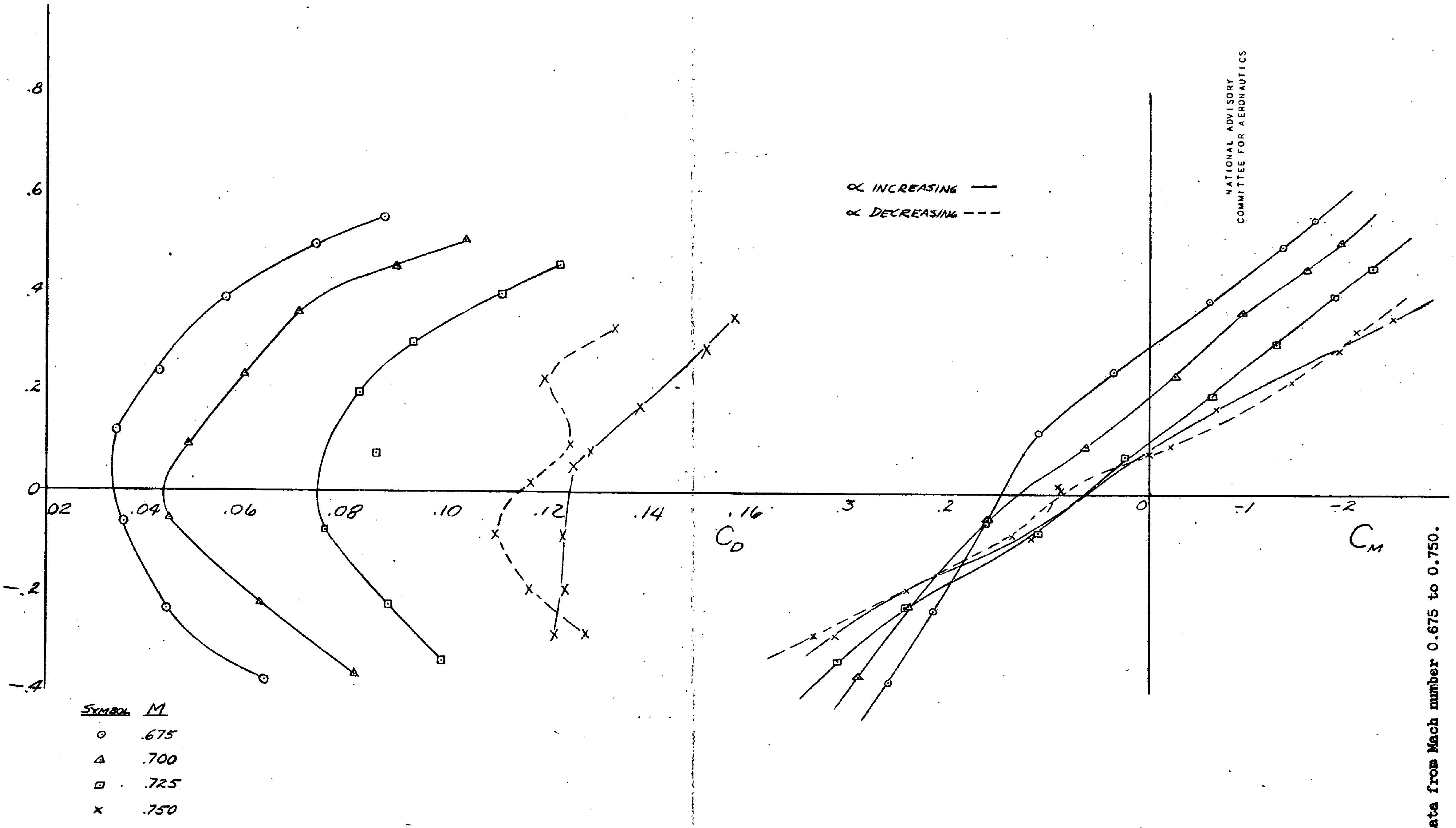

Figure 32. - Continued. Wing, booms, standard fuselage, and raised tail

(b) Basic data from Mach number 0.675 to 0.750.

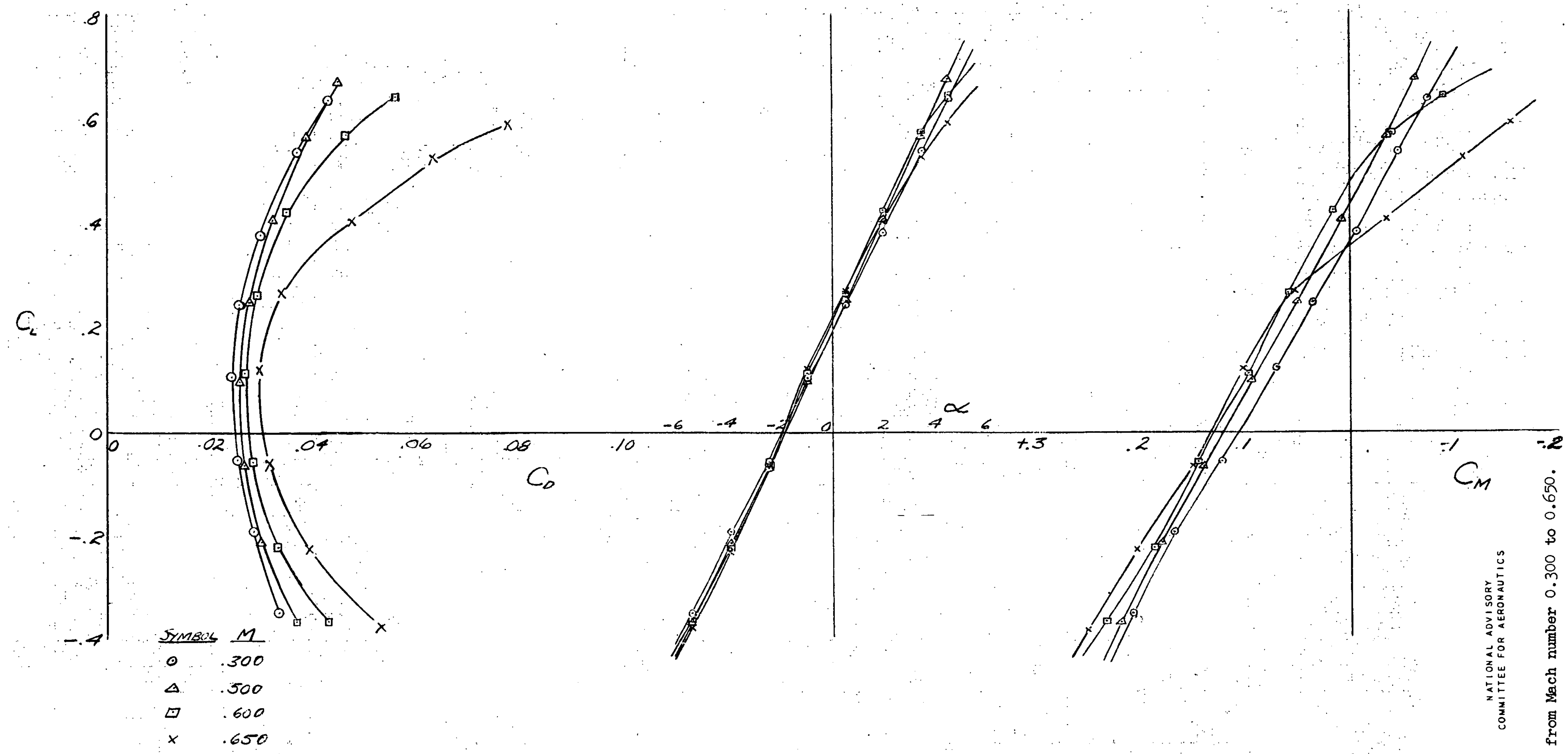

NATIONAL ADVISORY
COMMITTEE FOR AERONAUTICS

(a) Basic data from Mach number 0.300 to 0.650.

Figure 32. - Wing, booms, standard fuselage, and raised tail.

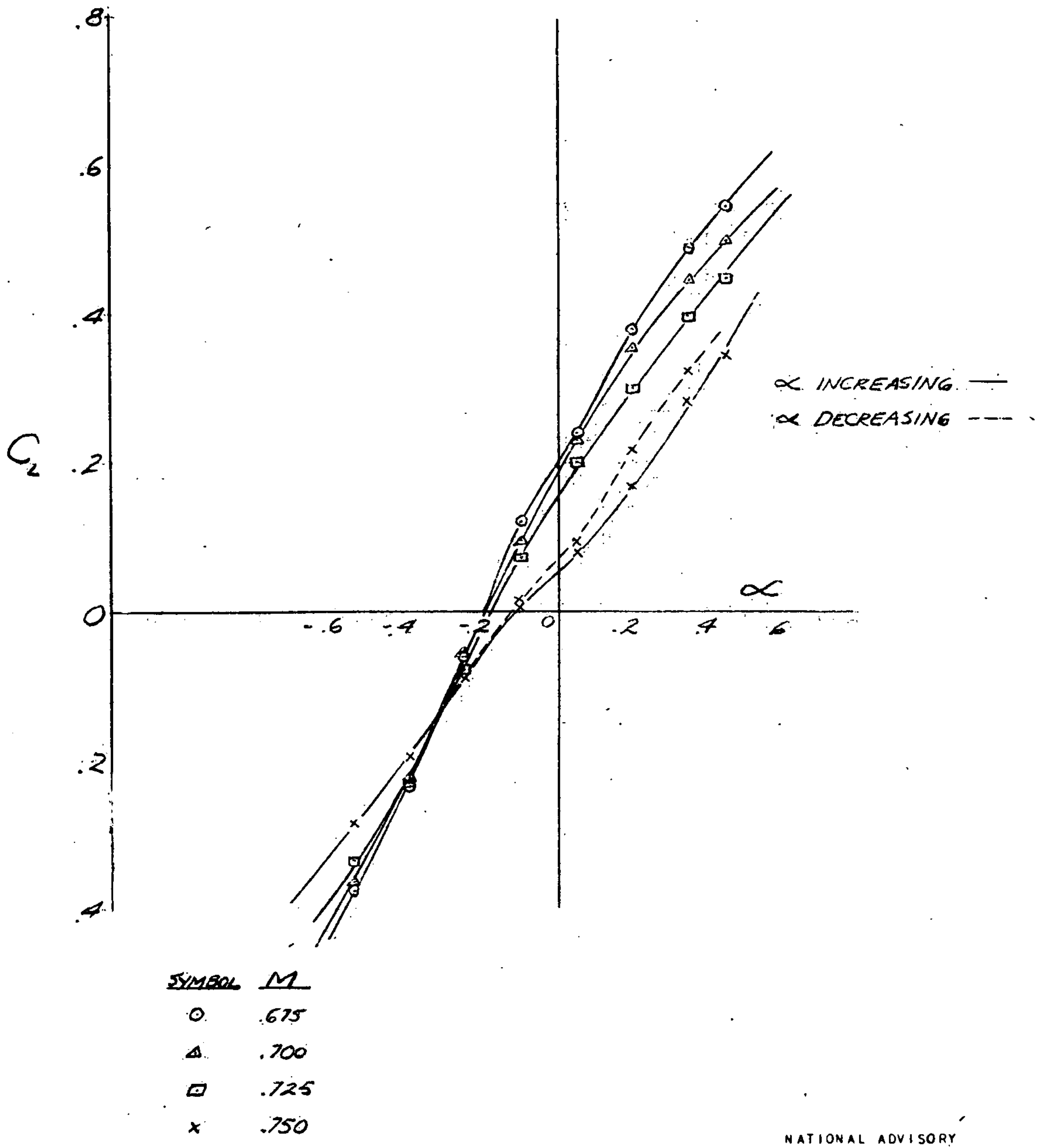

NATIONAL ADVISORY
COMMITTEE FOR AERONAUTICS

(b) Concluded. Basic data from Mach number 0.675 to 0.750.

Figure 32. - Continued. Wing, booms, standard fuselage, and raised tail.

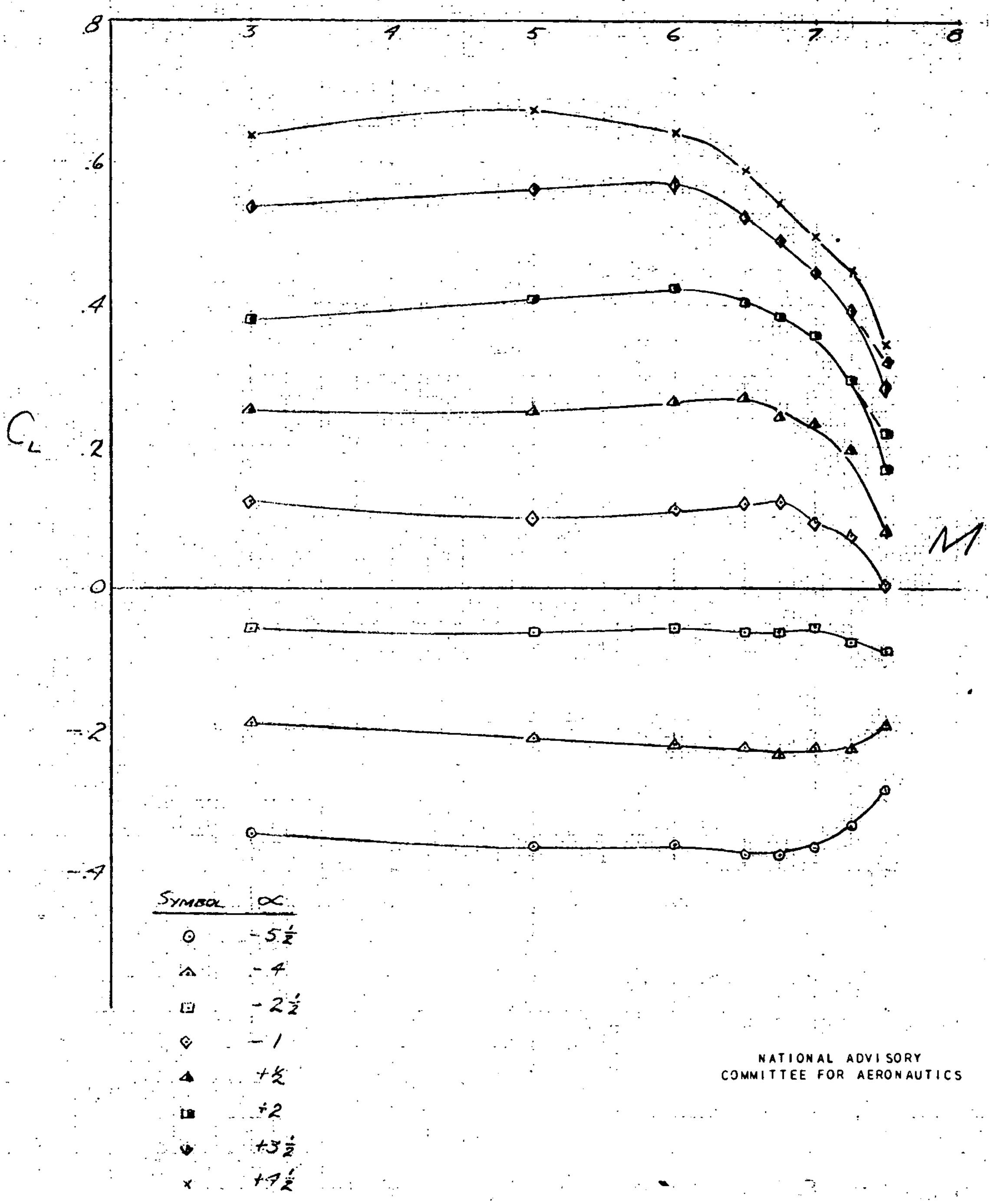

(c) Variation of C_L with Mach number at constant angles of attack.

Figure 32. - Continued. Wing, booms, standard fuselage, and raised tail.

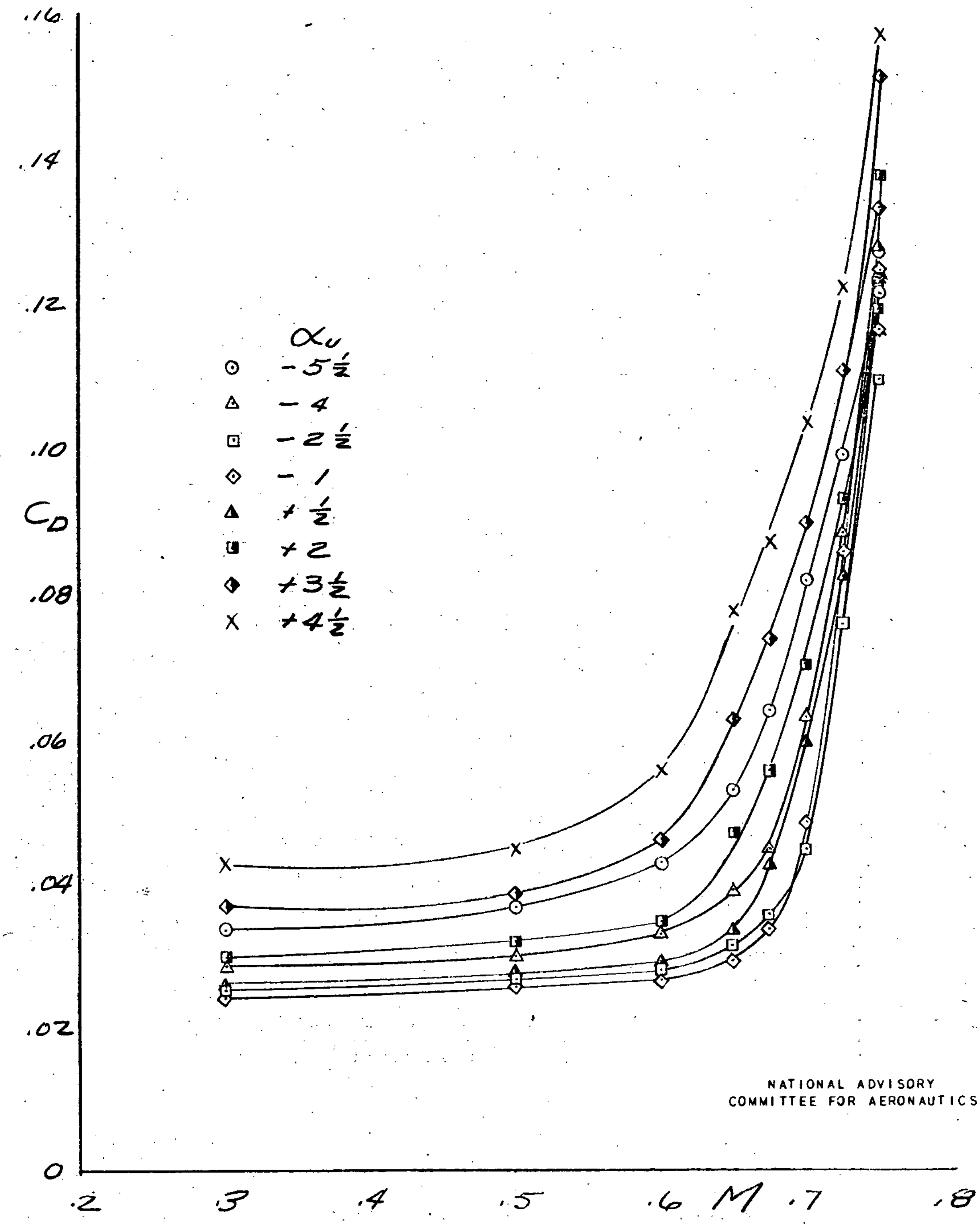

(d) Variation of C_D with Mach number at constant angles of attack.

Figure 32. - Continued. Wing, booms, standard fuselage, and raised tail.

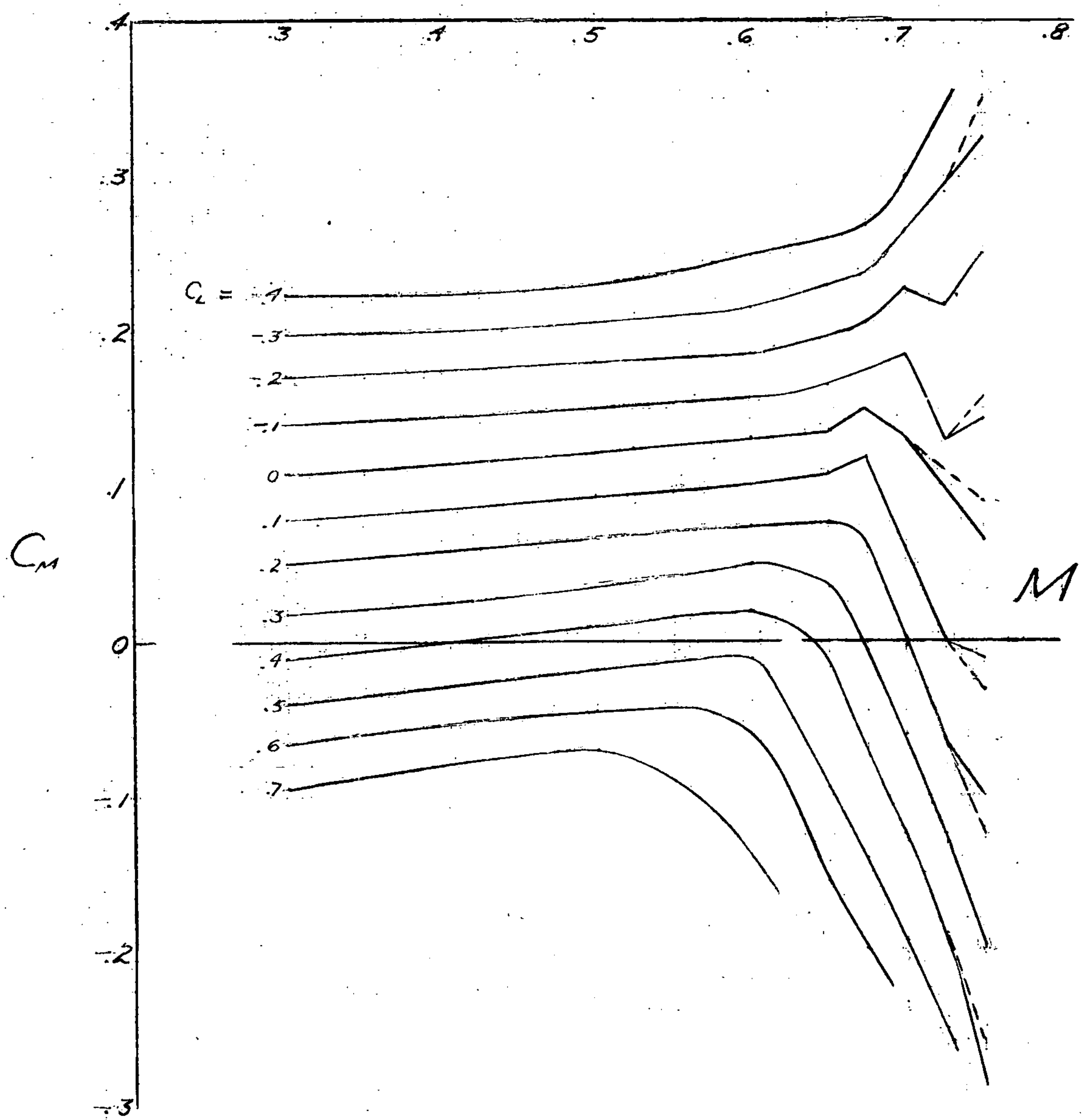

NATIONAL ADVISORY
COMMITTEE FOR AERONAUTICS

(e) Variation of C_M with Mach number at constant lift coefficients.

Figure 32. - Concluded. Wing, booms, standard fuselage, and raised tail.